Universität für Bodenkultur Wien

AUSTRIAN INSTITUTE OF TECHNOLOGY

Remediation of halogenated volatile organic compounds by phytoremediation and iron nano particles

DISSERTATION

zur Erlangung des Doktorgrades

an der Universität für Bodenkultur Wien

Durchgeführt am

AIT Austrian Institute of Technology GmbH
Dept. Health and Environment
Environmental Resources & Technologies
Konrad-Lorenz-Straße 24, 3430 Tulln a. d. Donau

Eingereicht von

PHILIPP SCHÖFTNER

Betreut durch:

Univ-Doz. Mag. Dr. Thomas G. Reichenauer (AIT/UNI WIEN/BOKU)

Dr. Georg Waldner (AIT)

Priv. Doz. Dr. MSc Andrea Watzinger (AIT/BOKU)

DI Dr. Bernhard Wimmer (AIT)

Priv. Doz. Dr. D.I. Gerhard Soja (AIT/BOKU)

Tulln, Juni, 2016

Universität für Bodenkultur Wien

AUSTRIAN INSTITUTE OF TECHNOLOGY

Remediation of halogenated volatile organic compounds by phytoremediation and iron nano particles

DISSERTATION

zur Erlangung des Doktorgrades

an der Universität für Bodenkultur Wien

Durchgeführt am

AIT Austrian Institute of Technology GmbH
Dept. Health and Environment
Environmental Resources & Technologies
Konrad-Lorenz-Straße 24, 3430 Tulln a. d. Donau

Eingereicht von

PHILIPP SCHÖFTNER

Betreut durch:

Univ-Doz. Mag. Dr. Thomas G. Reichenauer (AIT/UNI WIEN/BOKU)

Dr. Georg Waldner (AIT)

Priv. Doz. Dr. MSc Andrea Watzinger (AIT/BOKU)

DI Dr. Bernhard Wimmer (AIT)

Priv. Doz. Dr. D.I. Gerhard Soja (AIT/BOKU)

Tulln, Juni, 2016

Acknowledgements

I wish to thank

- My supervisor, Thomas G. Reichenauer, for his personal and academic support and numerous interesting discussions.
- Georg Waldner for his help whenever needed and the many, many times discussing even the smallest details. Without Georg Waldner it would not have been possible to implement the project NanoSan as we did.
- Philipp Holzknecht for an extraordinary teamwork in the framework of the Phytotop project, professionally as well as within numerous coffee breaks.
- Andrea Watzinger and Bernhard Wimmer for academic and technical supervision. Thanks for your open-door policy.
- Johann Riesing for technical support and a lot of coffee and cakes.
- Numerous students who helped me with my practical work but also brightened many days in the lab with lots of fun. Thanks to Sonja Feichtmaier, Dorothea Summer, Lisa Pum, Sarah Quast, Robert Müller, Hülya Hazler.
- Christian Mayer, Patrick Kobe, Marion Graser, Martha Klampfer and Christopher Nastl for technical support, very nice companion in the lab, around the table tennis table and at the tennis court. In specific Christian Mayer and Patrick Kobe for her inexhaustible technical support at the very beginning of my studies.
- Sandra Krissalis for proactive and perfect organization of my professional live.
- My parents without whose unquestioning support I would not have been able to realise school and university in a way as I did.
- My beloved family Stephanie, Verena and Magdalena for making me feel so very much at home.

The work was financially funded by the Federal Ministry of Agriculture, Environment and Water Management (BMLFUW) as well as partially by the AIT – Austrian Institute of Technology. The funding management for BMLFUW was done by Kommunalkredit Public Consulting (KPC).

Abstract

Soil and groundwater contamination poses a threat to groundwater quality all over the world. Therefore novel in-situ remediation technologies are investigated since conventional technologies as dig & dump, pump & treat or encapsulation are expensive. Especially in densely built areas conventional technologies are often not even technically feasible. In this study the applicability of two in-situ remediation technologies was investigated for remediation of trichloroethene (TCE). One project concentrated on the application of nanoscale zero valent iron (nZVI) particles for chemical-reductive dehalogenation of TCE. The other project concentrated on the capability of willow plants to take up, metabolize and transpire TCE from the soil and the groundwater stream. Both projects were implemented in lab scale.

Batch experiments were conducted to test the applicability of nZVI particles. Environmental conditions within these batches were varied to simulate conditions which are relevant in practice such as (i) different ionic strength, (ii) addition of polyelectrolytes (carboxymethylcellulose and ligninsulphonate), (iii) lowered water temperature, (iv) different dissolved oxygen concentrations and (v) different particle contents. Reduced ionic strength, addition of polyelectrolytes, temperature reduction, increased dissolved oxygen and reduced particle content decelerated particle reactivity but did not influence particle selectivity. Independent of environmental conditions solely about 3.4 ± 1.4 % of all electrons that were released via oxidation of nZVI reacted with TCE. These results suggest that particle selectivity is rather particle intrinsic than influenced by environmental conditions.

Greenhouse experiments were conducted to investigate the applicability of willow plants for remediation of TCE. Therefore willow trees were planted in glass pots which were filled with quartz sand and a compost layer was put on top of the quartz layer. TCE was added into these pots in nominal concentrations of 0, 144, 288 and 721 mgl^{-1}. The fate of TCE was then monitored by periodic measurements of the TCE concentration in the water as well as periodic measurements of TCE and its metabolites in the plant tissue. Water uptake was not inhibited by high TCE concentrations. Almost 1 % of the TCE was metabolized in the plant shoots, building mainly trichloroacetic acid and dichloroacetic acid. More than 98 % of the initially added TCE was transpirated without being metabolized. A potential microbial dehalogenation in the soil layers was ruled out by measurements of $\delta^{13}C$ of water and by measurements of phospholipid fatty acids.
In conclusion both technologies were capable to remove TCE from groundwater, but each technology has its potential for further optimization.

Zusammenfassung

Boden- und Grundwasserkontaminationen stellen auf der gesamten Welt ein Problem für die Grundwasserqualität dar. Derzeit werden neuartige in-situ Sanierungsverfahren entwickelt, da konventionelle Verfahren, wie dig & dump, pump & treat oder Umschließung, teuer sind. Insbesondere in dicht bebautem Gebiet sind diese Technologien oftmals auch technisch nicht einsetzbar. Im Rahmen dieser Studie wurde die Anwendbarkeit von zwei in-situ Sanierungsverfahren zur Sanierung von Trichlorethen (TCE) untersucht. Ein Projekt beschäftigte sich mit der Anwendung von nanoskaligen nullwertigen Eisenpartikeln zur reduktiven Dehalogenierung von TCE. Das zweite Projekt beschäftigte sich mit der Frage, ob Weidenbäume in der Lage sind TCE aufzunehmen und in der Pflanze zu metabolisieren.

Batch Experimente wurden durchgeführt um die Anwendbarkeit von Eisenpartikeln zur Dehalogenierung von TCE unter verschiedenen Umweltbedingungen auszutesten. Hierfür wurden Parameter variiert die auch in der Praxis als relevant angesehen werden: (i) verschiedene Ionenstärke im Wasser, (ii) Zugabe von Polyelektrolyten (Carboxymethylzellulose und Ligninsulfonat), (iii) geringere Reaktionstemperatur, (iv) verschiedene Konzentrationen an gelöstem Sauerstoff im Wasser und (v) verschiedene Partikelmengen. Eine Verringerung der Ionenstärke, die Zugabe von Polyelektrolyten, die Verringerung der Temperatur, eine Erhöhung der Sauerstoffkonzentration und eine Verringerung der Partikelmenge bewirkten eine Verlangsamung des Abbaus von TCE. Sie beeinflussten jedoch nicht die Selektivität der Partikel. Unabhängig von den Umweltbedingungen reagierten lediglich 3,4 ± 1,4 % der vom Eisen abgegebenen Elektronen mit TCE, was darauf hindeutet, dass die Selektivität der Partikel eher von den Partikeleigenschaften als von den Umweltbedingungen vorgegeben wird.

Die Anwendbarkeit von Weidenbäumen zur Sanierung von TCE wurde im Rahmen eines Glashausexperimentes untersucht. Hierfür wurden Weidenpflanzen in Glastöpfe eingesetzt, welche mit Quarzsand gefüllt wurden, auf den eine Kompostschicht aufgetragen wurde. Anschließend wurde mit TCE versetztes Wasser (nominal 0, 144, 288 & 721 mgl^{-1}) eingefüllt. Die TCE Konzentrationen wurden periodisch im Wasser, sowie die potentiellen TCE Metaboliten periodisch in der Pflanzenbiomasse gemessen. Das gelöste TCE wurde mit dem Wasserstrom aufgenommen, wo knapp 1 % des TCE in den Pflanzentrieben metabolisiert wurde. Rund 98 % des aufgenommenen TCE wurde transpiriert. Als Hauptmetaboliten wurden Di- und Trichloressigsäure identifiziert. Ein mikrobieller Abbau in der Bodenzone wurde ausgeschlossen, basierend auf durchgeführten $\delta^{13}C$ Messungen sowie durchgeführten Messungen von Phospholipid Fettsäuren.

Es konnte gezeigt werden, dass beide Technologien in der Lage sind TCE aus dem Grundwasser zu entfernen, wobei beide der Technologien noch Optimierungspotential aufweisen.

Contents

1. Introduction

1.1. Motivation

Soil and groundwater contamination poses a high risk to human health. Contaminants can be taken up via ingestion, inhalation, skin contact and dermal absorption. In Austria it is expected that about 1800 to 4200 severely contaminated sites will have to be remediated (Umweltbundesamt Österreich, 2007). The most frequent pollutants at contaminated sites worldwide are solvents, petroleum hydrocarbons, tar oil and heavy metals. Chlorinated hydrocarbons (CHCs) are especially toxic solvents which represent about 10 % of contaminants affecting soil and groundwater in Europe (Panagos et al., 2013). Particularly chemical industry, metal industry and laundries are known to be the major sources of CHCs at contaminated sites. In specific trichloroethene (TCE) represents a frequent and especially toxic pollutant. An intoxication with TCE can lead to failure of the central nervous system, injury of the liver and cancerogen effects at chronic exposure (IFA - Institut für Arbeitsschutz der Deutschen Gesetzlichen Unfallversicherung, 2013). TCE is denser than water (1.46 gml^{-1}), hardly soluble in water (~1 gl^{-1}) and volatile (boiling point 87 °C).

Due to its density higher than water TCE belongs to the so called DNAPLs (=Dense non-aqueous Phase Liquids). Most commonly DNAPLs infiltrate into the unsaturated zone from the surface (Figure 1a), for example by a leaking tank. Within the unsaturated zone DNAPLs migrate downwards to the water table (saturated zone) where a minimum pressure is needed to enable infiltration of DNAPLs into the saturated zone. This pressure corresponds to the pressure needed to create a network of interconnected pores from which water has to be removed. Initially the coarser pores will be filled by DNAPLs while fine pores may be filled subsequently. The pressure (P) needed for infiltration [N/m^2] depends on r (the soil pore radius [m]) and σ (the interfacial tension between water and DNAPL) which is 0,035 N/m in case of DNAPL (Appelo and Postma, 2005). According to that the necessary pressure head for infiltration of TCE in aquifers with coarse pores [50 µm] is about 0,10 m whilst the necessary pressure head can rise up to 24 m in case of very fine pores [0.2 µm]. After release into the underground DNAPLs migrate vertically since they are denser than water (Figure 1a). The DNAPLs accumulate on top of horizontal less permeable or impermeable layers (e.g. clay lense or rock). There they form pools. Such a DNAPL pool can migrate horizontally along such a horizontal layer and continues vertical migration at the impermeable layers edge (Figure 1a). Simultaneously the TCE begins to dissolve slowly and form groundwater plumes downstream and vapour plumes which migrate horizontally and vertically to the surface (Figure 1b). Such dissolution of DNAPLs like TCE can last for decades since they are hardly soluble in water. In the course of aging the DNAPL phase diffuses into the pores of the less

permeable layers. By that the DNAPL pools vanish. Once the DNAPL pools do not exist anymore the back diffusion of TCE from the less permeable layers to the more permeable layers dominates the plume formation. At this stage the mass discharge of TCE via the plume is already greatly reduced. Still the concentrations in the plume and the total amount of undissolved TCE can be quite high.

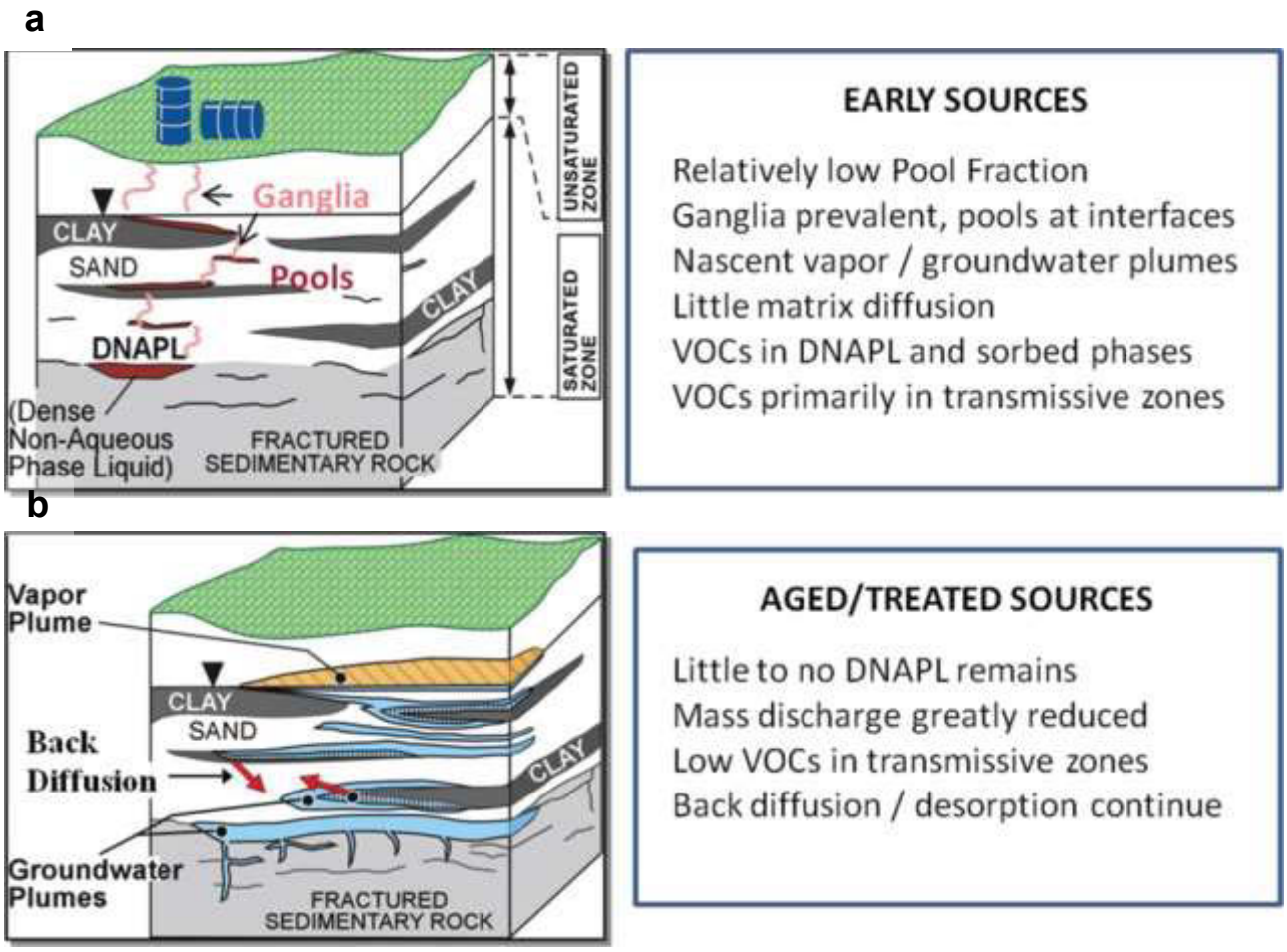

Figure 1: Evolution of a DNAPL source zone and key features of different stages (Stroo et al., 2012)

Remediation of all expected severely contaminated sites in Austria will cause estimated total costs of about 5 to 12 billion Euros (BMLFUW, 2007) if state of the art technologies will be applied for remediation of these sites. Decontamination of contaminated sites by such state of the art methods as “dig & dump” and “pump & treat” is very cost extensive. “Dig & dump” technologies are expensive since the infrastructure for digging, transport and the controlled disposal of contaminated soil is cost intensive. “Pump & treat” technologies pump contaminated water or air from the underground to the surface where the contaminated medium is treated. By that it is not possible to treat the contaminant source but solely the plume downstream of the source. The

treatment times of such technologies can be very long, in specific if the source dissolves or evaporates slowly over decades. Furthermore contaminated sites are often placed in densely built areas where dig & dump or encapsulation is technically not feasible.

Hence novel in-situ remediation technologies are developed to facilitate remediation in urban areas and to increase remediation cost efficiency. Table 1 illustrates a rough overview about different innovative remediation technologies and its stage of development and the state of the practice of these technologies in Austria.

Table 1: Assessment of the stage of development of innovative remediation technologies within Europe. Modified from (ÖVA, 2010)

Technology	Under Development	Technologically advanced	State of the art
Microbiological technologies			
Aerobic technologies			
Bioventing			■
Biosparging		■	■
Oxygen carrier addition	■	■	
Methan addition	■	■	
Aerisation of dumps		■	■
Anaerobic technologies			
Substrate addition	■	■	
Nitrate addition	■	■	
Phytoremediation			
Phytoremediation	■	■	
Chemical technologies			
In-situ chemical oxidation (ISCO)			
Permanganate	■	■	
Hydrogen peroxide	■	■	
Ozone	■	■	
Persulfate	■		
In-situ chemical reduction (ISCR)			
ISCR	■	■	
Physical technologies			
Thermal in-situ technologies			
Steam enhanced extraction		■	■
Electrical fixed heat source	■	■	
Radio frequency heating	■		
Electrical resistive heating	■		
Electro kinetic separation			
Electro kinetic separation	■		
Hydraulic and pneumatic technologies			
Air sparging			■
In situ flushing	■	■	■
Groundwater circulation wells			■
Permeable walls			
Adsorptive walls		■	■
Reactive walls	■	■	■
In-situ immobilisation			
In-situ immobilisation		■	■

All these technologies are called in-situ technologies because the contaminated material is not excavated but treated in the underground. The functional principles of these technologies are very diverse as are their possible applications and limitations. One approach is to stimulate microbial activity in the underground to trigger microbial degradation of the contaminant, for example via addition of oxygen or nutrients. Another one is to use the capability of plants to detoxify contaminated water. Plants can take up contaminated water and transform the substances into non-toxic metabolites or store the contaminants in their plant tissue. Furthermore plant root exudates can additionally trigger microbial decontamination processes. Another approach is to inject chemical substances into the underground which transform the contaminant via oxidation or reduction. Common substances for in-situ chemical oxidation (ISCO) are permanganate or persulfate. In-situ chemical reduction can be done via injection of zero-valent iron particles. Heating of the underground is one of the possible physical technologies. Heating of soil and contaminants can lead to transformation and detoxification of certain contaminants. Furthermore heating can be used to mobilize contaminants so they are available for other treatment methods. Via electro kinetic separation dissolved, ionisable contaminants are mobilized. Positively charged ions and molecules accumulate at the cathode while negatively charged ions and molecules accumulate at the anode. Electrodes that are enriched with contaminants can be washed and the concentrated water can be treated above site. Hydraulic and pneumatic technologies are used to mobilize contaminants, either via injection of gas or via injection or circulation of water. These technologies are commonly combined with other technologies to treat the mobilized contaminants and to prevent contamination downstream, for example by permeable walls. Such walls are built downstream of the contaminant source. The contaminated water flows through the wall where the contaminants get adsorbed (e.g. on activated carbon) or degraded (e.g. on the surface of zero-valent iron particles). Another conventional approach is to encapsulate the contaminated zone by construction of impermeable vertical walls in the underground. Such commonly cement based walls are expensive and the pollutants are not degraded but do stay in the underground. This disadvantage can be overcome by combining jet-grouting technologies with the injection of reactive additives as zero valent iron particles. By that the pollutant is encapsulated within the cement pylons while reactive additives degrade the encapsulated pollutants.

As written above Table 1 illustrates just an overview about different innovative remediation technologies. Detailed implementation of these technologies can be very different. Furthermore different technologies can be combined to enhance remediation efficiency. Such combination can be implemented simultaneously or sequentially. For example a groundwater circulation well can be used to mobilize contaminants as well as to inject and distribute substrates to improve microbial degradation. As well chemical technologies can be used to treat the main part of the contaminant source. Consecutively the residual contamination can be treated by less invasive technologies as microbial degradation.

1.2. Fundamentals of investigated remediation technologies

In this work the application of nanoscale zero valent iron particles (nZVI) and the application of willow plants were investigated to remediate TCE contaminations. In this chapter the fundamental background of these remediation technologies is explained.

1.2.1. Application of nZVI for remediation of TCE

The application of nZVI is an in-situ technology which is capable of transformation of CHCs and other contaminants. Nanoscale zero-valent iron (nZVI) particles are commonly injected into the aquifer via an injection well (Figure 2) where they detoxify inorganic or organic pollutants chemically due to their low redox potential. During injection process particles can be transported in the aquifer till they finally stick to aquifer grains and to the DNAPL phases in the contaminant source zone. It is important that the particles are mobile enough to reach the whole source zone area before they adsorb to the aquifer grains. To overcome these limitations special injection methods as for example jet grouting are nowadays investigated for particle injection.

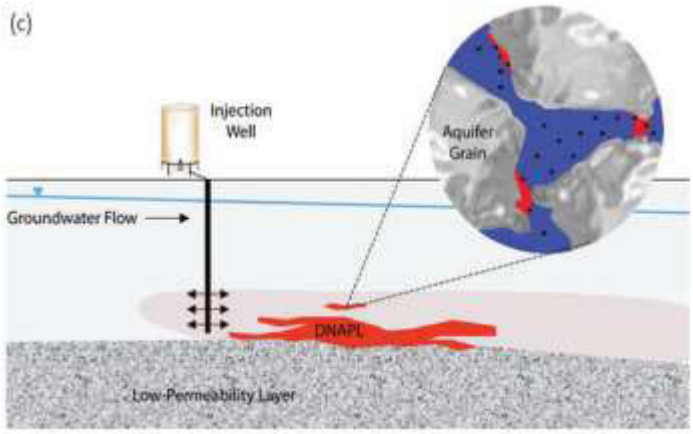

Figure 2: Injection of nZVI-solution into the DNAPL source zone (Tratnyek and Johnson, 2006).

NZVI can degrade or immobilize numerous organic and inorganic contaminants such as chlorinated organic solvents, polychlorinated biphenyls, antibiotics, nitroamines, various inorganic anions, alkaline earth metals, transition metals, post transition metals and metalloids (Crane and Scott, 2012; Sun et al., 2006; Yan et al., 2013; Zhang, 2003). After complete oxidation of nZVI particles, the particles remain in the aquifer as iron oxides which make up about 5 % of the Earth's crust.

Reaction pathways between nZVI and various reactants differ. In the case of trichloroethene (TCE), as representative substance for CHCs, complete reductive dechlorination proceeds by different mechanisms (Choe et al., 2001):

- Reductive dechlorination by direct contact
  $C_2HCl_3 + 3\ Fe^0 + 3\ H_2O \rightarrow C_2H_4 + 3\ Cl^- + 3\ Fe^{2+} + 3\ OH^-$.
- Reductive dechlorination by oxidation of solved or adsorbed Fe^{2+} on the iron oxide-hydroxide surface
- H_2-induced and Fe-catalyzed reduction

Other examples of reaction between nZVI and PCE, TCE, cis-DCE and CCl_4 are summarized in the paper of Karlický and Otyepka (2014). Besides the described reactions with target contaminants, unfavourable side reactions occur as:

- Iron corrosion ($2\ Fe^0 + 4\ H^+ + O_{2,}aq \rightarrow 2\ Fe^{2+} + 2\ H_2O$)
- Hydrogen evolution ($Fe^0 + 2\ H_2O \rightarrow Fe^{2+} + H_2 + 2\ OH^-$)
- Reactions with dissolved ions and organics

These side reactions consume electrons and decrease reduction potential for target contaminants. At this the main issues are to gain a better understanding regarding the influence of environmental conditions on reaction properties and to increase the selectivity of particles towards the target compound and to minimize unfavourable side reactions (e.g. with water).

Environmental conditions can determine the applicability of nZVI for in-situ remediation on site. As presented in Schöftner et al. (2015) in specific the pH-value (Liu and Lowry, 2006; Song and Carraway, 2005; Xie and Cwiertny, 2012), the redox potential (Dolfing et al., 2008; Shi et al., 2011), the applied mass of Fe^0 (Arnold and Roberts, 2000; Cwiertny and Roberts, 2005; Song and Carraway, 2008; Tratnyek and Johnson, 2006), the contaminant concentrations (Liu et al., 2007), the ionic strength and specific water constituents (Bi et al., 2009; Liu et al., 2007; Reinsch et al., 2010; Yu et al., 2012), the oxygen concentration (Reinsch et al., 2010; Xie and Cwiertny, 2010), the reaction temperature (Yang et al., 2002), the concentration of (dissolved) organics (Bouayed et al., 1998; Chen et al., 2011; Doong and Lai, 2006; Johnson et al., 2009; Tratnyek et al., 2001; Tsang et al., 2009) and the concentration of metal-ions in solution (Doong and Lai, 2006) can influence the applicability of nZVI. A detailed description how these environmental conditions can influence the mobility, the reaction rates, the electron efficiency and the particle aging of nZVI is written in the introduction of chapter 4, respectively in Schöftner et al. (2015).

Particle properties influence the reaction properties substantially as different particle types exhibit different reaction kinetics in respect to TCE (Liu et al., 2005a, 2005b; Su and Puls, 1999). Hence, under suitable environmental conditions nZVI particles should be applied that are optimized for a degradation of the target compound. Reaction properties of nZVI are highly determined by the particle size**,** specific surface area (SSA) of particles (m^2g^{-1}), chemical properties as impurities/dopants (e.g. presence of FeS), the particle structure (e.g. preferential orientation of the surface or crystallinity), structural defects, iron oxide-hydroxide shell, particle size distribution, magnetic attraction (in specific Fe^0 content), particle shape, particle porosity and application of surface stabilizers.

Smaller nano-particles show higher mass-normalized reaction rates than micro-particles. This is due to the higher specific surface area (m^2/g) of nano-particles. Therefore surface area normalized reaction rates are equal between nano and micro particles (Tratnyek and Johnson, 2006). Since nano-particles oxidize faster the longevity of nano-particles is lower what increases the necessity to transport nano-particles directly into the DNAPL phase to avoid excessive reaction with water. On the other hand nano-particles are more mobile what makes it easier to inject the particles near the DNAPL phase. Particles with iron sulfide impurities showed enhanced TCE degradation (Kim et al., 2013; Schöftner et al., submitted for publication). The enhanced reactivity was explained via enhancement of surface conductivity and iron corrosion as well as via enhanced surface hydrophobicity. Iron sulfides are less hydrated and introduce hydrophobic sites that preferentially adsorb hydrophobic substances (Park et al., 2006). Consequently increased affinities of FeS for chlorinated ethenes have been reported (Butler and Hayes, 2001, 1998; Weerasooriya and Dharmasena, 2001). The roughness of the particle surface as well as defects on the surface were shown to influence the reactive sorption of the hydrophobic substances TCE and tetrabrombisphenol A (Gotpagar et al., 1999; Luo et al., 2010). High magnetic attraction (Fe^0 content) and polydisperse particle distribution increase particle aggregation (Phenrat et al., 2009) what results in decreased particle reactivity and increased particle sedimentation. Such particle aggregation can be decreased by the application of surface stabilizers (Phenrat et al., 2010) leading to increase of nZVI reactivity. So high Fe^0 contents display some significant disadvantages in spite of its high efficiency in toxic compounds removal, such as the strong tendency of aggregation and rapid sedimentation (Ponder et al., 2000; Sun et al., 2007). Beside possible aggregation effects, the Fe^0 fraction of the particles in relation to the iron(hydr)oxides in the shell does not influence the particle reactivity regarding TCE (Liu and Lowry, 2006). Poorly ordered particles are capable to activate and use H_2 to reduce TCE whilst more crystalline particles are not (Liu et al., 2005a, 2005b). H_2 that is evolved through this reaction can be reused whereby particle selectivity can be increased. On the other hand poorly ordered particles create H_2 faster what decreases these particles longevity (Liu et al., 2005b). Increased specific surface area increases

reactivity of nZVI nanoparticles preferring to use nanoparticles instead of microparticles (Soukupova et al., 2015).

Numerous particle modifications were employed to increase adsorption of target substance on nZVI particles and decrease particle aggregation. For instance, particles were entrapped in chitosan beads to facilitate the reaction between nZVI and its reactant (Liu et al., 2012, 2010). Increased adsorption of TCE was achieved when nZVI particles were encapsulated in an Arabic gum stabilized oil-in-water emulsion (Long and Ramsburg, 2011) or integrated in colloidal active carbon (Bleyl et al., 2012; Mackenzie et al., 2012).

To sum up the main issues regarding the application of nZVI for remediation are:

- Homogenous distribution of the particles into the whole source zone area
- Better knowledge regarding the influence of environmental conditions on reaction properties
- Optimization of the particles regarding a selective reaction with the target compound
- Best possible understanding of potential toxic effects of nanoscale particles in the underground

1.2.2. Application of willow plants for remediation of TCE

Phytoremediation means using plant physiological mechanisms for the remediation of contaminated sites. By that it is possible to remediate inorganic and organic contaminations. Initially - beginning with about 1990 - phytoremediation was used mainly to remediate sites that were contaminated by heavy metals. Heavy metals can be taken up by plants and are stored in plant tissues. After harvesting of the plants it is possible to extract these heavy metals from plant tissues. Later the focus moved to organic contaminants, especially pesticides. Organic contaminants as TCE are not just stored in plant tissues but can be metabolized into other, less toxic substances. This metabolization can be compared with the metabolization of organic substances in the liver of mammals. Accordingly the "green liver concept" was established by Sandermann (1992).

In case of DNAPL contaminations, plants are planted around the source zone and downstream of the source zone (Figure 3). Plants take up the groundwater and redirect the groundwater stream towards the surface along the transpiration pathway (roots-stem-leaves-atmosphere). By that the plants act as a hydraulic barrier and prevent spreading of the dissolved DNAPL downstream. Additionally the plants can metabolize and detoxify the contaminant in their plant tissue according to the green liver concept. A site contaminated with DNAPL has to exhibit some requirements to be suitable for remediation by phytoremediation:

- The contaminated site has to be suitable for planting of trees at a scale that is big enough that the plants can act as a hydraulic barrier (surface sealing alone is no exclusion criterion).
- Rather low depth to water table so the plants can root into the aquifer
- Shallow aquifer and a low groundwater flow velocity

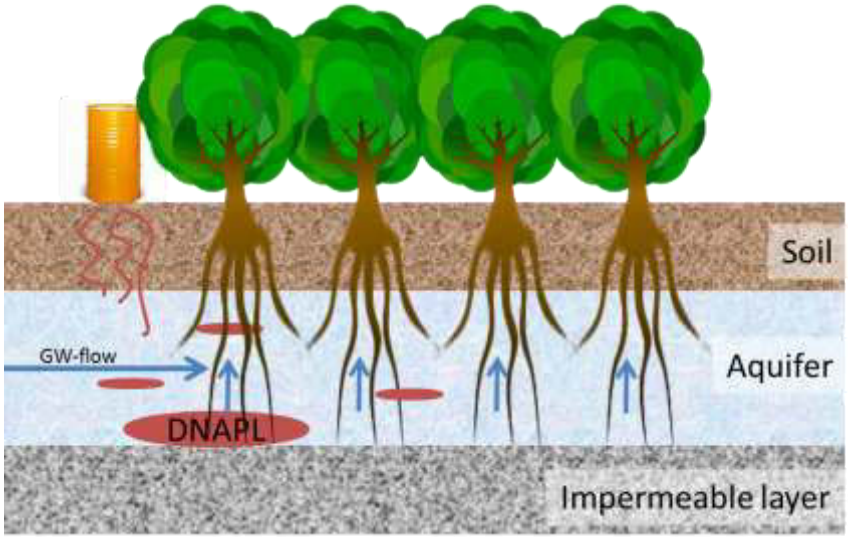

Figure 3: Schematic representation of a remediation set-up to remediate a site contaminated by DNAPL

Plant physiological processes of phytodegradation start after water uptake by plants. Plant roots are capable to take up CHCs as TCE because its chemical and physical properties facilitate root uptake. Its K_{ow} values (octanol-water partition coefficient) are between 1.8 (Briggs et al., 1982) and 3.1 (Hsu et al., 1990). Furthermore its strong polarity and water solubility and its low ionization potential facilitate CHC uptake (Dettenmaier et al., 2009). Once the contaminant is taken up it is metabolized according to the green liver concept which is divided into three phases (Reichenauer and Germida, 2008):

- Transformation (Phase I)
- Conjugation (Phase II)
- Compartmentalisation (Phase III)

In phase I, the transformation phase, the contaminants are chemically modified via oxidation, reduction or hydrolysis. By that the contaminants become more water soluble due to its increased polarity. Thus biochemical activity increases (Komives and Gullner, 2005). In case of TCE, it is state of the science that TCE becomes transformed into dichloroacetic acid, trichloroacetic acid and trichloroethanol (Figure 4). These substances can be conjugated within the second phase.

In phase II, the conjugation phase, the transformed contaminants are conjugated with endogenous molecules (sugars or peptides). By that the substances become less toxic for the plant and become capable to be compartmentalised in phase III. In case of TCE, TCE becomes conjugated into oxalic acid and trichloroethanol glucoside (Figure 4). These substances can still be toxic for mammals.

In phase III, the compartmentalisation phase, the conjugated substances are transferred into the vacuole (storage within the vacuole) or to the cell wall (covalent bonding to the molecules of the cell wall). Different to mammals the substances cannot be excreted but have to be stored in a place where the substances cannot harm the plant cells, as the vacuole or the cell wall.

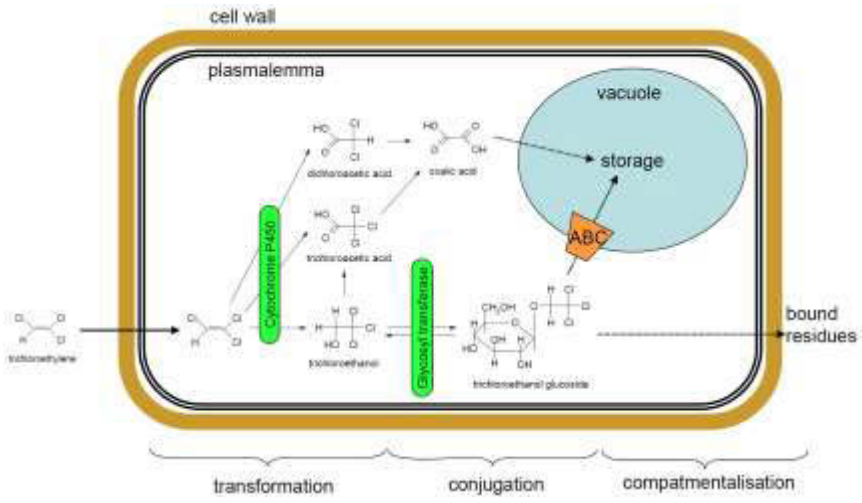

Figure 4: Metabolism of TCE in plant cells according to the green liver concept (Reichenauer and Germida, 2008)

Plant associated processes can improve the efficiency of phytoremediation complementary to the direct metabolization by plants as described above. *Endophytes* can support degradation of contaminants within plant tissues. Endophytes are often bacteria or fungi, which live within a plant without harming the plant. There they are capable to degrade contaminants. Plants can be inoculated with endophytes to enhance CHC degradation (Weyens et al., 2010, 2009a, 2009b). Another relevant CHC dehalogenating process is the dehalogenation in the rhizosphere. Plants can promote such microbial degradation of contaminants in the rhizosphere (*rhizodegradation*) (Anderson and Walton, 1995; Godsy et al., 2003; James et al., 2009) by (i) release of root exudates. Such root exudates can be nutrients, sugars, amino acids and secondary metabolites such as organic acids (Brigmon et al., 2003; Reichenauer and Germida, 2008; Walton and Anderson, 1990). These substances stimulate microbial growth in the rhizosphere (1 mm around the roots). During mineralization of these root exudates enzymes are built for mineralization. Some of these enzymes are also capable to degrade organic contaminants. This process of decontamination is called co-metabolism. Beside stimulation by root exudates rhizodegradation can also be enhanced by (ii) physical changes of the soil structure what causes enhanced gas exchange (enhanced oxygen supply) and regulation of soil moisture (McCully, 1999).

Phytovolatilization appears if processes described above are not efficient enough for complete metabolization of CHCs. In this case CHCs volatilize from the groundwater into the atmosphere, by passing the plants transpiration stream without being metabolized sufficiently (Ma and Burken, 2004; Orchard et al., 2000; Wang et al., 2004; Winters, 2008).

To summarize, following processes are relevant regarding fate and behaviour of CHC during phytoremediation:

- Phytodegradation
- Endophytic degradation within plant tissue
- Rhizodegradation
- Phytovolatilization

1.2.3. Isotopic fractionation of TCE during remediation

Isotopic fractionation is an analytical tool that was used within this study. It can be used to prove if a decrease of contaminant concentrations in water is caused by degradation of the contaminant or by dilution, by adsorption or by absorption of the contaminant. This method is based on the difference of the binding energy of different stable isotopes. Isotopes are variants of a chemical element as Carbon (C) which exhibit different numbers of neutrons in the nucleus of an atom but the same number of electrons and protons. The more neutrons an atom exhibit the higher the molecular mass of the isotope. Stable isotopes are is

topes which do not decay radioactively but are stable over time. In the case of carbon two stable isotopes with higher abundance exist; one with 12 neutrons (^{12}C) and one with 13 (^{13}C) neutrons. The heavier isotope (e.g. ^{13}C) is bound stronger within the initial product (e.g. TCE) than the lighter isotope (e.g. ^{12}C). So it is harder for microbes and chemical reactants to degrade organic substances which contain the heavier isotope. Therefore the molecules containing heavier isotopes accumulate during a degradation process while the molecules containing lighter isotopes are degraded preferentially. Figure 5 illustrates exemplary the accumulation of ^{13}C containing TCE molecules during degradation of TCE in a closed system. If the concentration in water decreases without accumulation of the heavier isotope the contaminant was not degraded but diluted, adsorbed or absorbed. Volatilization of TCE causes only minor shifts in isotopic composition of the residual contaminant compared to degradation processes. The intensity of this fractionation with degradation depends on specific degradation processes and vary significantly for different microbial communities and different nZVI particle types. The extent at which stable isotopes fractionate during degradation is described as C-enrichment factor or fractionation factor. This factor has to be defined for every microbial community and particle type in lab experiments. Carbon fractionation factors have already been defined for numerous (n)ZVI particles (Dayan et al., 1999; Elsner et al., 2008; Lojkasek-Lima et al., 2012; Slater et al., 2002) and microbial communities (Harding et al., 2013; Marco-Urrea et al., 2011; Numata et al., 2002).

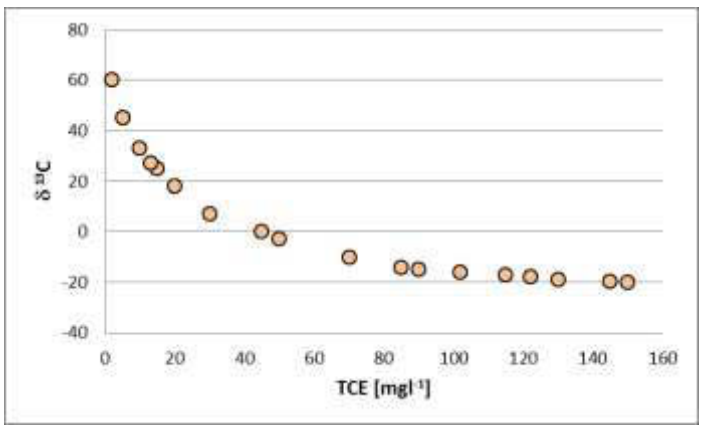

Figure 5: Schematic representation of accumulation of 13C during degradation of TCE in a closed system

1.3. Aims and objectives of this study

The aim of this study was to investigate the feasibility of two evolving in-situ remediation technologies for remediation of chlorinated hydrocarbons, in specific trichloroethene (TCE). One technology is the application of nanoscale zero valent iron particles (nZVI) for chemical reduction of TCE. The other investigated technology is the application of willow plants for remediation of TCE contaminations. Investigations were conducted in lab and greenhouse scale. Pilot scale applications were excluded since the stage of development of these technologies is still at a very early stage. Legal, economic and toxicological issues were excluded due to the same reason.

The thesis itself consists of two papers (chapter 2 and 3) which have been published in international peer reviewed journals. These two papers were published within the framework of two research Projects, NanoSan and PhytoTop, which were carried out at the Austrian Institute of Technology, Health & Environment Department, Environmental Resources & Technologies in 3430 Tulln, Austria. Both projects were funded by the Federal Ministry of Agriculture, Environment and Water Management (BMLFUW). The funding management was done by Kommunalkredit Public Consulting (KPC). Publication of further results of the two mentioned projects is planned but papers are not accepted at this time.

In case of the nZVI particle application, the reaction properties of ZVI particles that are produced differently can vary widely (Su and Puls, 1999). Furthermore it is known that environmental conditions can influence efficiency of remediation by nZVI substantially (Chen et al., 2011; Dolfing et al., 2008; Doong and Lai, 2006; Liu et al., 2007; Liu and Lowry, 2006; Reinsch et al., 2010; Song and Carraway, 2008; Yang et al., 2002). So the objective of this work was to (i) investigate the reaction properties of Nanofer Star particles produced by NANO IRON, s.r.o. (Rajhrad, Czech Republic) for dehalogenation of TCE. These particles are novel commercially available particles which are hardly investigated. This particle type is the only particle type that is commercially available within Europe nowadays. Only a few studies were conducted up to now using this particle type (Dong and Lo, 2013; Eglal and Ramamurthy, 2014; Honetschlägerová et al., 2012; Kim et al., 2014; Klimkova et al., 2011; Laumann et al., 2013; Li et al., 2012; Schmid et al., 2015; Zhuang et al., 2012). Another objective of this work was (ii) to explore the influence of environmental conditions on the reaction properties of Nanofer Star particles. Therefore conditions were simulated that are relevant for practical application, in specific under conditions that are representative conditions for Austrian porous groundwater bodies. Such as coarse grained highly productive aquifers (kf up to 10^{-2} m/s, 100 times higher than typically found in Germany or the USA), high content of carbonate sands (high surface charge heterogeneities) and alkaline earth causing carbonate waters with occasionally high Ca^{2+}, Mg^{2+}, NO_3^- and SO_4^{2-} content and high pH-values (high concentrations potentially increase nZVI aggregation, high pH-value decreases

particle reactivity). A detailed description of the conditions which were investigated in this study can be found in chapter 4.

In case of the application of willow plants for remediation of TCE, plants as willows are known to be capable to remediate sites contaminated with TCE (Newman et al., 1997; Shang et al., 2001; Shang and Gordon, 2002). But there is still a lack of knowledge regarding the fate of TCE once it is taken up by the plants. As described above TCE can be metabolized within the plant or can be transpired with the plants transpiration stream from the groundwater into the atmosphere. Obviously the second variant is unfavourable. Therefore the aim of this project was to get a balance of TCE uptake, TCE metabolization and TCE volatilization if willows are applied to remediate TCE-contaminated sites. For this reason, willows were grown within a greenhouse where its water was spiked with TCE. After spiking the fate of TCE was investigated. A detailed description of the experimental procedure can be found in chapter 5.

2. Main results and suggestions for further research

The application of ZVI was tested within this study for chemical reduction of TCE under different environmental conditions. In specific the application of Nanofer Star nZVI particles supplied by NANO IRON, s.r.o. (Rajhrad, Czech Republic) was tested under conditions that are relevant for practical application. The main observations of this study were:

- All tested environmental conditions (decreased ionic strength, addition of polyelectrolytes, addition O_2 and decreased temperature) decreased TCE and H_2 reaction rates but not particle selectivity regarding TCE and H_2.
- Particle selectivity appears to be particle intrinsic.
- In general selectivity of Nanofer Star particles was low (merely 3 % of released electron reacted with TCE).
- O_2 and NO_3^- were reduced and therefore it unfavourably consumed electrons supplied by nZVI.
- Application of nZVI in oxic aquifers can passivate particles, beside the fact that O_2 functions as electron acceptor. Hence pre-treatment is essential to eliminate dissolved oxygen prior to application of nZVI.
- Nanofer Star particle dehalogenated TCE without evolution of toxic intermediate products.

Based on these observations the following conclusions can be drawn for general application of nZVI and continued research:

1. Particle selectivity has to be enhanced for optimized remediation by:
   - Investigation of mechanisms causing different reaction characteristics of various particles as the influence of particle mineralogy or the influence of particle impurities (e.g. iron sulfides).
   - Production of optimized particles based on the results observed by the investigation of reaction mechanisms.
   - Modification of bare ZVI particles to enrich contaminant concentration on the particle surface (adsorption), to control particle longevity and to increase particle mobility.
2. Combination with other remediation technologies as microbial dehalogenation can improve remediation efficiency:
   - Usage of evolving H_2 as electron donor for TCE dehalogenating microbes (Wang and Tseng, 2009; Xiu et al., 2010).
   - Usage of evolving Fe^{2+}/Fe^{3+} iron (hydr)oxides for prolonged chemical dehalogenation (EPA, 2009) through Fe^{3+} -> Fe^{2+} reduction by microbial activity (Bosch et al., 2010).

The application of willow plants was tested for remediation of TCE contaminations. Therefore willows were grown in the greenhouse within microcosmsl aquifers that were spiked with TCE. The main observations of this study were:

- Willows were capable to take up TCE during the transpiration process without excluding TCE.
- Willows were tolerant regarding TCE toxicity. Even at TCE concentrations of 390 mgl^{-1} no detectable toxic effects were observed.
- Willows were capable to metabolize TCE and store these metabolites within its plant tissue.
- Metabolization of TCE within willows was not sufficient to avoid transition of TCE from the groundwater to the atmosphere via the transpiration pathway.

Based on these observations following conclusions can be drawn for general application of willows for remediation of TCE and continued research in this research field:

1. Plant intrinsic metabolization has to be improved to avoid transition of TCE into the atmosphere if willows are applied at remediation sites.
2. The influence of various parameters on transition of TCE has to be figured out. Such parameters as groundwater concentrations, tree size, season, microbial activity in the rhizosphere or plant health status. In specific since other studies than this one have shown that such transition of TCE can be very low.
3. Phytoremediation should be combined with plant associated dehalogenation processes to increase remediation potential:
   - Enhancement of rhizodegradation. Plants redirect the groundwater flow through the rhizosphere were microbes benefit from plant root exudates and physical changes of the soil structure caused by plant roots. Supplementary measures as addition of carbon sources may increase remediation potential.
   - Combination with endophytic degradation by inoculation of plants with endophytes. In this way complete mineralization of CHC, without evolution of toxic metabolites becomes possible.
4. Metabolites stored in plant tissue have to be treated following phytoremediation since metabolites as trichloroacetic acid are still harmful for humans. Therefore the fate of these metabolites during decomposition or burning of plant material has to be investigated.

In conclusion, both investigated technologies are capable to remediate TCE, even though each technology has its limitations. Beside optimization of limiting issues, the combination of different treatment technologies is reasonable to improve remediation efficiency. Furthermore, in recent years the establishment of advantageous consecutive treatments (treatment trains) got in the focus of the current research. Such a treatment train can for example be a short term application of nZVI for remediation of the source zone followed by phytoremediation to remediate the residual TCE contaminations.

3. References

Anderson, T.A., Walton, B.T., 1995. Comparative fate of [14C] trichloroethylene in the root zone of plants from a former solvent disposal site. Environmental Toxicology and Chemistry 14, 2041–2047.

Appelo, C.A.J., Postma, D., 2005. Geochemistry, groundwater and pollution, 2nd edition. ed. A.A. Balkema Publishers, Leiden.

Arnold, W.A., Roberts, A.L., 2000. Pathways and Kinetics of Chlorinated Ethylene and Chlorinated Acetylene Reaction with Fe(0) Particles. Environmental Science & Technology 34, 1794–1805. doi:10.1021/es990884q

Bi, E., Bowen, I., Devlin, J.F., 2009. Effect of Mixed Anions (HCO_3^- −SO_4^{2-} −ClO_4^-) on Granular Iron (Fe^0) Reactivity. Environmental Science & Technology 43, 5975–5981. doi:10.1021/es900599x

Bleyl, S., Kopinke, F.-D., Mackenzie, K., 2012. Carbo-Iron®—Synthesis and stabilization of Fe(0)-doped colloidal activated carbon for in situ groundwater treatment. Chemical Engineering Journal 191, 588–595. doi:10.1016/j.cej.2012.03.021

BMLFUW, B. für L.F., Umwelt und Wasserwirtschaft, 2007. Altlastensanierung in Österreich Effekte und Ausblick. Wien.

Bosch, J., Heister, K., Hofmann, T., Meckenstock, R.U., 2010. Nanosized Iron Oxide Colloids Strongly Enhance Microbial Iron Reduction. Applied and Environmental Microbiology 76, 184–189. doi:10.1128/AEM.00417-09

Bouayed, M., Rabaa, H., Srhiri, A., Saillard, J.-Y., Bachir, A.B., Beuze, A.L., 1998. Experimental and theoretical study of organic corrosion inhibitors on iron in acidic medium. Corrosion Science 41, 501–517. doi:10.1016/S0010-938X(98)00133-4

Briggs, G.G., Bromilow, R.H., Evans, A.A., 1982. Relationships between lipophilicity and root uptake and translocation of non-ionised chemicals by barley. Pesticide Science 13, 495–504.

Brigmon, L.R., Saunders, F.M., Altman, D., Wilde, E., Berry, C.J., Franck, M., McKinsey, P., Burdick, S., Loeffler, F., Harris, S., 2003. FY02 Final Report on Phytoremediation of Chlorinated Ethenes in Southern Sector Seepline Sediments of the Savannah River Site (No. WSRC-TR-2002-00557). United States Department of Energy.

Butler, E.C., Hayes, K.F., 2001. Factors Influencing Rates and Products in the Transformation of Trichloroethylene by Iron Sulfide and Iron Metal. Environmental Science & Technology 35, 3884–3891. doi:10.1021/es010620f

Butler, E.C., Hayes, K.F., 1998. Effects of solution composition and pH on the reductive dechlorination of hexachloroethane by iron sulfide. Environmental science & technology 32, 1276–1284.

Chen, J., Xiu, Z., Lowry, G.V., Alvarez, P.J.J., 2011. Effect of natural organic matter on toxicity and reactivity of nano-scale zero-valent iron. Water Research 45, 1995–2001. doi:10.1016/j.watres.2010.11.036

Choe, S., Lee, S.-H., Chang, Y.-Y., Hwang, K.-Y., Khim, J., 2001. Rapid reductive destruction of hazardous organic compounds by nanoscale Fe0. Chemosphere 42, 367–372. doi:10.1016/S0045-6535(00)00147-8

Crane, R.A., Scott, T.B., 2012. Nanoscale zero-valent iron: Future prospects for an emerging water treatment technology. Journal of Hazardous Materials 211-212, 112–125. doi:10.1016/j.jhazmat.2011.11.073

Cwiertny, D.M., Roberts, A.L., 2005. On the Nonlinear Relationship between k_{obs} and Reductant Mass Loading in Iron Batch Systems. Environmental Science & Technology 39, 8948–8957. doi:10.1021/es050472j

Dayan, H., Abrajano, T., Sturchio, N.C., Winsor, L., 1999. Carbon isotopic fractionation during reductive dehalogenation of chlorinated ethenes by metallic iron. Organic Geochemistry 30, 55–763.

Dettenmaier, E.M., Doucette, W.J., Bugbee, B., 2009. Chemical Hydrophobicity and Uptake by Plant Roots. Environmental Science & Technology 43, 324–329. doi:10.1021/es801751x

Dolfing, J., Van Eekert, M., Seech, A., Vogan, J., Mueller, J., 2008. In Situ Chemical Reduction (ISCR) Technologies: Significance of Low Eh Reactions. Soil and Sediment Contamination 17, 63–74. doi:10.1080/15320380701741438

Dong, H., Lo, I.M.C., 2013. Influence of calcium ions on the colloidal stability of surface-modified nano zero-valent iron in the absence or presence of humic acid. Water Research 47, 2489–2496. doi:10.1016/j.watres.2013.02.022

Doong, R., Lai, Y., 2006. Effect of metal ions and humic acid on the dechlorination of tetrachloroethylene by zerovalent iron. Chemosphere 64, 371–378. doi:10.1016/j.chemosphere.2005.12.038

Eglal, M.M., Ramamurthy, A.S., 2014. Nanofer ZVI: Morphology, Particle Characteristics, Kinetics, and Applications. Journal of Nanomaterials 2014, 1–11. doi:10.1155/2014/152824

Elsner, M., Chartrand, M., VanStone, N., Lacrampe Couloume, G., Sherwood Lollar, B., 2008. Identifying Abiotic Chlorinated Ethene Degradation: Characteristic Isotope Patterns in Reaction Products with Nanoscale Zero-Valent Iron. Environmental Science & Technology 42, 5963–5970. doi:10.1021/es8001986

EPA, U.S.E.P.A., 2009. Identification and characterization methods for reactive minerals responsible for natural attenuation of chlorinated organic compounds in ground water (No. EPA 600/R-09/115). EPA - United States environmental protection agency, Office of research and development, Oklahoma, USA.

Godsy, E.M., Warren, E., Paganelli, V.V., 2003. The role of microbial reductive dechlorination of TCE at a phytoremediation site. International Journal of Phytoremediation 5, 73–87.

Gotpagar, J., Lyuksyutov, S., Cohn, R., Grulke, E., Bhattacharyya, D., 1999. Reductive Dehalogenation of Trichloroethylene with Zero-Valent Iron: Surface Profiling Microscopy and Rate Enhancement Studies. Langmuir 15, 8412–8420. doi:10.1021/la990325x

Harding, K.C., Lee, P.K.H., Bill, M., Buscheck, T.E., Conrad, M.E., Alvarez-Cohen, L., 2013. Effects of Varying Growth Conditions on Stable Carbon Isotope Fractionation of Trichloroethene (TCE) by *tce* A-containing *Dehalococcoides mccartyi* strains. Environmental Science & Technology 47, 12342–12350. doi:10.1021/es402617q

Honetschlägerová, L., Janouskovcová, P., Soffer, Z., 2012. Nanoscale zero valent iron coating for subsurface application. Presented at the Proceedings of the 4th international conference NANOCAN 2012, “NANOCAN 2012” Proceedings of the 4th international conference, Brno, Czech Republic.

Hsu, F.C., Marxmiller, R.L., Yang, A.Y., 1990. Study of root uptake and xylem translocation of cinmethylin and related compounds in detopped soybean roots using a pressure chamber technique. Plant Physiology 93, 1573–1578.

IFA - Institut für Arbeitsschutz der Deutschen Gesetzlichen Unfallversicherung, 2013. GESTIS Stoffdatenbank [WWW Document]. GESTIS Stoffdatenbank. URL http://gestis.itrust.de (accessed 10.28.13).

James, C.A., Xin, G., Doty, S.L., Muiznieks, I., Newman, L., Strand, S.E., 2009. A mass balance study of the phytoremediation of perchloroethylene-contaminated groundwater. Environmental Pollution 157, 2564–2569. doi:10.1016/j.envpol.2009.02.033

Johnson, R.L., Johnson, G.O., Nurmi, J.T., Tratnyek, P.G., 2009. Natural Organic Matter Enhanced Mobility of Nano Zerovalent Iron. Environmental Science & Technology 43, 5455–5460. doi:10.1021/es900474f

Karlický, F., Otyepka, M., 2014. Challenges in the theoretical description of nanoparticle reactivity: Nano zero-valent iron. International Journal of Quantum Chemistry 114, 987–992. doi:10.1002/qua.24627

Kim, E.-J., Le Thanh, T., Kim, J.-H., Chang, Y.-S., 2013. Synthesis of metal sulfide-coated iron nanoparticles with enhanced surface reactivity and biocompatibility. RSC Advances 3, 5338. doi:10.1039/c3ra00009e

Kim, H.-S., Ahn, J.-Y., Kim, C., Lee, S., Hwang, I., 2014. Effect of anions and humic acid on the performance of nanoscale zero-valent iron particles coated with polyacrylic acid. Chemosphere 113, 93–100. doi:10.1016/j.chemosphere.2014.04.047

Klimkova, S., Cernik, M., Lacinova, L., Filip, J., Jancik, D., Zboril, R., 2011. Zero-valent iron nanoparticles in treatment of acid mine water from in situ uranium leaching. Chemosphere 82, 1178–1184. doi:10.1016/j.chemosphere.2010.11.075

Komives, T., Gullner, G., 2005. Phase I xenobiotic metabolic systems in plants. Z Naturforsch C 60, 179–185.

Laumann, S., Micić, V., Lowry, G.V., Hofmann, T., 2013. Carbonate minerals in porous media decrease mobility of polyacrylic acid modified zero-valent iron nanoparticles used for groundwater remediation. Environmental Pollution 179, 53–60. doi:10.1016/j.envpol.2013.04.004

Li, S., Fang, Y.-L., Romanczuk, C.D., Jin, Z., Li, T., Wong, M.S., 2012. Establishing the trichloroethene dechlorination rates of palladium-based catalysts and iron-based reductants. Applied Catalysis B: Environmental 125, 95–102. doi:10.1016/j.apcatb.2012.05.025

Liu, T., Wang, Z.-L., Zhao, L., Yang, X., 2012. Enhanced chitosan/Fe0-nanoparticles beads for hexavalent chromium removal from wastewater. Chemical Engineering Journal 189-190, 196–202. doi:10.1016/j.cej.2012.02.056

Liu, T., Zhao, L., Sun, D., Tan, X., 2010. Entrapment of nanoscale zero-valent iron in chitosan beads for hexavalent chromium removal from wastewater. Journal of Hazardous Materials 184, 724–730. doi:10.1016/j.jhazmat.2010.08.099
Liu, Y., Choi, H., Dionysiou, D., Lowry, G.V., 2005a. Trichloroethene Hydrodechlorination in Water by Highly Disordered Monometallic Nanoiron. Chemistry of Materials 17, 5315–5322. doi:10.1021/cm0511217
Liu, Y., Lowry, G.V., 2006. Effect of Particle Age (Fe^0 Content) and Solution pH On NZVI Reactivity: H_2 Evolution and TCE Dechlorination. Environmental Science & Technology 40, 6085–6090. doi:10.1021/es060685o
Liu, Y., Majetich, S.A., Tilton, R.D., Sholl, D.S., Lowry, G.V., 2005b. TCE Dechlorination Rates, Pathways, and Efficiency of Nanoscale Iron Particles with Different Properties. Environmental Science & Technology 39, 1338–1345. doi:10.1021/es049195r
Liu, Y., Phenrat, T., Lowry, G.V., 2007. Effect of TCE Concentration and Dissolved Groundwater Solutes on NZVI-Promoted TCE Dechlorination and H_2 Evolution. Environmental Science & Technology 41, 7881–7887. doi:10.1021/es0711967
Lojkasek-Lima, P., Aravena, R., Shouakar-Stash, O., Frape, S.K., Marchesi, M., Fiorenza, S., Vogan, J., 2012. Evaluating TCE Abiotic and Biotic Degradation Pathways in a Permeable Reactive Barrier Using Compound Specific Isotope Analysis. Ground Water Monitoring & Remediation 32, 53–62.
Long, T., Ramsburg, C.A., 2011. Encapsulation of nZVI particles using a Gum Arabic stabilized oil-in-water emulsion. Journal of Hazardous Materials 189, 801–808. doi:10.1016/j.jhazmat.2011.02.084
Luo, S., Yang, S., Wang, X., Sun, C., 2010. Reductive degradation of tetrabromobisphenol A over iron–silver bimetallic nanoparticles under ultrasound radiation. Chemosphere 79, 672–678. doi:10.1016/j.chemosphere.2010.02.011
Mackenzie, K., Bleyl, S., Georgi, A., Kopinke, F.-D., 2012. Carbo-Iron – An Fe/AC composite – As alternative to nano-iron for groundwater treatment. Water Research 46, 3817–3826. doi:10.1016/j.watres.2012.04.013
Marco-Urrea, E., Nijenhuis, I., Adrian, L., 2011. Transformation and Carbon Isotope Fractionation of Tetra- and Trichloroethene to *Trans* -Dichloroethene by *Dehalococcoides* sp. Strain CBDB1. Environmental Science & Technology 45, 1555–1562. doi:10.1021/es1023459
Ma, X., Burken, J., 2004. Modeling of TCE Diffusion to the Atmosphere and Distribution in Plant Stems. Environmental Science & Technology 38, 4580–4586. doi:10.1021/es035435b
McCully, M.E., 1999. Roots in soil: Unearthing the Complexities of Roots and Their Rhizospheres. Annual Review of Plant Physiology and Plant Molecular Biology 50, 695–718. doi:10.1146/annurev.arplant.50.1.695
Newman, L.A., Strand, S.E., Choe, N., Duffy, J., Ekuan, G., Ruszaj, M., Shurtleff, B.B., Wilmoth, J., Heilman, P., Gordon, M.P., 1997. Uptake and biotransformation of trichloroethylene by hybrid poplars. Environmental Science & Technology 31, 1062–1067.
Numata, M., Nakamura, N., Koshikawa, H., Terashima, Y., 2002. Chlorine Isotope Fractionation during Reductive Dechlorination of Chlorinated Ethenes by Anaerobic Bacteria. Environmental Science & Technology 36, 4389–4394. doi:10.1021/es025547n
Orchard, B.J., Doucette, W.J., Chard, J.K., Bugbee, B., 2000. Uptake of trichloroethylene by hybrid poplar trees grown hydroponically in flow-through plant growth chambers. Environmental Toxicology and Chemistry 19, 895–903.
ÖVA, Ö.V. für A., 2010. Technologiequickscan: In-situ-Sanierungstechnologien. Österreichischer Verein für Altlastensanierung, Wien.
Panagos, P., Van Liedekerke, M., Yigini, Y., Montanarella, L., 2013. Contaminated Sites in Europe: Review of the Current Situation Based on Data Collected through a European Network. Journal of Environmental and Public Health 2013, 1–11. doi:10.1155/2013/158764
Park, S.-W., Kim, S.-K., Kim, J.-B., Choi, S.-W., Inyang, H.I., Tokunaga, S., 2006. Particle Surface Hydrophobicity and the Dechlorination of Chloro-Compounds by Iron Sulfides. Water, Air, & Soil Pollution: Focus 6, 97–110. doi:10.1007/s11267-005-9016-z
Phenrat, T., Kim, H.-J., Fagerlund, F., Illangasekare, T., Lowry, G.V., 2010. Empirical correlations to estimate agglomerate size and deposition during injection of a polyelectrolyte-modified Fe0 nanoparticle at high particle concentration in saturated sand. Journal of Contaminant Hydrology 118, 152–164. doi:10.1016/j.jconhyd.2010.09.002
Phenrat, T., Kim, H.-J., Fagerlund, F., Illangasekare, T., Tilton, R.D., Lowry, G.V., 2009. Particle Size Distribution, Concentration, and Magnetic Attraction Affect Transport of Polymer-Modified Fe^0 Nanoparticles in Sand Columns. Environmental Science & Technology 43, 5079–5085. doi:10.1021/es900171v

Ponder, S.M., Darab, J.G., Mallouk, T.E., 2000. Remediation of Cr(VI) and Pb(II) Aqueous Solutions Using Supported, Nanoscale Zero-valent Iron. Environmental Science & Technology 34, 2564–2569. doi:10.1021/es9911420
Reichenauer, T.G., Germida, J.J., 2008. Phytoremediation of Organic Contaminants in Soil and Groundwater. ChemSusChem 1, 708–717. doi:10.1002/cssc.200800125
Reinsch, B.C., Forsberg, B., Penn, R.L., Kim, C.S., Lowry, G.V., 2010. Chemical Transformations during Aging of Zerovalent Iron Nanoparticles in the Presence of Common Groundwater Dissolved Constituents. Environmental Science & Technology 44, 3455–3461. doi:10.1021/es902924h
Sandermann, H., 1992. Plant metabolism of xenobiotics. Trends in Biochemical Sciences 17, 82–84. doi:10.1016/0968-0004(92)90507-6
Schmid, D., Micić, V., Laumann, S., Hofmann, T., 2015. Measuring the reactivity of commercially available zero-valent iron nanoparticles used for environmental remediation with iopromide. Journal of Contaminant Hydrology. doi:10.1016/j.jconhyd.2015.01.006
Schöftner, P., Waldner, G., Freitag, P., Lottermoser, W., Reichenauer, T., submitted for publication. Selectivity of trichloroethene dehalogenation differs between zerovalent nano iron particles.
Schöftner, P., Waldner, G., Lottermoser, W., Stöger-Pollach, M., Freitag, P., Reichenauer, T.G., 2015. Electron efficiency of nZVI does not change with variation of environmental parameters. Science of The Total Environment. doi:10.1016/j.scitotenv.2015.05.033
Shang, T.Q., Doty, S.L., Wilson, A.M., Howald, W.N., Gordon, M.P., 2001. Trichloroethylene oxidative metabolism in plants: the trichloroethanol pathway. Phytochemistry 58, 1055–1065.
Shang, T.Q., Gordon, M.P., 2002. Transformation of [14C] trichloroethylene by poplar suspension cells. Chemosphere 47, 957–962.
Shi, Z., Nurmi, J.T., Tratnyek, P.G., 2011. Effects of Nano Zero-Valent Iron on Oxidation−Reduction Potential. Environmental Science & Technology 45, 1586–1592. doi:10.1021/es103185t
Slater, G.F., Sherwood Lollar, B., Allen King, R., O'Hannesin, S., 2002. Isotopic fractionation during reductive dechlorination of trichloroethene by zero-valent iron: influence of surface treatment. Chemosphere 49, 587–596.
Song, H., Carraway, E.R., 2008. Catalytic hydrodechlorination of chlorinated ethenes by nanoscale zero-valent iron. Applied Catalysis B: Environmental 78, 53–60. doi:10.1016/j.apcatb.2007.07.034
Song, H., Carraway, E.R., 2005. Reduction of Chlorinated Ethanes by Nanosized Zero-Valent Iron: Kinetics, Pathways, and Effects of Reaction Conditions. Environmental Science & Technology 39, 6237–6245. doi:10.1021/es048262e
Soukupova, J., Zboril, R., Medrik, I., Filip, J., Safarova, K., Ledl, R., Mashlan, M., Nosek, J., Cernik, M., 2015. Highly concentrated, reactive and stable dispersion of zero-valent iron nanoparticles: Direct surface modification and site application. Chemical Engineering Journal 262, 813–822. doi:10.1016/j.cej.2014.10.024
Stroo, H.F., Leeson, A., Marqusee, J.A., Johnson, P.C., Ward, C.H., Kavanaugh, M.C., Sale, T.C., Newell, C.J., Pennell, K.D., Lebrón, C.A., Unger, M., 2012. Chlorinated Ethene Source Remediation: Lessons Learned. Environmental Science & Technology 46, 6438–6447. doi:10.1021/es204714w
Su, C., Puls, R.W., 1999. Kinetics of Trichloroethene Reduction by Zerovalent Iron and Tin: Pretreatment Effect, Apparent Activation Energy, and Intermediate Products. Environmental Science & Technology 33, 163–168. doi:10.1021/es980481a
Sun, Y.-P., Li, X., Cao, J., Zhang, W., Wang, H.P., 2006. Characterization of zero-valent iron nanoparticles. Advances in Colloid and Interface Science 120, 47–56. doi:10.1016/j.cis.2006.03.001
Sun, Y.-P., Li, X.-Q., Zhang, W.-X., Wang, H.P., 2007. A method for the preparation of stable dispersion of zero-valent iron nanoparticles. Colloids and Surfaces A: Physicochemical and Engineering Aspects 308, 60–66. doi:10.1016/j.colsurfa.2007.05.029
Tratnyek, P.G., Johnson, R.L., 2006. Nanotechnologies for environmental cleanup. Nano Today 1, 44–48.
Tratnyek, P.G., Scherer, M.M., Deng, B., Hu, S., 2001. Effects of natural organic matter, anthropogenic surfactants, and model quinones on the reduction of contaminants by zero-valent iron. Water Research 35, 4435–4443.
Tsang, D.C.W., Graham, N.J.D., Lo, I.M.C., 2009. Humic acid aggregation in zero-valent iron systems and its effects on trichloroethylene removal. Chemosphere 75, 1338–1343. doi:10.1016/j.chemosphere.2009.02.058
Umweltbundesamt Österreich, 2007. Umweltsituation in Österreich - Achter Umweltkontrollbericht des Umweltministers and den Nationalrat. Umweltbundesamt GmbH, Wien.

Walton, B.T., Anderson, T.A., 1990. Microbial degradation of trichloroethylene in the rhizosphere: potential application to biological remediation of waste sites. Applied and Environmental Microbiology 56, 1012–1016.
Wang, S.-M., Tseng, S., 2009. Reductive dechlorination of trichloroethylene by combining autotrophic hydrogen-bacteria and zero-valent iron particles. Bioresource Technology 100, 111–117. doi:10.1016/j.biortech.2008.05.033
Wang, X., Dossett, M.P., Gordon, M.P., Strand, S.E., 2004. Fate of carbon tetrachloride during phytoremediation with poplar under controlled field conditions. Environmental science & technology 38, 5744–5749.
Weerasooriya, R., Dharmasena, B., 2001. Pyrite-assisted degradation of trichloroethene (TCE). Chemosphere 42, 389–396. doi:10.1016/S0045-6535(00)00160-0
Weyens, N., Taghavi, S., Barac, T., Lelie, D., Boulet, J., Artois, T., Carleer, R., Vangronsveld, J., 2009a. Bacteria associated with oak and ash on a TCE-contaminated site: characterization of isolates with potential to avoid evapotranspiration of TCE. Environmental Science and Pollution Research 16, 830–843. doi:10.1007/s11356-009-0154-0
Weyens, N., Truyens, S., Dupae, J., Newman, L., Taghavi, S., van der Lelie, D., Carleer, R., Vangronsveld, J., 2010. Potential of the TCE-degrading endophyte Pseudomonas putida W619-TCE to improve plant growth and reduce TCE phytotoxicity and evapotranspiration in poplar cuttings. Environmental Pollution 158, 2915–2919. doi:10.1016/j.envpol.2010.06.004
Weyens, N., Van der Lelie, D., Artois, T., Smeets, K., Taghavi, S., Newman, L., Carleer, R., Vangronsveld, J., 2009b. Bioaugmentation with Engineered Endophytic Bacteria Improves Contaminant Fate in Phytoremediation. Environmental Science & Technology 43, 9413–9418. doi:10.1021/es901997z
Winters, R.M., 2008. Volatilization of trichloroethylene from shallow subsurface environments: trees and soil (PhD-thesis). Utah State University, Logan, Utah.
Xie, Y., Cwiertny, D.M., 2012. Influence of Anionic Cosolutes and pH on Nanoscale Zerovalent Iron Longevity: Time Scales and Mechanisms of Reactivity Loss toward 1,1,1,2-Tetrachloroethane and Cr(VI). Environmental Science & Technology 46, 8365–8373. doi:10.1021/es301753u
Xie, Y., Cwiertny, D.M., 2010. Use of Dithionite to Extend the Reactive Lifetime of Nanoscale Zero-Valent Iron Treatment Systems. Environmental Science & Technology 44, 8649–8655. doi:10.1021/es102451t
Xiu, Z., Jin, Z., Li, T., Mahendra, S., Lowry, G.V., Alvarez, P.J.J., 2010. Effects of nano-scale zero-valent iron particles on a mixed culture dechlorinating trichloroethylene. Bioresource Technology 101, 1141–1146. doi:10.1016/j.biortech.2009.09.057
Yang, S.Y., Chen, Y.F., Ke, Y.H., Tse, W.S., Horng, H.E., Hong, C.-Y., Yang, H.C., 2002. Effect of temperature on the structure formation in the magnetic fluid film subjected to perpendicular magnetic fields. Journal of Magnetism and Magnetic Materials 252, 290–292.
Yan, W., Lien, H.-L., Koel, B.E., Zhang, W., 2013. Iron nanoparticles for environmental clean-up: recent developments and future outlook. Environmental Science: Processes & Impacts 15, 63. doi:10.1039/c2em30691c
Yu, J., Liu, W., Zeng, A., Guan, B., Xu, X., 2012. Effect of SO on 1,1,1-Trichloroethane Degradation by Fe^0 in Aqueous Solution. Ground Water 286–292. doi:10.1111/j.1745-6584.2012.00957.x
Zhang, W., 2003. Nanoscale iron particles for environmental remediation: an overview. Journal of nanoparticle Research 5, 323–332.
Zhuang, Y., Jin, L., Luthy, R.G., 2012. Kinetics and pathways for the debromination of polybrominated diphenyl ethers by bimetallic and nanoscale zerovalent iron: Effects of particle properties and catalyst. Chemosphere 89, 426–432. doi:10.1016/j.chemosphere.2012.05.078

Science of the Total Environment 535 (2015) 69–78

Contents lists available at ScienceDirect

Science of the Total Environment

journal homepage: www.elsevier.com/locate/scitotenv

Electron efficiency of nZVI does not change with variation of environmental parameters

Philipp Schöftner [a], Georg Waldner [a], Werner Lottermoser [b], Michael Stöger-Pollach [c], Peter Freitag [d], Thomas G. Reichenauer [a,*]

[a] AIT Austrian Institute of Technology GmbH, Konrad-Lorenz-Straße 24, 3430 Tulln a.d. Donau, Austria
[b] Salzburg University, FB Materialforschung und Physik, Hellbrunnerstr. 34, 5020 Salzburg, Austria
[c] Technical University of Vienna, Universitäre Service-Einrichtung für Transmissionselektronenmikroskopie — USTEM
[d] Keller Grundbau Ges. mbH, Mariahilfer Straße 127a, 1150 Vienna, Austria

HIGHLIGHTS

- We investigated the degradation kinetics of trichloroethene by zerovalent nanoiron particles.
- Electron efficiency of the tested particles was very low (about 3%).
- The tested environmental conditions had no significant influence on the degradation kinetics and electron efficiency.
- We conclude that particle type is more important for degradation rates than environmental conditions.

ARTICLE INFO

Article history:
Received 14 October 2014
Received in revised form 8 May 2015
Accepted 8 May 2015
Available online 23 May 2015

Editor: D. Barcelo

Keywords:
Halogenated hydrocarbons
TCE
nZVI
Dechlorination

ABSTRACT

Nanoscale zero-valent iron particles (nZVI) are already applied for in-situ dechlorination of halogenated organic contaminants in the field. We performed batch experiments whereby trichloroethene (TCE) was dehalogenated by nZVI under different environmental conditions that are relevant in practice. The tested conditions include different ionic strengths, addition of polyelectrolytes (carboxymethylcellulose and ligninsulphonate), lowered temperature, dissolved oxygen and different particle contents. Particle properties were determined by Mössbauer spectroscopy, XRD, TEM, SEM, AAS and laser obscuration time measurements.

TCE dehalogenation and H_2 evolution were decelerated by reduced ionic strength, addition of polyelectrolytes, temperature reduction, the presence of dissolved oxygen and reduced particle content. The partitioning of released electrons between reactions with the contaminant vs. with water (selectivity) was low, independent of the tested conditions. Basically out of hundred electrons that were released via nZVI oxidation only 3.1 ± 1.4 were used for TCE dehalogenation. Even lower selectivities were observed at TCE concentrations below 3.5 mg l^{-1}, hence particle modifications and/or combination of nZVI with other remediation technologies seem to be necessary to reach target concentrations for remediation.

Our results suggest that selectivity is particle intrinsic and not as much condition dependent, hence particle synthesis and potential particle modifications of nZVI particles may be more important for optimization of the pollutant degradation rate, than tested environmental conditions.

1. Introduction

Chlorinated hydrocarbons (CHC) are toxic pollutants that are frequently found at contaminated sites. Particularly, the chemical industry, metal working industry and laundries are known to be the major sources of CHCs. These industries exist all over the world hence CHC contaminated soil and groundwater can be regarded to be a global problem. Although CHC usage is better controlled nowadays contaminated sites are still frequent due to CHC persistence. As DNAPLs (dense non-aqueous phase liquids) CHC drops migrate through the aquifer and accumulate on surfaces with higher density like intermittent clay layers or the aquiclude. By solution from this source zone CHCs can form large plumes in the groundwater.

The application of nanoscale zero valent iron (nZVI) for in situ remediation of CHC contaminated sites via reductive dehalogenation (Choe

* Corresponding author.
E-mail addresses: philipp.schoeftner@ait.ac.at (P. Schöftner), werner.lottermoser@sbg.ac.at (W. Lottermoser), stoeger@ustem.tuwien.ac.at (M. Stöger-Pollach), p.freitag@kellergrundbau.at (P. Freitag), thomas.reichenauer@ait.ac.at (T.G. Reichenauer).

http://dx.doi.org/10.1016/j.scitotenv.2015.05.033
0048-9697/

et al., 2001; Liu and Lowry, 2006) is a promising technology for remediation of CHC contaminated sites. Nano sized particles can be injected and migrate to the source in the underground (Elliott and Zhang, 2001) although particle modifications may be useful to further increase particle migration (Mackenzie et al., 2012; Mueller et al., 2011; Zhan et al., 2008). Besides mobility the reaction characteristics, especially "electron efficiency" of the used nZVI are crucial for the practical applicability of these materials. TCE and H_2 electron efficiencies were calculated via balancing of electrons that were released by particle oxidation (calculated from the change in Fe^0 content) and electrons that were "consumed" by reaction with TCE and its reaction products (calculated from final concentrations of end products) on one hand and with water (calculated from the generated H_2) on the other hand. A detailed description of the calculation can be found in the Materials and methods section. The following hydrochemical and hydrogeological properties can significantly influence mobility, reaction rates, "electron efficiency" and particle aging of nZVI: pH-value (Liu and Lowry, 2006; Song and Carraway, 2005; Xie and Cwiertny, 2012), redox potential (Dolfing et al., 2008; Shi et al., 2011), applied mass of Fe^0 (Arnold and Roberts, 2000; Cwiertny and Roberts, 2005; Song and Carraway, 2008; Tratnyek and Johnson, 2006), contaminant concentration (Liu et al., 2007), ionic strength and specific water constituents (Bi et al., 2009; Liu et al., 2007; Reinsch et al., 2010; Yu et al., 2012), oxygen concentration (Reinsch et al., 2010; Xie and Cwiertny, 2010), reaction temperature (Yang et al., 2002), concentration of (dissolved) organics (Bouayed et al., 1998; Chen et al., 2011; Doong and Lai, 2006; Johnson et al., 2009; Tratnyek et al., 2001; Tsang et al., 2009) and the concentration of metal-ions in solution (Doong and Lai, 2006). Organic materials such as polyacrylic acid (Laumann et al., 2013) and carboxymethylcellulose (Johnson et al., 2013) are commonly used to increase particle mobility in the underground, but they can block reactive particle sites (Tratnyek et al., 2001) and consequently decrease electron transfer (Bouayed et al., 1998). On the other hand quinones can increase electron transfer (Doong and Lai, 2006; Tratnyek et al., 2001; Xie and Shang, 2005). Reduction of dissolved oxygen consumes electrons supplied by nZVI. Besides, that oxygen can influence the iron (hydr)oxide shell formed during particle oxidation and thereby can change reaction characteristics (Reinsch et al., 2010; Xie and Cwiertny, 2010). Anions like NO_3^-, HCO_3^-, SO_4^{2-}, HPO_4^{2-} can increase particle reactivity (Bi et al., 2009; D'Andrea et al., 2005; Liu et al., 2007) however a number of studies indicate a decreasing particle reactivity with increasing ionic strength (Bi et al., 2009; Liu et al., 2007; Reinsch et al., 2010; Yu et al., 2012). Reduced reaction temperature in the aquifer decreases reaction rate (according to the Arrhenius equation) and increases particle agglomeration (Yang et al., 2002) causing reduced reactivity. In full scale and pilot scale applications it is very difficult to distinguish the influence of all these parameters. Therefor batch experiments are a proper way to discover useful operation ranges of nZVI.

ZVI particle types are known to show differing reaction characteristics (Su and Puls, 1999) so the objective of this work was to explore reaction characteristics of novel hardly investigated Nanofer Star nZVI particles supplied by NANO IRON, s.r.o. (Rajhrad, Czech Republic) with TCE under environmental conditions that are relevant for practical application. So our study complements previous work performed by Dong and Lo (2013), Eglal and Ramamurthy (2014), C. Kim et al. (2014), H.-S. Kim et al. (2014) and Sarathy et al. (2010) which investigated the reactivity of Nanofer particles. The investigated conditions in this study were carboxymethylcellulose and ligninsulphonate as potential amendments to improve particle mobility in the field, oxygen, carbonate content, temperature and different particle concentration. Reactivity tests were performed in batch experiments and particles were characterized using scanning electron microscopy (SEM), high-resolution transmission electron microscopy (HRTEM), X-ray diffraction (XRD) and Mössbauer spectroscopy.

2. Materials and methods

2.1. Chemicals and materials

Dry Nanofer Star powder supplied by NANO IRON, s.r.o. (Rajhrad, Czech Republic) was used for reactivity experiments. Nanofer Star particles were stored in the original packaging in the fridge for two months at maximum prior to use. Further chemicals used in these experiments are listed in SI.

2.1.1. Reactivity experiments

For batch experiments 42.2 ml vials (VWR) capped with Teflon Mininert valves (Sigma-Aldrich) were used as reactors. Anoxic batch experiments were prepared under argon (Ar) atmosphere, maintaining a water:headspace ratio of 1:1. As reaction media Millipore water and Ca–Mg–Na–HCO_3–SO_4–Cl groundwater with an ionic strength of 15 mM were used. Vials were shaken on a horizontal shaker at 160 spm and measured amounts of TCE and reaction products were corrected for overpressure and sampling induced headspace losses. CH_4 was used as internal standard to validate headspace loss measurements. The detailed correction procedure is described in SI. Three vials of each treatment were used for GC measurements and additional vials were used to measure changes in Fe^0 content, pH-value, redox potential (ORP(H)), dissolved oxygen, concentrations of dissolved Fe^{2+} and anion concentrations (Cl^-, F^-, NO_3^-, SO_4^{2-}, PO_4^{3-}).

The influence of environmental conditions was investigated with Fe^0 concentrations of 2.5 g l^{-1} Fe^0 where the Fe^0 concentration of Nanofer Star particles was around 58 ± 16% (w/w) and with initial TCE concentrations of 35 mg l^{-1}. Due to its high volatility about 30% of TCE were in the headspace of the vials (Henry constant at 22 ° C: 0.130 M/Atm according to Sander, 1999). The initial concentration in the aqueous phase was therefore about 25 mg l^{-1} and whenever TCE was degraded in the aqueous phase, TCE from the headspace was dissolved again until a new equilibrium was reached. Reported concentrations (mg l^{-1}) are the amount of total TCE (headspace + aqueous phase) related to the volume of the aqueous phase. Experimental conditions were varied (Table 1) and results were compared to a reference experiment in anoxic groundwater at 22 °C. These reference conditions were changed by using anoxic Millipore water (MQ), adding 50 mg l^{-1} ligninsulphonate (LS) or carboxymethylcellulose (CMC), reducing the reaction temperature to 12 °C and by using oxygen saturated water and headspace (21% O_2). Polyelectrolytes were dissolved in a groundwater stock-solution which was used subsequently as reaction medium. Fe^0 was added via a stock solution (50 g particles/200 ml water) into reaction vials after preparation of reaction vials and addition of TCE. To break up aggregates, Iron particles in stock solutions were mixed in deoxygenized Millipore water with a high-shear mixer at 15,500 rpm (Ultra-turrax® IKA T18, Germany) for 2 min under inert gas atmosphere. The iron stock solution was prepared directly before starting a reaction experiment. The concentration of Fe^0 was verified after addition via measurement of H_2 evolution by addition of HCl. Experiments under reference conditions, in Millipore water (MQ) and under oxic conditions (O2) were examined two times to verify reproducibility of obtained results. Reported reaction specific values represent pooled data of both batch experiments in the case of Reference and MQ conditions. Reported data of O_2 experiments represent those of the first batch experiment. Besides the influence of environmental conditions the influence of nZVI particle mass was investigated under reference conditions with 1.0, 2.5 and 4.6 g l^{-1} Fe^0 of particle mass.

2.1.2. Calculation of electron efficiencies, reaction rates and rate constants

The electron efficiency describes the fraction of electrons released during oxidation of Fe^0 that reacted with TCE and its reaction products (TCE electron efficiency, α) or with water to form H_2 (H_2 electron

Table 1
Overview of performed experiments to test the influence of environmental parameters.

Variation	Acronym	Polyelectrolyte [mg l^{-1}]	Oxygen status	Water type	Temperature [°C]	Fe^0 [g l^{-1}]
Reference	Ref	0	Anoxic	Groundwater	22	2.5
Ligninsulphonate	LS	**50**	Anoxic	Groundwater	22	2.5
Carboxymethylcellulose	CMC	**50**	Anoxic	Groundwater	22	2.5
Oxygen	O2	0	**Oxic**	Groundwater	22	2.5
Millipore	MQ	0	Anoxic	**Millipore**	22	2.5
Temperature	12 °C	0	Anoxic	Groundwater	**12**	2.5
Low nZVI mass	1.0 g/l	0	Anoxic	Groundwater	22	**1.0**
Medium nZVI mass[a]	2.5 g/l	0	Anoxic	Groundwater	22	2.5
High nZVI mass	4.6 g/l	0	Anoxic	Groundwater	22	**4.6**

[a] Same batches as reported under reference conditions.

efficiency, β). The efficiency calculation from Liu et al. (2005) was modified (Eqs. (1), (2) and (3)).

$$\epsilon TCE_{n+1} = \frac{([TCE_n] - [TCE_{n+1}]) * [e^-_{TCE}]}{\left(\left[Fe^0{}_n\right] - \left[Fe^0{}_{n+1}\right]\right) * \left[e^-_{Fe^0}\right]} \quad (1)$$

$$\epsilon H2_{n+1} = \frac{([H2_n] - [H2_{n+1}]) * \left[e^-_{H_2}\right]}{\left(\left[Fe^0{}_n\right] - \left[Fe^0{}_{n+1}\right]\right) * \left[e^-_{Fe^0}\right]} \quad (2)$$

$$e^-_{TCE} = \frac{\sum_i ni * pi}{\sum_i pi} \quad (3)$$

ϵTCE_{n+1} or $\epsilon H2_{n+1}$ TCE or H_2 electron efficiency during reaction period between two TCE or H_2 measurements n and n + 1.
TCE_n or $H2_n$ TCE or H_2 in a reaction vessel at reaction time n
TCE_{n+1} or $H2_{n+1}$ TCE or H_2 in a reaction vessel at reaction time n + 1
$Fe^0{}_n$ Fe^0 in a reaction vessel at reaction time n
$Fe^0{}_{n+1}$ Fe^0 in a reaction vessel at reaction time n + 1
e^-_{TCE} or $e^-_{H_2}$ or $e^-_{Fe^0}$ electrons consumed per TCE degraded (dependent on measured reaction products) or H_2 evolved ($2e^-/H_2$) or electrons derived from Fe^0 oxidized ($2.5e^-/Fe^0$)
n_i number of electrons needed to transform TCE into a specific endproduct (e.g. ethane = 6 e^-)
p_i moles of endproducts (ethane, ethene, ethine) generated

Reported TCE and H_2 electron efficiency values represent average values and standard deviations of single time period efficiencies (ϵTCE_{n+1} or $\epsilon H2_{n+1}$) for time intervals between two consecutive CHC and H_2 measurements and TCE concentrations between 5 and 25 mg l^{-1} in the water phase (stable reaction phase). Therefor data from all three replicates were merged. Further modifications were that H_2 efficiencies were calculated and that an average number of $2.5e^-$ was assumed to be released per oxidized Fe^0. Calculation of H_2 efficiencies enables balancing of TCE degradation and H_2 evolution to 100%. Assumption of $2.5e^-$ per Fe^0 were based on evolved Fe^{2+} and Fe^{3+} (hydr)oxides that were measured via Mössbauer Spectroscopy measurements l^{-1}.

Zero-order Fe^0-oxidation rates (k^0_{Fe}) and H_2-reaction rates ($k_{H_2,obs}$) as well as pseudo first-order TCE-reaction rate constants ($k_{TCE,obs}$) were calculated according to Eqs. (4)–(6), n representing the amount of Fe^0 [mg], H_2 [μmol] and TCE [μmol] in the reaction vessels at the times t1 and t2 [d]. n was calculated from linear regression curves (amount vs. time) for every specific time interval.

$$k_{Fe(0)} = \frac{n1-n2}{t2-t1} \quad \left[mg * d^{-1}\right] \quad (4)$$

$$k_{H2,obs} = \frac{n2-n1}{t2-t1} \quad \left[\mu mol * d^{-1}\right] \quad (5)$$

$$k_{TCE,obs} = -\left[\frac{\ln\left(\frac{C2}{C_1}\right)}{t2-t1}\right] \quad \left[h^{-1}\right]. \quad (6)$$

Surface-area-normalized rates and rate constants for TCE ($k_{TCE,SA}$) [$l*h^{-1}*m^{-2}$] and H_2 ($k_{H_2,SA}$) [$l*\mu mol*d^{-1}*m^{-2}$] were calculated based on observed reaction rates and rate constants (Eq. (4)), where a_s represents the specific surface area of the iron particles before reaction [m^2/g] and p_m the total amount of Fe in the reaction vessels [g l^{-1}]. The specific surface area of unreacted Nanofer particles is 20–25 m^2/g (Klimkova et al., 2011; Zhuang et al., 2012; Honetschlägerová et al., 2012 and the MSDS of NANO IRON, s.r.o.). Hence, 25 m^2/g were assumed for calculation of reaction rate constants.

$$k_{TCE,SA} \text{ or } k_{H2,SA} = \frac{k_{obs}}{a_s \times \rho_m} \quad (7)$$

Calculation of surface area normalized reaction rate constants were based on the initial surface area of 25 m^2/g that was obtained for Nanofer particles by Honetschlägerová et al. (2012), Klimkova et al. (2011) Zhuang et al. (2012) and the MSDS of NANO IRON, s.r.o.

For reaction kinetics, it is as well relevant that TCE is not fully available in the aqueous phase but that there is a reservoir in the non-reactive headspace. If TCE is degraded in the aqueous phase, TCE from the headspace dissolves again until a new equilibrium is reached. Thus, the reported rate constants for TCE degradation are values, which depend on the gas/liquid ratio. Real rate constants in the water phase therefore would be higher than the reported ones.

2.2. Analytical methods

Headspace samples were measured on a Carlo Erba GC 8000 Top GC provided with a flame ionization detector (FID) and a thermal conductivity detector (TCD). Chlorinated hydrocarbons (CHC), hydrocarbons and H_2 were measured simultaneously within one run. 100 μl headspace samples were injected manually on-column. Aqueous concentrations were calculated based on published Henry constant data (Sander, 1999). Solubility of carbon species and H_2 was considered according to the IFA (2013) database (IFA — Institut für Arbeitsschutz der Deutschen Gesetzlichen Unfallversicherung, 2013). Monitoring of

solution redox potential (ORP_H), pH-value and O_2 concentration of suspensions were measured following filtration with a syringe filter (<0.2 μm) in an Ar-filled glovebag. Detailed information on measurement methodology and calibration can be found in supporting information (SI).

Anion concentrations (Cl^-, F^-, NO_3^-, SO_4^{2-}, PO_4^{3-}) were analyzed via ion chromatography (for details see SI).

2.3. Iron characterization

The Fe^0 content of the reaction particles and the amount of Fe^0 in the reactors were determined by indirectly measuring the H_2 evolved during acidification of iron suspensions with HCl, followed by analyzing the total Fe content of acidified suspensions. The amount of dissolved total Fe in the reaction suspensions was measured at the end of reaction experiments: water samples were taken from the supernatant after sedimentation of particles and were immediately analyzed using a PerkinElmer Analyst 400 atomic absorption spectroscope (AAS).

Iron oxide species were identified using Mössbauer Spectroscopy (time mode arrangement, Halder Elektronik GmbH) and XRD (X-Ray Diffraction; Bruker D8 Advance, A25X1; Bruker Analytical X-ray Systems GmbH, Germany) analyses. Accordingly, samples from suspensions were prepared in an Ar-filled glovebag (see SI for details). Spatial distribution of oxygen, magnesium, calcium, iron (hydr-)oxides and iron before and after reactions was analyzed using HRTEM (high resolution transmission electron microscopy). For TEM analysis sample carrier grids were immersed in the suspensions and dried in N_2 filled exsiccators before analysis. Fresh, unreacted particle samples were therefore mixed with a high shear mixing according to section reactivity experiments and immediately sampled and dried.

3. Results

3.1. Particle characterization

Multiple measurements of the Fe^0 content of unused Nanofer Star particles revealed a mean value of 58 ± 16%. Mössbauer and XRD measurements of one specific Nanofer Star sample showed a content of 81% (Table 2). Relatively high Fe^0 content measured by Mössbauer spectroscopy can be explained by the fact that Mössbauer measurement was only conducted once with only 2 mg of particles what is not sufficient to rule out the possibility of errors caused by measurement of local Fe^0 agglomerations in the sample and minor measurement inaccuracies.

According to Klimkova et al. (2011), Zhuang et al. (2012) and Honetschlägerová et al. (2012) and the technical data sheets from NANO IRON s.r.o. the specific surface area of fresh Nanofer (Nanfoer 25, 25S and Star) particles is 20–25 m^2/g and the primary particle size is about 50 nm. HRTEM measurements showed a primary particle size of around 100 nm and particle aggregation of the primary particles before (Fig. S6) and after 6 days of reaction under reference conditions (Figs. S6 and S7). Furthermore EELS-line scans (electron energy loss spectroscopy) exhibited iron cores of primary particles surrounded by ~10 nm thick oxide shells, before and after reaction. The iron oxide shell of fresh, not reacted iron-particles consisted mainly of magnetite and partially of superparamagnetic goethite and traces of amakinite (Table 2). During oxidation under reference conditions (anoxic groundwater) mainly hydroxides amakinite and superparamagnetic goethite were formed (Table 2) whereas the percentage of magnetite of the total iron decreased slightly from 13% to 11%. About 6 ± 5 mg l^{-1} of dissolved Fe-ions (Fe^{2+} and Fe^{3+}) were detected (Fig. S8) with no significant differences between different experimental conditions and oxidation states of the particles. Compared to the amount of added Fe^0 (2.5 g l^{-1}) the proportion of detected Fe^{2+} in solution was rather low with a maximum equilibrium concentration of 5% of the consumed Fe^0 (Fig. S8).

3.2. Influence of environmental conditions

3.2.1. Changes in reaction rates and rate constants

Nanofer Star particles showed a lag phase during the first four to five days. TCE degradation was slower in this lag phase followed by an accelerated degradation showing a pseudo first order TCE kinetics (Figs. 1 and 3). Graphs show the TCE concentrations which were measured and corrected for losses of TCE due to sampling and H_2 induced overpressure as explained in SI in detail. So the shown values are higher than the measured concentrations since they also contain the lost TCE. Since the amount of lost TCE accounted for about 0.2–0.4 μmol (depending on H_2 evolution), the calculated values in Fig. 1 cannot be smaller than these values, although the measured concentrations were much lower (e.g. 0.05 ± 0.07 μmol in Ref 1 on day 21).

Addition of polyelectrolytes, addition of dissolved oxygen, the use of Millipore water instead of groundwater and a reduction of the reaction temperature caused decreasing zero order H_2 reaction rates and decreasing pseudo first order TCE reaction rate constants ($\alpha = 0.05$ Scheffé post-hoc test). Temperature reduction from 22 °C to 12 °C reduced H_2 reaction rates and TCE reaction rate constants by a factor of 3.04 (for H_2) and 2.44 (for TCE) which is consistent with expected temperature induced decelerated reactivity of a factor of 2–4 per 10 °C according to the Van't Hoff equation (Gramatke, 2013). The H_2 reaction rate of the reference (0.70 ± 0.03 $l*\mu mol*d^{-1}\ m^{-2}$) was decreased to 79% (for addition of ligninsulphonate) and 14% (for Millipore water). The TCE reaction constant of the reference (0.15 ± 0.02 $l*h^{-1}\ m^{-2}$) was decreased to 60% (for addition of ligninsulphonate) and to 26% (for Millipore water) (Fig. 2I, II). Iron oxidation rates decreased similarly as did TCE rate constants and H_2 rates (Table S1). Dissolved oxygen inhibited TCE degradation and hindered reaction reproducibility. Reactivity under oxic conditions was tested in two independent batch experiments (three replicates each). In the first batch experiment (Batch 1) TCE was not degraded and no H_2 was generated in the first 10–15 days (Fig. 3I). Only after the oxygen was consumed degradation of TCE started. In Batch 2 no degradation and negligible hydrogen generation (≤2 μmol) were observed within 22 days whereby Fe^0 cores were not oxidized.

The reduction potential under oxic conditions in batch 2 showed a similar trend as in batch 1 although particles were passivated, so eventually pH dropped due to reaction with O_2. In general ORPs were unstable, with potentials fluctuating within single vials in the range of −300 mV_H.

The reaction in anoxic Millipore water (MQ) and in oxic groundwater (O_2) also showed two phases. In Millipore water after a comparable long lag-phase of 14 days with a slower TCE degradation and H_2

Table 2
Chemical composition of Nanofer Star particles before and after reaction under reference conditions (anoxic groundwater at room temperature) measured by XRD and Mössbauer spectroscopy.

	Iron	Magnetite	Goethite superpar.	Amakinite	Magnetite	Goethite superpar.	Amakinite
	Fe^0	Fe_3O_4	FeO(OH)	$Fe(OH)_2$	Fe_3O_4	FeO(OH)	$Fe(OH)_2$
	[%] of total iron				[%] of Iron(hydr)oxides only		
Fresh particles	**81**	13	5	1	**69**	**28**	3
Oxidized particles	**42**	11	25	22	20	**43**	**37**

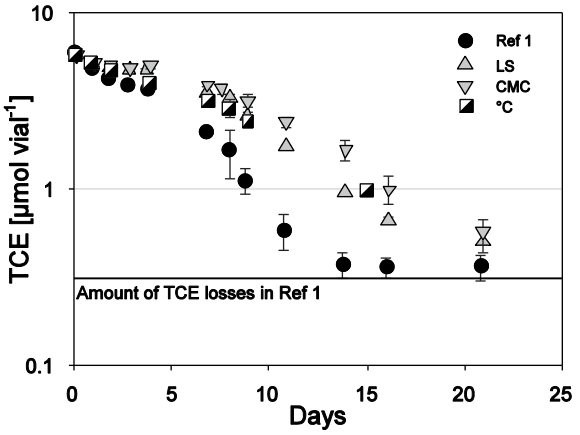

Fig. 1. TCE degradation under reference conditions (Ref 1), in combination with the polyelectrolytes ligninsulphonate (LS) and carboxymethylcellulose (CMC) and under reduced reaction temperature (12 °C). Error bars represent standard deviation of three replicates.

evolution reactivity finally increased (Fig. 3). Under oxic conditions the start of reactivity was delayed. The delayed start under oxic conditions and the start of the increasing reactivity in Millipore water were accompanied with a decreasing redox potentials (ORP) (Fig. 3 II). Under other environmental conditions the redox potentials alternated around -300 mV_H with the exception of reactions under oxic conditions (Table S1). Furthermore reactivity in Millipore water was associated with a decline in the pH-value to about 6 (see Fig. S2).

The pH-values increased under all conditions in groundwater from 8.4 ± 0.2 to 8.8 ± 0.1 within the first 10 days of reaction whereas those in Millipore water decreased from 8.8 to 6.1 Detailed pH and ORP data are given in Fig. 4 and Table S1.

3.2.2. Electron use efficiency

Selectivity with respect to TCE was not affected by the environmental conditions investigated in our experiments ($\alpha = 0.05$ Scheffé post-hoc test) Independent of environmental conditions TCE electron efficiencies were about 3.1 ± 1.4% (Fig. 2 III). Compared to previously tested particle types these values are rather low, as e.g. RNIP particles (Toda Kogyo) were reported to utilize about 50% of its electron capacity for degradation of TCE (Berge and Ramsburg, 2010; Liu et al., 2005). Complementary to this about 100 ± 50% of electrons that were released from zero valent iron reduced H^+ to H_2 (Fig. 2 IV). These relatively broad ranges of the standard deviation result from natural deviations of the replicates, from assumptions that have to be made for calculation of electron efficiencies, namely steady Fe^0 oxidation with a fixed amount of $2.5e^-$ released per Fe^0 oxidized and to a lesser extent from inaccuracies of Fe^0, TCE and H_2 measurements. Deviations are discussed

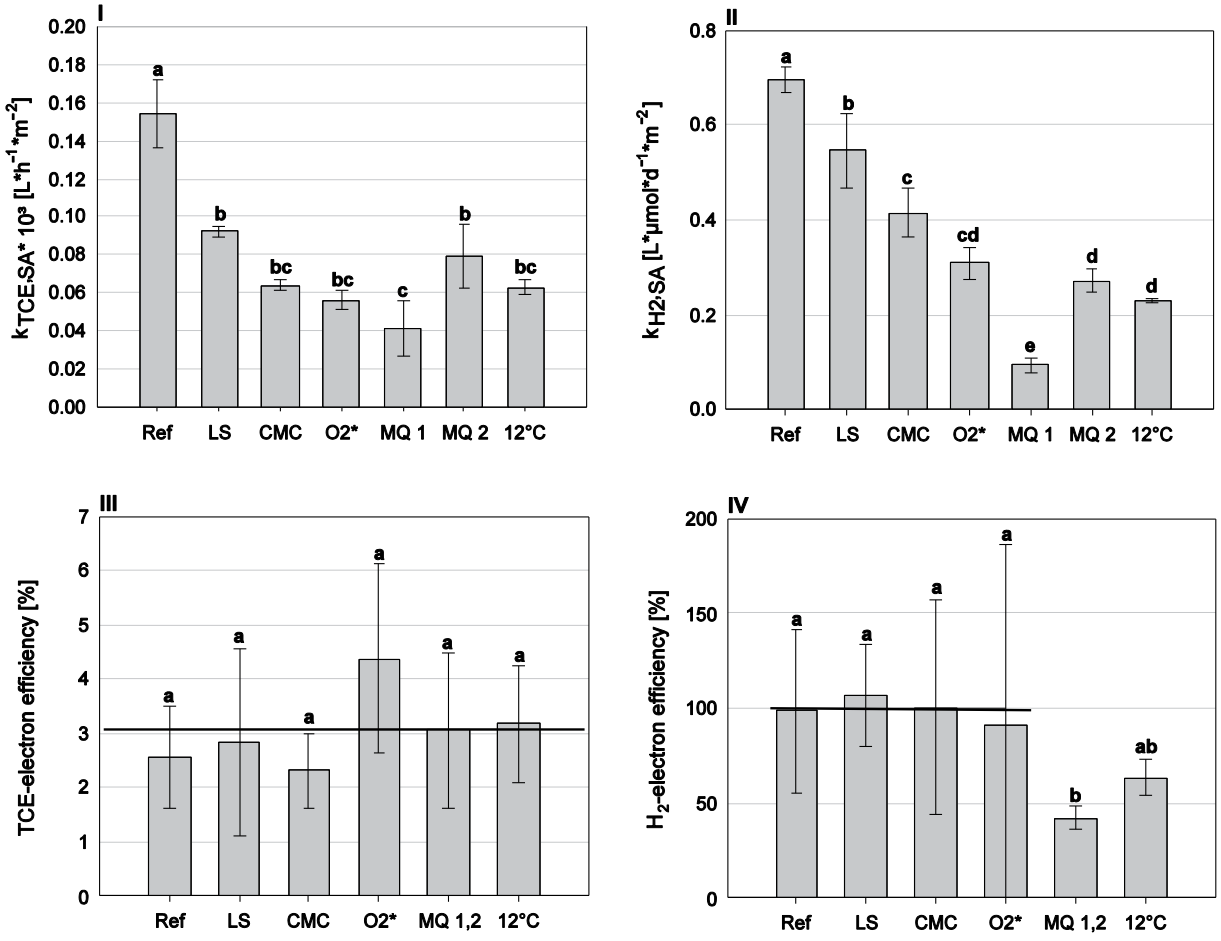

Fig. 2. Surface area normalized reaction rate constants (original specific surface) of (I) TCE and (II) H_2 and electron efficiencies of (III) TCE and (IV) H_2 under different conditions. Reference conditions (Ref), 50 mg l^{-1} ligninsulphonate (LS) or carboxymethylcellulose (CMC), oxic conditions (O2), Millipore water (MQ) and reduced temperature (12 °C). Straight horizontal lines above bars represent the mean value of these bars. MQ 1 and MQ 2 represent two stable reaction phases. MQ 1 values are pooled data from two batch experiments under equal conditions (first days of reaction). MQ 2 values are data from one of these two experiments that was implemented for a longer period of time. Electron-efficiencies were averaged because there was no difference between phase 1 and 2. Error bars represent standard deviation of three replicates. Different letters (a, b, c and d) above bars indicate statistically significant differences between respective bars ($\alpha = 0.05$ Scheffé post-hoc test). * Reaction rate constants and electron efficiencies in vials containing O_2 were calculated after consumption of oxygen and with the start of the subsequent TCE degradation and H_2 evolution.

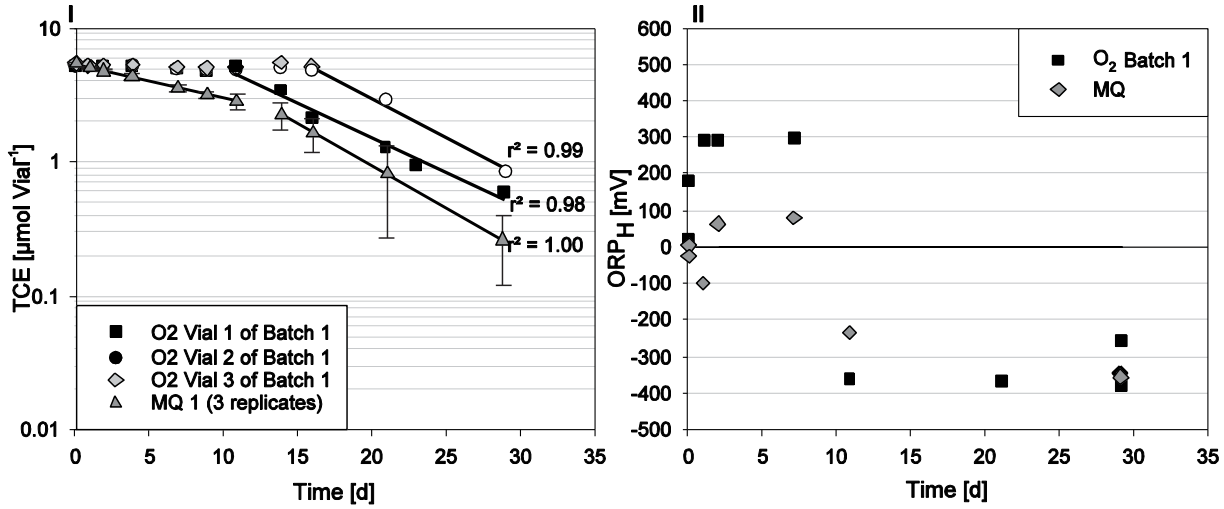

Fig. 3. Development of (I) TCE concentration under oxic conditions in vials 1, 2 and 3 of batch 1 and in Millipore water (MQ) (3 replicates) and development of (II) oxidation-reduction potential (ORP) under oxic conditions (Batch 1) and in Millipore water (MQ). Error bars represent standard deviation of three replicates.

in more detail in the discussion section. TCE degradation and H_2 evolution together consumed only 43% of released electrons in Millipore water and about 67% under reduced temperature (12 °C). What the remaining 57% and 33% of electrons reacted with under these environmental conditions cannot be explained on the basis of the parameters we measured. The TCE electron efficiency was independent if the TCE concentration (total TCE per volume of aqueous phase) was between 5 and 25 mg l^{-1} (Fig. S3). These concentrations amounted to real concentrations of 3.5 and 17.5 mg l^{-1} of TCE in the aqueous phase. As soon as the TCE concentration in the aqueous phase fell below 3.5 mg l^{-1}, TCE electron efficiencies fell proportionally with TCE concentration. In the frame of the experiment with 4.6 g/l Fe^0 TCE was added a second time after complete dehalogenation of initial TCE. In this case TCE electron efficiencies were around 14% in the beginning (TCE 17.5 mg l^{-1}) and fell proportionally with TCE concentration from the very beginning of the reactivity experiment.

3.2.3. Reaction products

The two major reaction products after dehalogenation of ≥ 71% of initial TCE were ethene with 73 ± 4% and ethane with 26 ± 4% (mol%) independent of environmental conditions (Table 3). As TCE disappeared, ethene was increasingly transformed to ethane. A fraction of 24 ± 3% of measured peak areas were not identified whereby obtained C-balances of 86 ± 5% (after dehalogenation of >90% of initial TCE) could be explained. Vinyl chloride was not detected (limit of detection 0.02 mg l^{-1}) and dichloroethenes were identified at minor concentrations around 0.05–0.2 mg l^{-1} near their detection limits.

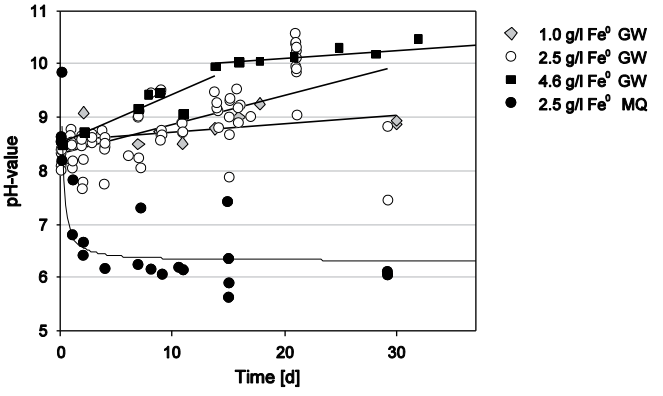

Fig. 4. Development of pH-values with different iron mass loadings in groundwater (GW) and with 2.5 g/l Fe^0 particle mass in Millipore water (MQ).

3.2.4. Evolution of NO_3^-, SO_4^{2-} and Cl^- concentrations in the suspensions

Nitrate (initial concentration of 12 mg l^{-1}) was no more detectable after 2 days under reference conditions, after 3 days at reaction temperature of 12 °C and within 7 days under oxic conditions. SO_4^{2-} was only slightly reduced in our experiments (Fig. S4). Thus NO_3^- reduction to NH_4 represented a remarkable competition reaction to TCE dehalogenation while SO_4^{2-} was not reduced by iron particles. NO_3 can occur in aquifers at very high concentrations, therefore NO_3 can cause remarkable iron depletion since it reacts faster than TCE, requires 8 electrons for complete reduction to NH_3/NH_4 and will not be depleted in the aquifer. In our test system nitrate reduction was about 12 mg in 2 days in 1 l of water what equals about 100 µmol/d. Simultaneously Fe^0 was depleted with a rate of about 2200 µmol/d. Accordingly, nitrate reduction accounted for about 4–5% of iron depletion. Assuming constant and higher NO_3 concentration this value might be much higher within the plume of real sites. Cl^- concentrations increased as TCE was dehalogenated showing a significant correlation (Fig. S5). Initial Cl^- concentrations in groundwater suspensions containing iron particles were slightly lower than in suspensions without iron particles (Fig. S5a). Measured Cl^- evolution in groundwater suspensions was higher than Cl^- release calculated on the basis of measured TCE dehalogenation if initial Cl^- concentration of iron containing suspensions was set as total initial amount of Cl^- within the vessel (Fig. S5b). To the contrary in Millipore water the measured Cl^- concentration was lower than the concentration calculated from TCE dehalogenation (Fig. S5b).

3.3. Influence of nZVI concentration

Observed TCE reaction rate constants and H_2 reaction rates (k_{obs}) increased linearly with the initial mass of nZVI (Fig. 5 I). Upon surface area normalization (k_{SA}), the influence of nZVI mass on TCE reaction rate constants disappeared and H_2 reaction rates decreased slightly with increasing nZVI content (Fig. 5 II) ($\alpha = 0.05$ Scheffé post-hoc test) from 0.75 $l*\mu mol*d^{-1}*m^{-2}$ (1 g l^{-1} Fe^0) to 0.60 $l*\mu mol*d^{-1}*m^{-2}$ (4.6 g l^{-1} Fe^0). The iron oxidation rate rose from 1.3 mg d^{-1} to 3.1 ± 0.9 mg d^{-1} if nZVI mass was increased from 1.0 to 2.5 g l^{-1} Fe^0, but showed no further increase, if Fe^0 mass was increased from 2.5 to 4.6 g l^{-1} Fe^0. Thus TCE and H_2 electron efficiencies at nZVI loadings of 1.0 and 2.5 were similar whereas if Fe^0 loading was 4.6 g l^{-1} electron efficiencies increased from 2.8 ± 1.1% to 5.5 ± 0.6% (TCE) and from

Table 3
Reaction products of batch experiments under different environmental conditions: percent of ethene, ethine and ethane whereby unidentified peaks were neglected. Values: mean ± standard deviation (n = 3). Detailed description of variations can be found in Table 1 of the main publication. Batch experiments of "Ref" and "MQ" were implemented two times. Ref 1 and MQ 1 represent the first of the two batch experiments implemented. Ref 2 represents the second experiment.

Variation	Acronym	Reaction products			Reaction time	TCE dehalogenated[a]
		Ethene	Ethine	Ethane		
		[% µmol]	[days]	[%]		
Reference 1	Ref 1	69 ± 1	0 ± 0	31 ± 1	13.8	94 ± 1
Reference 2	Ref 2	72 ± 0	0 ± 0	28 ± 0	8.9	93 ± 0
Ligninsulphonate	LS	73 ± 0	0 ± 0	27 ± 1	13.9	88 ± 1
Carboxymethylcellulose	CMC	75 ± 0	1 ± 0	24 ± 0	13.9	71 ± 4
Oxygen	O2	77 ± 1	0 ± 0	23 ± 1	29.0	86 ± 4
Millipore 1	MQ 1	79 ± 1	1 ± 1	20 ± 1	21.0	85 ± 10
Temperature	12 °C	74 ± 0	0 ± 0	26 ± 0	15.0	83 ± 1
Low nZVI mass	1.0 g/l	74 ± 0	0 ± 0	26 ± 0	13.8	74 ± 1
Medium nZVI mass[a]	2.5 g/l	69 ± 1	0 ± 0	31 ± 1	13.8	94 ± 1
High nZVI mass	4.6 g/l	70 ± 1	0 ± 0	30 ± 1	8.7	96 ± 0

[a] [%] values represent TCE dehalogenated from originally measured amount of TCE in the vials [C/C_0]. At this it has to be kept in mind that TCE losses due to sampling and H_2 induced overpressure do not count as dehalogenation. Hence values of around 95% mean that there is almost 0% of originally TCE left in the vials. A detailed description of correction for headspace losses can be found in SI.

nearly 94 ± 43% to overstoichiometric 170 ± 23% (H_2). Mechanisms that led to overstoichiometric H_2 evolution in the case of higher nZVI concentration remained unclear. The rise of pH-values was accelerated as nZVI mass was increased, complementary TCE degradation was increased. So within the period at which rates, rate constants and efficiencies were calculated pH-values were similar (~8.7) between different nZVI loadings (Table S1). Data of the reaction experiment with 2.5 g l^{-1} are the same as reported in section Influence of environmental conditions as reference conditions.

4. Discussion

4.1. Mechanism

All tested amendments and environmental conditions decreased reaction rates and reaction rate constants compared to reference conditions. The mechanisms of electron transfer seemed to be independent of conditions. This assumption is supported by the observation that no differences were obtained regarding reaction products, TCE electron efficiencies and dissolved iron concentrations between different conditions. Adsorption of TCE and H^+ is assumed to be an important process that determines particle reactivity. This process is primarily dependent on structural properties like preferential orientation, iron impurities such as sulfide inclusions (Butler and Hayes, 1998, 2001; He et al., 2010; Kim et al., 2011, 2013; Lee and Batchelor, 2002; Park et al., 2006; Uegami et al., 2003; Weerasooriya and Dharmasena, 2001), structural defects (Gotpagar et al., 1999; Luo et al., 2010) of the surface and iron oxide types in the particle shell. Adsorption properties may be related to the surface hydrophobicity, which can be monitored by contact angle measurements. Thus selectivity of Nanofer Star particles is particle intrinsic but not significantly influenced by changes in reaction conditions in our experiment. Particle synthesis and potential particle modifications may be more important than environmental conditions within the investigated ranges. Accordingly previous studies showed great differences of reactivity between particle types (Su and Puls, 1999). Previously tested RNIP nZVI particles showed much higher TCE reaction rate constants (Liu et al., 2005, 2007; Liu and Lowry, 2006) and much higher selectivity regarding TCE (Berge and Ramsburg, 2010; Liu et al., 2005). Of course it has to be mentioned that other environmental conditions than tested here may influence reactivity to a greater extent. Such conditions could be for example the presence of other metals (Doong and Lai, 2006) in the aquifer. Furthermore reaction characteristics may change in the long-term, as indicated by rising k_{TCE} and k_{H_2} after 14 days in Millipore water. Cl^- ions that were released via dehalogenation of TCE could be balanced with measured increase of Cl^- ions in the reaction vessels. In cases that Cl^- evolution was slightly higher than TCE degradation (Fig. S5) this may have been due to Cl^- particle sorption at the start of incubation followed by a partial release of sorbed Cl^-. In Millipore water right at the start released Cl^- ions may have been adsorbed and as sorption sites were saturated Cl^-

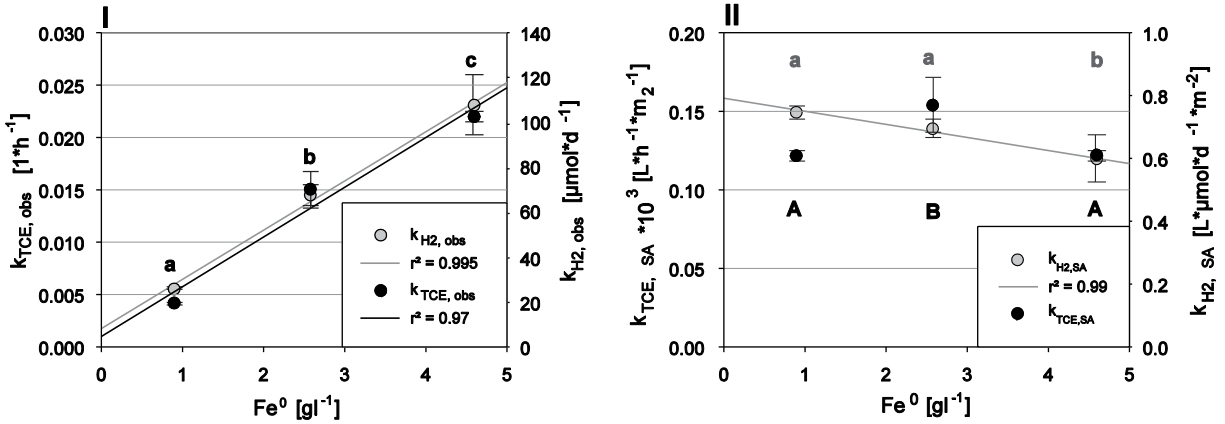

Fig. 5. (I) Observed TCE and H_2 reaction rate constants (k_{obs}) and (II) surface area normalized reaction rate constants (k_{SA}) according to particle mass in the system. Error bars represent standard deviation of three replicates. In (I) a, b and c represent statistically different groups (α = 0.05 Scheffé post-hoc test). In (II) small letters (a, b, c) were used for $k_{TCE,SA}$ and capital letters (A, B, C) were used for $k_{H_2,SA}$.

evolution balanced TCE dehalogenation. A considerable co-precipitation of TCE together with the build-up of iron oxides as proposed by Noubactep (2009) can therefore be neglected.

Mechanisms by which electron transfer was hindered may be different for various environmental conditions. Summed TCE and H_2 electron efficiencies showed relatively high standard deviations but accounted for about 100% of released electrons with the exceptions of reactions in Millipore water (67%) and reactions under temperature reduced conditions (43%). Relatively high standard deviations of electron efficiencies as well as lacking electrons in the balances of Millipore water and temperature reduced conditions can at least partially be explained. For calculation of efficiency it was assumed that the same iron (hydr)oxides were formed in Millipore water and under low temperature conditions as those which were observed under reference conditions by Mössbauer and XRD measurements. Furthermore it was assumed that identified reaction products are representative for electron absorption per dehalogenated TCE. Hence the gap to 100% can at least partially be explained if preferentially Fe^{2+} (hydr)oxides were built up instead of Fe^{3+} (hydr)oxides as amakinite and goethite that were built-up under reference conditions. The amount of iron that was dissolved during reactions was negligible. Furthermore Fe(0) measurements showed remarkable deviations. Even though the influence of one of these factors may be negligible, the sum of them causes rather high deviations. Type and amount of unidentified reaction products did not differ between conditions and therefore are unlikely to be responsible for the missing electrons. Finally the reason for missing electrons and the mechanisms of electron transfer remain in question under reduced temperature and in Millipore water.

4.2. Influence of ionic strength on reactivity

In groundwater (15 mM ionic strength) we observed increased particle reactivity compared to reactivity in Millipore water. With previously investigated (RNIP) particles it was generally assumed that high ionic strengths generated passivating shells (Bi et al., 2009; Liu et al., 2007; Reinsch et al., 2010; Yu et al., 2012) compared to reaction in deionized water and only low ionic strength caused removal of passivating (hydr)oxide shells (Bi et al., 2009). Furthermore presence of Ca^{2+} can lead to particle agglomeration of Nanofer particles (Dong and Lo, 2013). Hence previous studies obtained increased reaction rate constants only if NO_3^-, $CaCO_3$ and $NaHCO_3$ were present in the solution at concentrations <1 mM (D'Andrea et al., 2005; H.-S. Kim et al., 2014; Liu et al., 2007). Studies that tested suspensions with 5 and 10 mM Cl^-, SO_4^{2-}, HCO_3^-, NO_3^-, and HPO_4^{2-} and 1 mM KNO_3^- showed reduced reaction rate constants by factors between 1.4 and 7 (D'Andrea et al., 2005; Liu et al., 2007; Reinsch et al., 2010). NO_3^- at concentrations of 5 and 10 mM is known to be capable of stopping particle oxidation completely (Liu et al., 2007; Reinsch et al., 2010). Natural groundwater with different ionic strengths decreased TCE reaction rate constants by a factor of 3.5 (5 mM) and 7.4 (15 mM) (Liu et al., 2007). Besides TCE reaction rate constants also the types of formed iron (hydr)oxides of Nanofer Star particles differed in comparison to other iron particles. In Nanofer Star particles reacting in groundwater mainly amakinite and goethite were formed. In the shell of RNIP particles on the other hand mainly schwertmannite was found if the reaction took place in 10 mM NO_3^- and 10 mM SO_4^{2-} suspensions (Reinsch et al., 2010) and magnetite (Reinsch et al., 2010) or magnetite/maghemite (Nurmi et al., 2005), if they reacted in deionized water. Particle shells of other nZVI particle types transformed in pH 8 buffered (HEPES buffer) suspensions with 5, 25 and 100 mM Cl^-, SO_4^{2-}, ClO_4^-, NO_3^-, and HCO_3^- to magnetite independent of ionic strength (Xie and Cwiertny, 2012). So the transformation of the particle shell seems to be particle dependent that could explain the reaction characteristics of Nanofer Star particles which differ from other nZVI particles. Nitrate was reduced immediately; hence high NO_3^- concentrations have the potential to be electron consumptive besides the fact that NO_3^- can passivate particles.

To sum up, contrary to previously studied particles, high ionic strength seems not to adversely affect particle applicability of Nanofer Star particles.

4.3. Influence of polyelectrolytes on reactivity

Application of polyelectrolytes may be indispensable if particles are injected at field scale applications to improve particle mobility (Johnson et al., 2009; Schrick et al., 2004; Tiraferri and Sethi, 2008; Zhan et al., 2009). 50 mg l^{-1} ligninsulphonate and carboxymethylcellulose reduced particle reactivity significantly which is consistent with previous studies (Chen et al., 2011; Doong and Lai, 2006; Tratnyek et al., 2001). Probably that was because organics adsorb on ZVI particles (Johnson et al., 2009; Tratnyek et al., 2001), whereby reactive sites got partially blocked (Tratnyek et al., 2001) and the electron transfer was reduced (Bouayed et al., 1998). Merely quinones are known to be capable of increasing electron transfer (Doong and Lai, 2006; Tratnyek et al., 2001; Xie and Shang, 2005). To our knowledge solely Tsang et al. (2009) found increased reactivity due to addition of 20 mg l^{-1} of various humic acids. Even if polyelectrolytes reduced reactivity, they did not reduce particle selectivity that makes the application of polyelectrolytes favorable to improve particle mobility.

4.4. Influence of dissolved oxygen on reactivity

Dissolved oxygen reduced reactivity and finally fully prevented particle reaction with TCE in the case of 4 of 6 replicates. Although the amount of Fe^0 (0.95 mmol Fe^0) was clearly overstoichiometric in respect to oxygen (0.17 mmol O_2). Probably a small, not measurable part of Fe^0 was oxidized and caused reduced reactivity or passivation by fast particle oxidation that hindered Fe^{2+} diffusion leading to the build-up of a passivating layer of iron oxides as supposed by Xie and Cwiertny (2010) who obtained particle passivation induced by dissolved oxygen at pH-values > 8 but not at pH-values between 6 and 7. According to Nagayama and Cohen (1962) and Tamura (2008) even thin passivating films (1-3 nm) can build up in aqueous solutions which prevent further corrosion. RNIP particles were oxidized up to 98% if suspensions were aerated (p_{O_2} = 0.21 bar) for 24 h (Reinsch et al., 2010). So besides the fact that dissolved oxygen causes electron depletion it is able to passivate particles. Hence, for application of nZVI particles in oxygen containing aquifers pre-treatment of oxygen is indispensable.

4.5. Influence of reaction temperature on reactivity

A reduction of reaction temperature from 22 °C to 12 °C reduced reaction rates and rate constants by a factor 2–3 as well as nitrate reduction. This is consistent with the expected temperature induced decelerated reactivity according to Van't Hoff equation (Gramatke, 2013). Furthermore potentially increased particle aggregation (Yang et al., 2002) may have lowered the reactivity. Summed TCE and H_2 electron efficiencies accounted for 67% of released electrons. Efficiencies were calculated based on formed (hydr)oxides under reference conditions (at 22 °C). Electron efficiencies would account for 79 ± 12% if preferentially Fe^{2+} (hydr)oxides were built-up at 12 °C instead of assumed Fe^{2+} (Amakinite), $Fe^{2,66+}$ (Goethite) and Fe^{3+} (Goethite) (hydr)oxides. So potential differences in formed iron (hydr)oxides cannot completely explain missing electrons in the electron balance and what the remaining 33% of electrons reacted with under these environmental conditions was not figured out.

4.6. Influence of TCE concentration

At TCE concentrations <3.5 mg l^{-1} TCE specific selectivity decreased proportionally with TCE concentration (Fig. S3). Low selectivities at low TCE concentrations probably inhibit achievement of target

concentrations for remediation through solely application of Nanofer Star particles without additional measures such as combination with biological remediation (Fernandez-Sanchez et al., 2004; Lacinová et al., 2013; Rosenthal et al., 2004; Wang and Tseng, 2009; Xiu et al., 2010) or particle modification (Long and Ramsburg, 2011; Mackenzie et al., 2012; Zhan et al., 2009).

4.7. Influence of nZVI mass

Increasing nZVI mass did not influence surface area normalized reaction rates and rate constants, nor did it influence selectivity. But longevity was increased. Hence injection of higher nZVI mass loadings may prolong periods between injections and therefore may perhaps reduce costs but is not expected to influence remediation efficiency. In this respect it has to be mentioned that spatial limitations in the pore space may limit the injection of higher nZVI mass loadings especially in fine-pored aquifers.

5. Conclusion

All tested amendments and environmental conditions (decreased ionic strength, addition of polyelectrolytes, addition of O_2 and decreased temperature) decreased TCE and H_2 reaction rates but not particle selectivity. Selectivity seemed to be particle intrinsic, so particle synthesis and particle modifications may influence TCE dehalogenation efficiency more than the tested environmental conditions. NO_3^- and O_2 consumed electrons while SO_4^{2-} was not reduced by nZVI, so high NO_3^- and O_2 concentrations may decrease dehalogenation efficiency. In many tests oxygen even caused total particle passivation that may be caused by a very fast build-up of a thick passivating layer. These results cannot be transferred into field directly due to numerous possible environmental conditions on different sites that may change particle reactivity and which were not tested within this study. But they strongly indicate that particle synthesis or particle modification may influence remediation success stronger than tested environmental parameters.

In general electron efficiency of Nanofer Star particles was low. Merely about 3% of released electrons reacted with TCE and this percentage further decreased as TCE concentration decreased. At these selectivities achievement of target concentrations for remediation through solely application of Nanofer Star particles seems very difficult to achieve. But high H_2 evolution and known interactions of iron (hydr)oxides with microbiology indicate a potential for combination of Nanofer Star particles with biological degradation. For instance nZVI could be used as remediation technology that additionally triggers biological degradation. In specific if additional measures are taken to enhance biological degradation simultaneously.

Acknowledgment

This research was funded by the Federal Ministry of Agriculture, Forestry, Environment and Water Management of Austria (B020004). The authors want to thank Karl Moder (BOKU — University of applied life science, Institut für Angewandte Statistik und EDV, Vienna, Austria) for statistical consultancy and Lisa Pum for support in the lab. Furthermore we want to thank Frank-Dieter Kopinke, Katrin Mackenzie and Steffen Bleyl (Helmholtz-Centre for Environmental Research, Department Environmental Engineering) for numerous discussions. The research was funded by the Austrian Federal Ministry of Agriculture, Forestry, Environment and Water (BMLFUW); Management by Kommunalkredit Public Consulting (KPC) (Proj. Nr.: B020004).

Appendix A. Supplementary data

Description of analytical methods (Ion chromatography and HRTEM measurements). Obtained iron oxidation rates pH values and redox conditions at different reaction conditions. Representation of two stable reaction phases in reactions with Millipore water. Influence of TCE concentration on TCE electron efficiency. Development of Anion concentrations during dehalogenation. Particle characterization: TEM analysis and monitoring of dissolved Fe^{2+} concentrations.

References

Arnold, W.A., Roberts, A.L., 2000. Pathways and kinetics of chlorinated ethylene and chlorinated acetylene reaction with Fe(0) particles. Environ. Sci. Technol. 34, 1794–1805. http://dx.doi.org/10.1021/es990884q.

Berge, N.D., Ramsburg, C.A., 2010. Iron-mediated trichloroethene reduction within non-aqueous phase liquid. J. Contam. Hydrol. 118, 105–116. http://dx.doi.org/10.1016/j.jconhyd.2010.07.006.

Bi, E., Bowen, I., Devlin, J.F., 2009. Effect of mixed anions (HCO_3^-–SO_4^{2-}–ClO_4^-) on granular iron (Fe 0) reactivity. Environ. Sci. Technol. 43, 5975–5981. http://dx.doi.org/10.1021/es900599x.

Bouayed, M., Rabaa, H., Srhiri, A., Saillard, J.-Y., Bachir, A.B., Beuze, A.L., 1998. Experimental and theoretical study of organic corrosion inhibitors on iron in acidic medium. Corros. Sci. 41, 501–517. http://dx.doi.org/10.1016/S0010-938X(98)00133-4.

Butler, E.C., Hayes, K.F., 1998. Effects of solution composition and pH on the reductive dechlorination of hexachloroethane by iron sulfide. Environ. Sci. Technol. 32, 1276–1284.

Butler, E.C., Hayes, K.F., 2001. Factors influencing rates and products in the transformation of trichloroethylene by iron sulfide and iron metal. Environ. Sci. Technol. 35, 3884–3891. http://dx.doi.org/10.1021/es010620f.

Chen, J., Xiu, Z., Lowry, G.V., Alvarez, P.J.J., 2011. Effect of natural organic matter on toxicity and reactivity of nano-scale zero-valent iron. Water Res. 45, 1995–2001. http://dx.doi.org/10.1016/j.watres.2010.11.036.

Choe, S., Lee, S.-H., Chang, Y.-Y., Hwang, K.-Y., Khim, J., 2001. Rapid reductive destruction of hazardous organic compounds by nanoscale Fe^0. Chemosphere 42, 367–372. http://dx.doi.org/10.1016/S0045-6535(00)00147-8.

Cwiertny, D.M., Roberts, A.L., 2005. On the nonlinear relationship between k_{obs} and reductant mass loading in iron batch systems. Environ. Sci. Technol. 39, 8948–8957. http://dx.doi.org/10.1021/es050472j.

D'Andrea, P., Lai, K.C.K., Kjeldsen, P., Lo, I.M.C., 2005. Effect of groundwater inorganics on the reductive dechlorination of TCE by zero-valent iron. Water Air Soil Pollut. 162, 401–420.

Dolfing, J., Van Eekert, M., Seech, A., Vogan, J., Mueller, J., 2008. In situ chemical reduction (ISCR) technologies: significance of low Eh reactions. Soil Sediment Contam. 17, 63–74. http://dx.doi.org/10.1080/15320380701741438.

Dong, H., Lo, I.M.C., 2013. Influence of calcium ions on the colloidal stability of surface-modified nano zero-valent iron in the absence or presence of humic acid. Water Res. 47, 2489–2496. http://dx.doi.org/10.1016/j.watres.2013.02.022.

Doong, R., Lai, Y., 2006. Effect of metal ions and humic acid on the dechlorination of tetrachloroethylene by zerovalent iron. Chemosphere 64, 371–378. http://dx.doi.org/10.1016/j.chemosphere.2005.12.038.

Eglal, M.M., Ramamurthy, A.S., 2014. Nanofer ZVI: morphology, particle characteristics, kinetics, and applications. J. Nanomater. 2014, 1–11. http://dx.doi.org/10.1155/2014/152824.

Elliott, D.W., Zhang, W., 2001. Field assessment of nanoscale bimetallic particles for groundwater treatment. Environ. Sci. Technol. 35, 4922–4926. http://dx.doi.org/10.1021/es0108584.

Fernandez-Sanchez, J.M., Sawvel, E.J., Alvarez, P.J.J., 2004. Effect of Fe^0 quantity on the efficiency of integrated microbial-Fe^0 treatment processes. Chemosphere 54, 823–829. http://dx.doi.org/10.1016/j.chemosphere.2003.08.037.

Gotpagar, J., Lyuksyutov, S., Cohn, R., Grulke, E., Bhattacharyya, D., 1999. Reductive dehalogenation of trichloroethylene with zero-valent iron: surface profiling microscopy and rate enhancement studies. Langmuir 15, 8412–8420. http://dx.doi.org/10.1021/la990325x.

Gramatke, S., 2013. ANORGANISCH: Einstieg in die anorganische Chemie. epubli GmbH.

He, Y.T., Wilson, J.T., Wilkin, R.T., 2010. Impact of iron sulfide transformation on trichloroethylene degradation. Geochim. Cosmochim. Acta 74, 2025–2039. http://dx.doi.org/10.1016/j.gca.2010.01.013.

Honetschlägerová, L., Janouskovcová, P., Soffer, Z., 2012. Nanoscale zero valent iron coating for subsurface application. Presented at the Proceedings of the 4th international conference NANOCAN 2012, "NANOCAN 2012" Proceedings of the 4th international conference, Brno, Czech Republic.

IFA — Institut für Arbeitsschutz der Deutschen Gesetzlichen Unfallversicherung, 2013. GESTIS Stoffdatenbank [WWW Document]. GESTIS Stoffdatenbank (URL http://gestis.itrust.de (accessed 10.28.13)).

Johnson, R.L., Johnson, G.O., Nurmi, J.T., Tratnyek, P.G., 2009. Natural organic matter enhanced mobility of nano zerovalent iron. Environ. Sci. Technol. 43, 5455–5460. http://dx.doi.org/10.1021/es900474f.

Johnson, R.L., Nurmi, J.T., O'Brien Johnson, G.S., Fan, D., O'Brien Johnson, R.L., Shi, Z., Salter-Blanc, A.J., Tratnyek, P.G., Lowry, G.V., 2013. Field-scale transport and transformation of carboxymethylcellulose-stabilized nano zero-valent iron. Environ. Sci. Technol. 47, 1573–1580. http://dx.doi.org/10.1021/es304564q.

Kim, E.-J., Kim, J.-H., Azad, A.-M., Chang, Y.-S., 2011. Facile synthesis and characterization of Fe/FeS nanoparticles for environmental applications. ACS Appl. Mater. Interfaces 3, 1457–1462. http://dx.doi.org/10.1021/am200016v.

Kim, E.-J., Le Thanh, T., Kim, J.-H., Chang, Y.-S., 2013. Synthesis of metal sulfide-coated iron nanoparticles with enhanced surface reactivity and biocompatibility. RSC Adv. 3, 5338. http://dx.doi.org/10.1039/c3ra00009e.

Kim, C., Ahn, J.-Y., Hwang, K.-Y., Kim, H.-S., Kwon, D.-Y., Hwang, I., 2014a. Effects of groundwater solutes on colloidal stability of polymer-coated and bare nanosized zero-valent iron particles. Desalin. Water Treat. 1–9 http://dx.doi.org/10.1080/19443994.2014.903873.

Kim, H.-S., Ahn, J.-Y., Kim, C., Lee, S., Hwang, I., 2014b. Effect of anions and humic acid on the performance of nanoscale zero-valent iron particles coated with polyacrylic acid. Chemosphere 113, 93–100. http://dx.doi.org/10.1016/j.chemosphere.2014.04.047.

Klimkova, S., Cernik, M., Lacinova, L., Filip, J., Jancik, D., Zboril, R., 2011. Zero-valent iron nanoparticles in treatment of acid mine water from in situ uranium leaching. Chemosphere 82, 1178–1184. http://dx.doi.org/10.1016/j.chemosphere.2010.11.075.

Lacinová, L., Černíková, M., Hrabal, J., Černík, M., 2013. In-situ combination of bio and abio remediation of chlorinated ethenes. Ecol. Chem. Eng. S 20 http://dx.doi.org/10.2478/eces-2013-0034.

Laumann, S., Micić, V., Lowry, G.V., Hofmann, T., 2013. Carbonate minerals in porous media decrease mobility of polyacrylic acid modified zero-valent iron nanoparticles used for groundwater remediation. Environ. Pollut. 179, 53–60. http://dx.doi.org/10.1016/j.envpol.2013.04.004.

Lee, W., Batchelor, B., 2002. Abiotic reductive dechlorination of chlorinated ethylenes by iron-bearing soil minerals. 1. Pyrite and magnetite. Environ. Sci. Technol. 36, 5147–5154. http://dx.doi.org/10.1021/es025836b.

Liu, Y., Lowry, G.V., 2006. Effect of particle age (Fe^0 content) and solution pH On NZVI reactivity: H_2 evolution and TCE dechlorination. Environ. Sci. Technol. 40, 6085–6090. http://dx.doi.org/10.1021/es060685o.

Liu, Y., Majetich, S.A., Tilton, R.D., Sholl, D.S., Lowry, G.V., 2005. TCE dechlorination rates, pathways, and efficiency of nanoscale iron particles with different properties. Environ. Sci. Technol. 39, 1338–1345. http://dx.doi.org/10.1021/es049195r.

Liu, Y., Phenrat, T., Lowry, G.V., 2007. Effect of TCE concentration and dissolved groundwater solutes on NZVI-promoted TCE dechlorination and H_2 evolution. Environ. Sci. Technol. 41, 7881–7887. http://dx.doi.org/10.1021/es0711967.

Long, T., Ramsburg, C.A., 2011. Encapsulation of nZVI particles using a Gum Arabic stabilized oil-in-water emulsion. J. Hazard. Mater. 189, 801–808. http://dx.doi.org/10.1016/j.jhazmat.2011.02.084.

Luo, S., Yang, S., Wang, X., Sun, C., 2010. Reductive degradation of tetrabromobisphenol A over iron–silver bimetallic nanoparticles under ultrasound radiation. Chemosphere 79, 672–678. http://dx.doi.org/10.1016/j.chemosphere.2010.02.011.

Mackenzie, K., Bleyl, S., Georgi, A., Kopinke, F.-D., 2012. Carbo–Iron – an Fe/AC composite – as alternative to nano-iron for groundwater treatment. Water Res. 46, 3817–3826. http://dx.doi.org/10.1016/j.watres.2012.04.013.

Mueller, N.C., Braun, J., Bruns, J., Černík, M., Rissing, P., Rickerby, D., Nowack, B., 2011. Application of nanoscale zero valent iron (NZVI) for groundwater remediation in Europe. Environ. Sci. Pollut. Res. 19, 550–558. http://dx.doi.org/10.1007/s11356-011-0576-3.

Nagayama, M., Cohen, M., 1962. The anodic oxidation of iron in a neutral solution I. The nature and composition of the passive film. J. Electrochem. Soc. 109, 781–790. http://dx.doi.org/10.1149/1.2425555.

Noubactep, C., 2009. The suitability of metallic iron for environmental remediation. Environ. Prog. Sustainable Energy 29, 286–291. http://dx.doi.org/10.1002/ep.10406.

Nurmi, J.T., Tratnyek, P.G., Sarathy, V., Baer, D.R., Amonette, J.E., Pecher, K., Wang, C., Linehan, J.C., Matson, D.W., Penn, R.L., Driessen, M.D., 2005. Characterization and properties of metallic iron nanoparticles: spectroscopy, electrochemistry, and kinetics. Environ. Sci. Technol. 39, 1221–1230. http://dx.doi.org/10.1021/es049190u.

Park, S.-W., Kim, S.-K., Kim, J.-B., Choi, S.-W., Inyang, H.I., Tokunaga, S., 2006. Particle surface hydrophobicity and the dechlorination of chloro-compounds by iron sulfides. Water Air Soil Pollut. Focus 6, 97–110. http://dx.doi.org/10.1007/s11267-005-9016-z.

Reinsch, B.C., Forsberg, B., Penn, R.L., Kim, C.S., Lowry, G.V., 2010. Chemical transformations during aging of zerovalent iron nanoparticles in the presence of common groundwater dissolved constituents. Environ. Sci. Technol. 44, 3455–3461. http://dx.doi.org/10.1021/es902924h.

Rosenthal, H., Adrian, L., Steiof, M., 2004. Dechlorination of PCE in the presence of Fe^0 enhanced by a mixed culture containing two *Dehalococcoides* strains. Chemosphere 55, 661–669. http://dx.doi.org/10.1016/j.chemosphere.2003.11.053.

Sander, R., 1999. Compilation of Henry's Law Constants for Inorganic and Organic Species of Potential Importance in Environmental Chemistry. Max-Planck Institute of Chemistry, Air Chemistry Department.

Sarathy, V., Salter, A.J., Nurmi, J.T., O'Brien Johnson, G., Johnson, R.L., Tratnyek, P.G., 2010. Degradation of 1,2,3-Trichloropropane (TCP): Hydrolysis, Elimination, and Reduction by Iron and Zinc. Environ. Sci. Technol. 44, 787–793. http://dx.doi.org/10.1021/es902595j.

Schrick, B., Hydutsky, B.W., Blough, J.L., Mallouk, T.E., 2004. Delivery vehicles for zerovalent metal nanoparticles in soil and groundwater. Chem. Mater. 16, 2187–2193. http://dx.doi.org/10.1021/cm0218108.

Shi, Z., Nurmi, J.T., Tratnyek, P.G., 2011. Effects of nano zero-valent iron on oxidation–reduction potential. Environ. Sci. Technol. 45, 1586–1592. http://dx.doi.org/10.1021/es103185t.

Song, H., Carraway, E.R., 2005. Reduction of chlorinated ethanes by nanosized zero-valent iron: kinetics, pathways, and effects of reaction conditions. Environ. Sci. Technol. 39, 6237–6245. http://dx.doi.org/10.1021/es048262e.

Song, H., Carraway, E.R., 2008. Catalytic hydrodechlorination of chlorinated ethenes by nanoscale zero-valent iron. Appl. Catal. B Environ. 78, 53–60. http://dx.doi.org/10.1016/j.apcatb.2007.07.034.

Su, C., Puls, R.W., 1999. Kinetics of trichloroethene reduction by zerovalent iron and tin: pretreatment effect, apparent activation energy, and intermediate products. Environ. Sci. Technol. 33, 163–168. http://dx.doi.org/10.1021/es980481a.

Tamura, H., 2008. The role of rusts in corrosion and corrosion protection of iron and steel. Corros. Sci. 50, 1872–1883. http://dx.doi.org/10.1016/j.corsci.2008.03.008.

Tiraferri, A., Sethi, R., 2008. Enhanced transport of zerovalent iron nanoparticles in saturated porous media by guar gum. J. Nanoparticle Res. 11, 635–645. http://dx.doi.org/10.1007/s11051-008-9405-0.

Tratnyek, P.G., Johnson, R.L., 2006. Nanotechnologies for environmental cleanup. Nano Today 1, 44–48.

Tratnyek, P.G., Scherer, M.M., Deng, B., Hu, S., 2001. Effects of natural organic matter, anthropogenic surfactants, and model quinones on the reduction of contaminants by zero-valent iron. Water Res. 35, 4435–4443.

Tsang, D.C.W., Graham, N.J.D., Lo, I.M.C., 2009. Humic acid aggregation in zero-valent iron systems and its effects on trichloroethylene removal. Chemosphere 75, 1338–1343. http://dx.doi.org/10.1016/j.chemosphere.2009.02.058.

Uegami, M., Kawano, J., Okita, T., Fujii, Y., Okinaka, K., Kakuya, K., Yatagai, S., 2003. Iron particles for purifying contaminated soil or ground water, process for producing the iron particles, purifying agent comprising the iron particles, process for producing the purifying agent and method of purifying contaminated soil or ground water (20030217974A1).

Wang, S.-M., Tseng, S., 2009. Reductive dechlorination of trichloroethylene by combining autotrophic hydrogen-bacteria and zero-valent iron particles. Bioresour. Technol. 100, 111–117. http://dx.doi.org/10.1016/j.biortech.2008.05.033.

Weerasooriya, R., Dharmasena, B., 2001. Pyrite-assisted degradation of trichloroethene (TCE). Chemosphere 42, 389–396. http://dx.doi.org/10.1016/S0045-6535(00)00160-0.

Xie, Y., Cwiertny, D.M., 2010. Use of dithionite to extend the reactive lifetime of nanoscale zero-valent iron treatment systems. Environ. Sci. Technol. 44, 8649–8655. http://dx.doi.org/10.1021/es102451t.

Xie, Y., Cwiertny, D.M., 2012. Influence of anionic cosolutes and pH on nanoscale zerovalent iron longevity: time scales and mechanisms of reactivity loss toward 1,1,1,2-tetrachloroethane and Cr(VI). Environ. Sci. Technol. 46, 8365–8373. http://dx.doi.org/10.1021/es301753u.

Xie, L., Shang, C., 2005. Role of humic acid and quinone model compounds in bromate reduction by zerovalent iron. Environ. Sci. Technol. 39, 1092–1100. http://dx.doi.org/10.1021/es049027z.

Xiu, Z., Jin, Z., Li, T., Mahendra, S., Lowry, G.V., Alvarez, P.J.J., 2010. Effects of nano-scale zero-valent iron particles on a mixed culture dechlorinating trichloroethylene. Bioresour. Technol. 101, 1141–1146. http://dx.doi.org/10.1016/j.biortech.2009.09.057.

Yang, S.Y., Chen, Y.F., Ke, Y.H., Tse, W.S., Horng, H.E., Hong, C.-Y., Yang, H.C., 2002. Effect of temperature on the structure formation in the magnetic fluid film subjected to perpendicular magnetic fields. J. Magn. Magn. Mater. 252, 290–292.

Yu, J., Liu, W., Zeng, A., Guan, B., Xu, X., 2012. Effect of SO on 1,1,1-trichloroethane degradation by Fe^0 in aqueous solution. Ground Water 286–292 http://dx.doi.org/10.1111/j.1745-6584.2012.00957.x.

Zhan, J., Zheng, T., Piringer, G., Day, C., McPherson, G.L., Lu, Y., Papadopoulos, K., John, V.T., 2008. Transport characteristics of nanoscale functional zerovalent iron/silica composites for in situ remediation of trichloroethylene. Environ. Sci. Technol. 42, 8871–8876.

Zhan, J., Sunkara, B., Le, L., John, V.T., He, J., McPherson, G.L., Piringer, G., Lu, Y., 2009. Multifunctional colloidal particles for in situ remediation of chlorinated hydrocarbons. Environ. Sci. Technol. 43, 8616–8621. http://dx.doi.org/10.1021/es901968g.

Zhuang, Y., Jin, L., Luthy, R.G., 2012. Kinetics and pathways for the debromination of polybrominated diphenyl ethers by bimetallic and nanoscale zerovalent iron: effects of particle properties and catalyst. Chemosphere 89, 426–432. http://dx.doi.org/10.1016/j.chemosphere.2012.05.078.

4.1 Supporting Information

Electron efficiency of nZVI does not change with variation of environmental parameters

*Philipp Schöftner[1], Georg Waldner[1], Werner Lottermoser[2], Michael Stöger-Pollach[3], Peter Freitag[4], Thomas Reichenauer[1]**

[1]AIT Austrian Institute of Technology GmbH, Konrad-Lorenz-Strasse 24, 3430 Tulln an der Donau, Austria.

[2] Salzburg University, FB Materialforschung und Physik

[3] Technical University of Vienna, Universitäre Service-Einrichtung für Transmissionselektronenmikroskopie - USTEM

[4] Keller Grundbau

Contents

Section 1: Chemicals and Materials

Chemicals used in these experiments were hydrochloric acid (37 %, PA, Merck), sulfuric acid (≥ 99.5 %, PA, Merck), ethanol (≥ 99.5 %, PA, Merck), trichloroethene (≥99.5 %, Sigma), 1,1-dichloroethene (99 %, Sigma), trans-1,2-dichloroethene (98 %, Sigma) and cis-1,2-dichloroethene (≥ 95 %, GC grade, Fluka). Gases were purchased from Linde AG (Austria): H2 (5.0), Ar (5.0), He (5.0), N2 (5.0), ethine (flame photometry), methane (60 % ± 1 % in CO2), carbon dioxide (380 ppm (V/V) ± 2% in N2), hydrogen (1% ± 2% (V/V) in N2), ethene (997 ppm (V/V) ± 2 % in N2), ethine (985 ppm (V/V) ± 2 % in N2), ethane (992 ppm (V/V) ± 2 % in N2), chloroethene (1047 ppm (V/V) ± 2 % in N2), synthetic air (HC free, 20 % O2 in N2) and a multicomponent standard (methane 1007 ppm (V/V) ± 2 %, ethene 993 ppm (V/V) ± 2 %, ethane 976 ppm (V/V) ± 2 %, ethane 1013 ppm (V/V) ± 2 %, chloroethene 1032 ppm (V/V) ± 2 % and trichloroethene 2438 ppm (V/V) ± 2 % in N2). Additionally for ion chromatography a Merck Certipur Anion multi-element standard I (1 g/L Cl-, NO3-, SO42-) und standard II (1 g/L F-, PO43-, Br-) were used.

Section 2: Detailed analytical methods

CHC and H_2 headspace concentrations were detected using a GS-Q, 30 m plot column, 0.53 mm (Agilent) for analysis of (C)HC (FID) and a packed Molsieve column (5 Å) for analysis of H_2 (TCD); the injector temperatures were set at 110 °C in both cases. An oven temperature program (40 °C for 3 min, ramp 30 °C/min to 180 °C, and hold for 5 min) was developed to separate the analyzed species. He 5.0 (2.5 ml/min) was used as carrier gas to measure carbon species via FID, while Ar 5.0 was used as carrier gas (16 ml/min) and as reference gas (17 ml/min) to measure H_2 via TCD. Carbon species and H_2 were calibrated using a gaseous multi-component (methane, ethene, ethine, ethane, chloroethene and trichloroethene) and a gaseous H_2 standard supplied by Linde AG, Stadl-Paura, Austria. Dichloro-intermediate products 1,1-DCE, 1,2-trans DCE and 1,2-cis DCE were calibrated using liquid standards supplied by Sigma-Aldrich.

Measured amounts of TCE and reaction products were corrected for overpressure and sampling induced headspace losses. Before analyzing headspace samples via GC, H_2-induced excess pressure was equalized using a pressure-equalizing syringe. Additionally CH_4 was used as internal standard to validate headspace losses.

CH_4 in the headspace was measured at each sampling point and the amount of CH_4 in the liquid phase was calculated. So it was possible to derive a total amount of CH_4 within the vials at each sampling point. Over time the total amount of CH_4 within the vials decreased due to losses of the headspace.

Additionally the decrease of total CH_4 in the vials was calculated based on the overpressure and sampling induced headspace losses. Therefore the measured amount of CH_4 in the vials was corrected for CH_4 losses that were calculated by:

$$[CH4_{total}\ t_{n+1}] = [CH4_{total}\ t_n]\ -\ (\ [CH4_{HS}\ t_n] * \frac{HS\ t_{n+1}}{HS\ t_{n+1} + EP\ t_{n+1} + SA\ t_{n+1}}\ )$$

$CH4_{total}\ t_{n+1}$	CH_4 [µmol] in the headspace and aqueous phase at t_{n+1}
$CH4_{total}\ t_n$	CH_4 [µmol] in the headspace and aqueous phase at t_n
$CH4_{HS}\ t_n$	CH_4 [µmol] in the headspace at t_n
$HS\ t_{n+1}$	Volume of the headspace of the vials at t_{n+1}
$EP\ t_{n+1}$	Volume lost due to excess pressure (measured with the pressure equalizing syringe at t_{n+1})
$SA\ t_{n+1}$	Volume lost by sampling the headspace (2*100 µl)
$CH4_{HS}\ t_n$	CH_4 [µmol] in the headspace at t_n

As explained before the total amount of CH_4 within the vials decreased over time due to losses of the headspace. Deviations between measured decreases of CH_4 [µmol] within the vials (headspace + aqueous phase) and calculated decreases (based on pressure equalization) were negligible (Ref 1.01 ± 0.05, LS 0.97 ± 0.18, CMC 1.02 ± 0.06, O_2 1.04 ± 0.09, MQ1 0.97 ± 0.04, 12 °C 1.04 ± 0.04).

Measured concentrations of TCE and its reaction products and of H_2 were corrected based on measured overpressure and sampling induced headspace losses, not based on measured internal CH_4 standards. This was useful because an internal standard was used for correction which is present in the gas phase all the time, whereas TCE concentration decreases (higher mass loss at the beginning) and H_2 is formed (higher mass loss at the end) over the reaction. Using this method we proved that measurements of overpressure were precise and can be used to calculate losses of H_2 and TCE based on real headspace concentrations of H_2 and TCE at the time of sampling.

Figure S1 illustrates the differences in TCE concentrations if measured concentrations were corrected for headspace losses. In case of the first replicate of the first reference experiment the TCE losses due to headspace losses accounted for 0.24 µmol on day 9 (about 4 % of initial TCE). This amount of lost TCE was similar under all conditions, but increased with increasing reaction time. In case of more volatile compounds - as H_2, ethane, ethane and ethine - headspace losses were substantially higher.

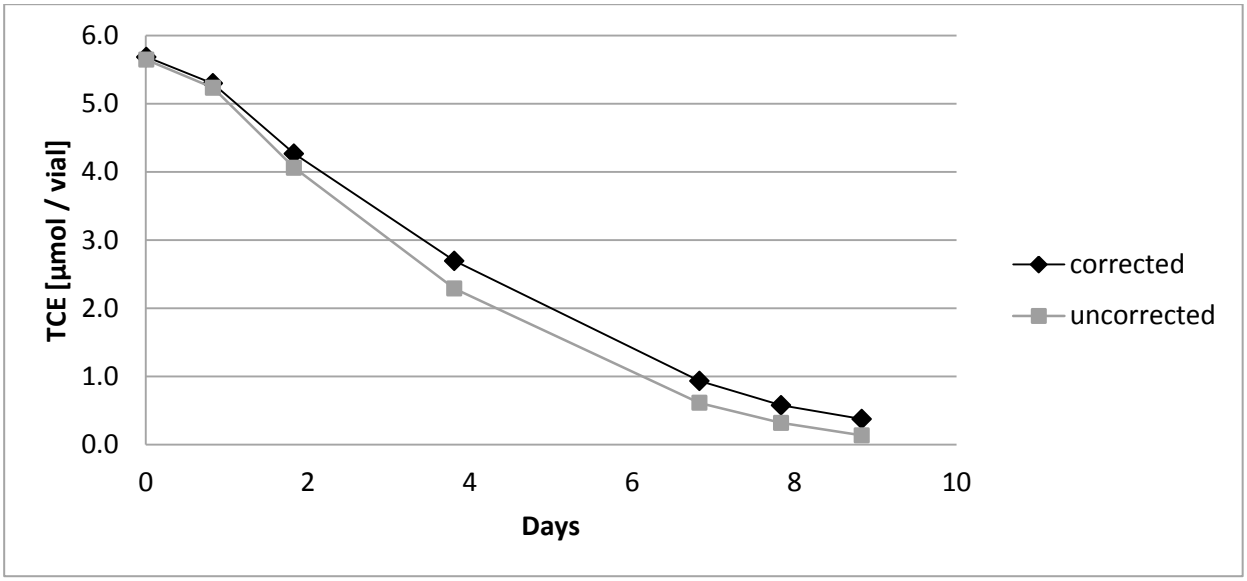

Figure S6: TCE concentrations in the first replicate of the first reference experiment. Measured amount of TCE in the vials which were not corrected for headspace losses (uncorrected) and measured amount of TCE in the vials which were corrected for headspace losses (corrected).

Solution redox potential (ORP_H), pH value and O_2 concentration were measured using the following electrodes: WTW Sentix® ORP 900 platinum electrode (reported values are referred to the normal hydrogen electrode (NHE); WTW SenTix® 41 pH-electrode, WTW FDO® 925 optical D.O. sensor).

Iron oxide species were identified using Mössbauer Spectroscopy and XRD (X-Ray Diffraction) analyses. The powder samples were prepared on Mössbauer absorbers with 5 mg Fe/cm^2 and a diameter of 7 mm by embedding the samples homogeneously, airtight in an epoxy glue with good thermal conductivity and fixing them in a copper ring sandwiched by aluminum foils. Samples from suspensions were prepared in an argon-filled glovebag: These were dropped on sample carrier plates and embedded in airtight epoxy glue after evaporation of the water phase. Subsequently, the gaseous oxygen concentration in the glovebox was monitored with a GMH 3691 air oxygen measuring device with GGO 370 sensor (Greisinger electronic GmbH). These absorbers were mounted in a conventional Mössbauer apparatus (time mode arrangement, Halder Elektronik GmbH) with constant acceleration and exposed to a nominal 1.8 GBq source of Co-57 in Rh (Wissel GmbH). The transmitted intensities were stored in a multichannel analyzer with 1024 channels and subsequently folded to 510 channels in order to improve statistics. Before and after a sequence of experiments with identical velocity adjustments, an alpha-iron spectrum was recorded in order to determine the calibration factor – the velocity scale was subsequently recalculated from channels to mm/s. The spectra were then fitted with a conventional refinement routine with Lorentzian lines (MOESALZ)(Lottermoser et al., 1993). Mössbauer phase analysis was performed by attributing the different subspectra to calculated patterns with Mössbauer parameters characteristic for the iron phases mentioned in the main section. The different phases mentioned below were found by comparison with the relevant parameter sets published in the Mössbauer Mineral Handbook(Stevens et al., 1998). XRD measurements were performed on the above-mentioned powder samples using a BRUKER D8 Advance, A25X1 (Fa. Bruker Analytical X-ray Systems GmbH, Karlsruhe) powder diffractometer with tube tension/current values of 40 kV and 40 mA, respectively. The diffractometer has a Bragg-Brentano beam geometry with a divergence slit of 0.5°. The patterns were recorded between 5° and 80° (2Θ), a step width of 0.02° and a step time of 57.3 s. This yielded well-resolved powder patterns that could be attributed to the different phases with high accuracy.

Anion concentrations (Cl^-, F^-, NO_3^-, SO_4^{2-}, PO_4^{3-}) were analyzed with a Dionex DX-120 Ion Chromatography (IC) connected to an AS 50 autosampler using Thermo Scientific Dionex Ion PacTM AG14 4*50 mm as precolumn and a Thermo Scientific Dionex Ion PacTM AS14 4*250 mm as separation column. As eluent $NaHCO_3/Na_2CO_3$ (1.0/3.5 mM) was used.

Section 3: Obtained iron oxidation rates, pH-values and redox conditions (ORP_H) at different reaction conditions

Table S2: Fe^0 oxidation rates, pH-values and ORP_H (standard hydrogen electrode) under different conditions and different iron particle mass. Reference conditions, 50 mg/l lignosulphonate (LS) or carboxymethylcellulose (CMC), oxic conditions (O_2), Millipore water (MQ) and reduced temperature (12 °C).

Variation	Fe^0 oxidation rate	pH-value			ORP_H
	[mg/d]	μ ± σ[4]	Start	End[5]	[mV_H]
Reference	3.1 ± 0.9	8.7 ± 0.6	8.4	9.0	-334 ± 151
LS	2.4	8.9 ± 0.6	8.4	8.8	-267 ± 172
CMC	2.0	8.8 ± 0.3	8.6	8.7	-310 ± 229
O_2[1]	0.8	8.6 ± 0.5	8.0	8.7	-31 ± 308
MQ Phase 1[2]	1.0 ± 0.4	7.0 ± 1.1	8.8	6.1	-10 ± 117
MQ Phase 2[2]	1.3	6.1 ± 0.05	8.8	6.1	-311 ± 68
12 °C	1.5	8.3 ± 0.6	8.4	8.7	-205 ± 100
1.0 g/l Fe^0	1.3	8.6 ± 0.1	8.2	8.6	-437 ± 20
2.5 g/l Fe^0 [3]	3.1 ± 0.9	8.7 ± 0.6	8.4	9.0	-334 ± 151
4.6 g/l Fe^0	2.4	8.9 ± 0.4	8.5	9.5	-451 ± 52

[1] 4 of 6 batches passivated under oxic conditions. Values represent data from two reactive batches after reduction of dissolved oxygen.

[2] MQ showed two stable reaction phases (pseudo first order regarding TCE).

[3] Same batches as reported under reference conditions

[4] Mean and std. deviation of measured values within the reaction period in which reaction constants and electron efficiencies were calculated

[5] pH-values after 10 days of reaction

Section 4: Representation of two stable reaction phases in reactions with Millipore water

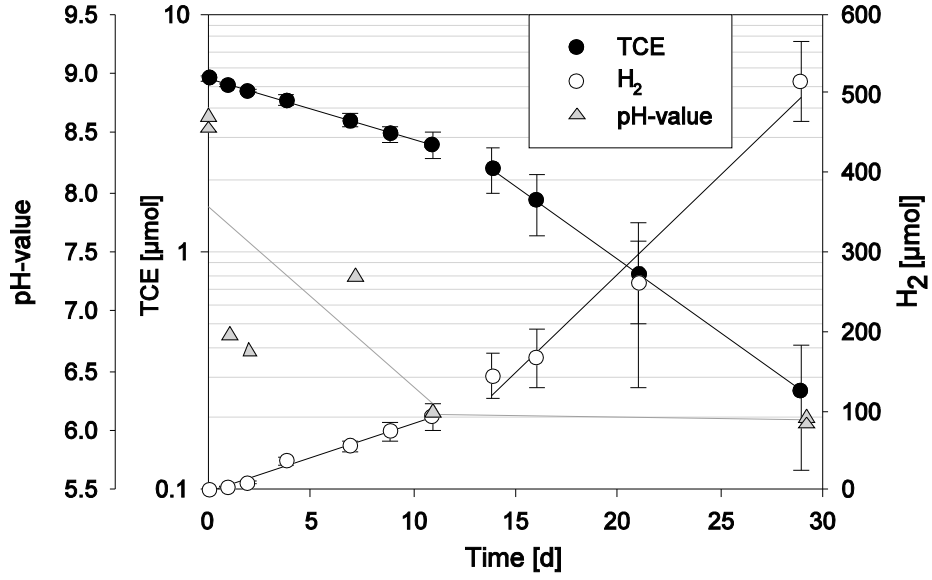

Figure S7: Development of TCE concentration, pH-value and H_2 concentration in reaction vials with Millipore water as reaction media (Batch 1 of 2).

Section 5: Influence of TCE concentration on TCE electron efficiency

Reported TCE and H_2 electron efficiency values represent average values and standard deviations of single time period efficiencies (ϵTCE_{n+1} or $\epsilon H2_{n+1}$) for time intervals between two consecutive CHC and H_2 measurements on condition that the TCE concentration was between 5 and 25 mgl^{-1} (total TCE per volume of water phase) (stable reaction phase). These concentrations amount to real TCE concentrations of 3.5 and 17.5 mgl^{-1} in the aqueous phase.

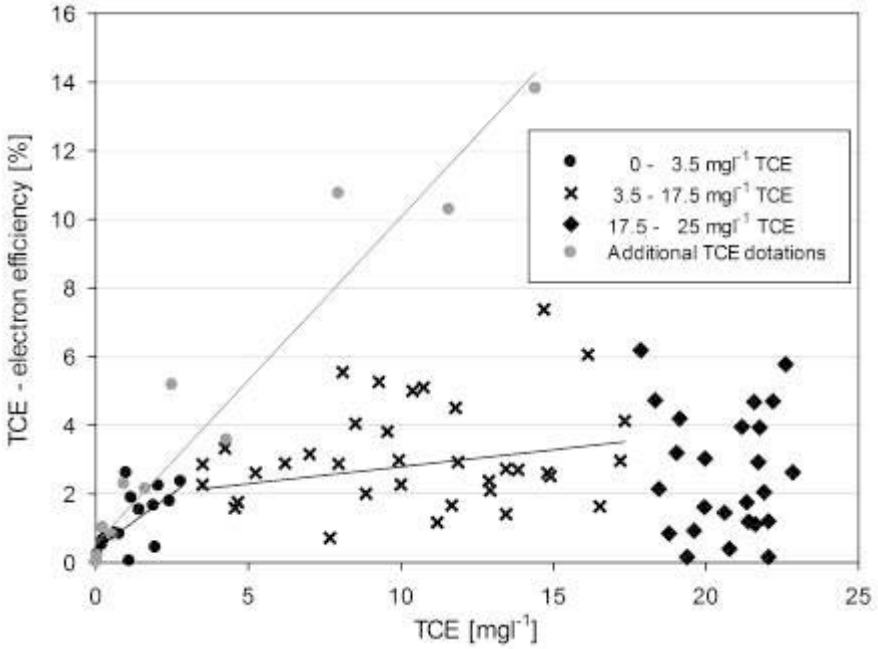

Figure S8: Summary of TCE electron efficiencies in dependence of TCE concentration in reaction vessels under different conditions. Reference conditions, 50 mg/l lignosulphonate (LS) or carboxymethylcellulose (CMC), Millipore water (MQ), reduced temperature (12 °C) and oxic conditions (O_2) and after second and third TCE addition into vessel with 4.6 g/l Fe(0) Batch vials after complete dehalogenation of initial TCE. TCE concentrations represent measured TCE concentrations in the water phase which were not corrected for overpressure headspace losses. TCE from the headspace was not included. Hence concentrations start from slightly lower than 25 mgl^{-1} and not 35 mgl^{-1} as explained in the papers method section.

Section 6: Development of Anion concentrations during dehalogenation

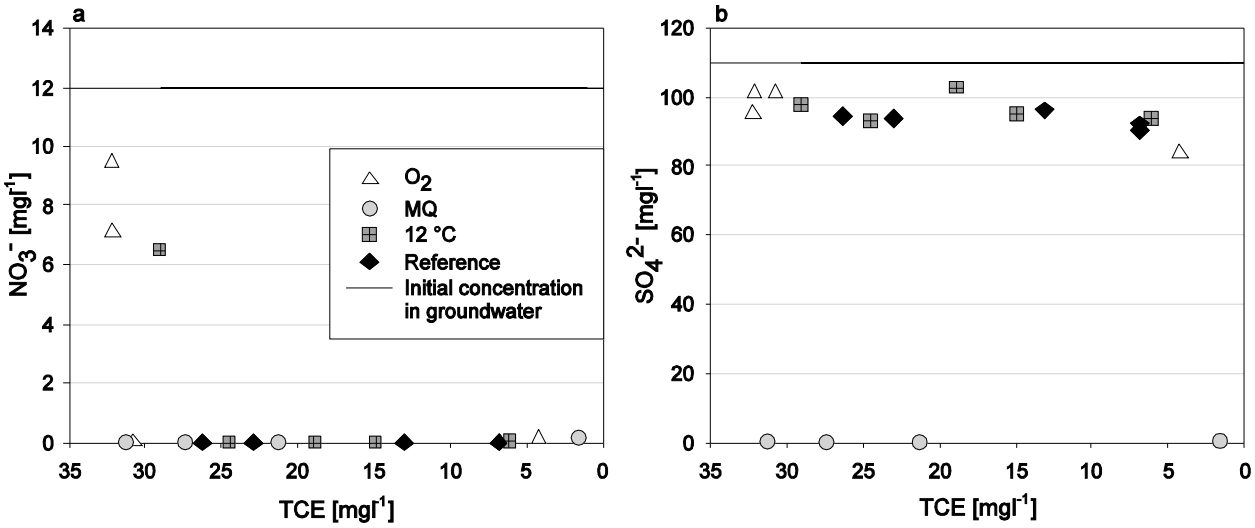

Figure S9: Development of NO_3^- and SO_4^{2-} concentrations in reaction vessels under different conditions. Reference conditions, Millipore water (MQ), reduced temperature (12 °C) and oxic conditions (O_2). TCE concentrations represent concentrations that were corrected for losses induced by overpressure.

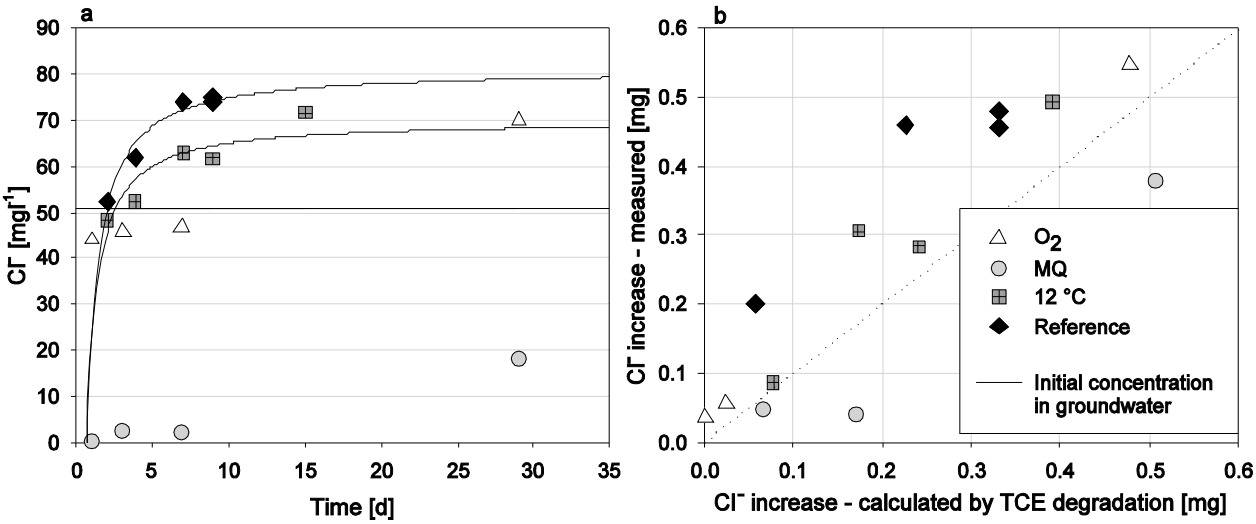

Figure S10: (a) Cl^- concentration in reaction vessels under different conditions. (b) Comparison of measured Cl^- amounts and Cl^- concentrations that were calculated by the dehalogenation of TCE (corrected for losses induced by overpressure) under different conditions. Reference conditions, Millipore water (MQ), reduced temperature (12 °C) and oxic conditions (O_2).

Section 7: Particle characterization: TEM analysis and monitoring of dissolved Fe^{2+} concentrations

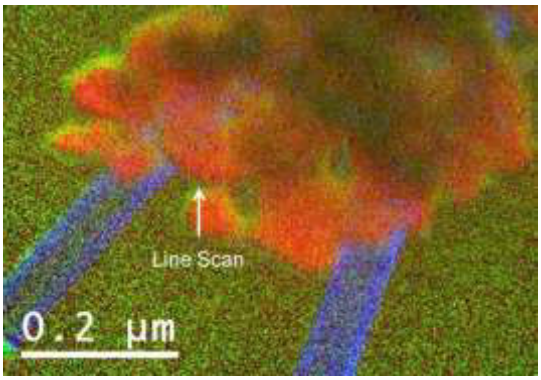

Figure S11: HRTEM (high resolution transmission electron microscopy): Elemental map of fresh unreacted Nanofer Star particles. red-Fe, blue-C, green-O

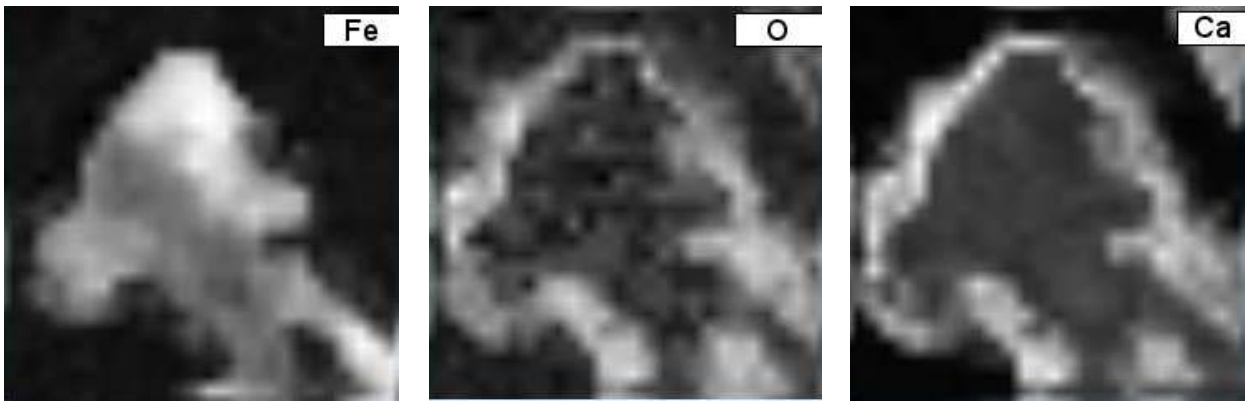

Figure S12: HRTEM (high resolution transmission electron microscopy): Elemental map of Nanofer Star particles that reacted for 6 days under reference conditions (200nm * 200nm). Lightened areas represent particular elements.

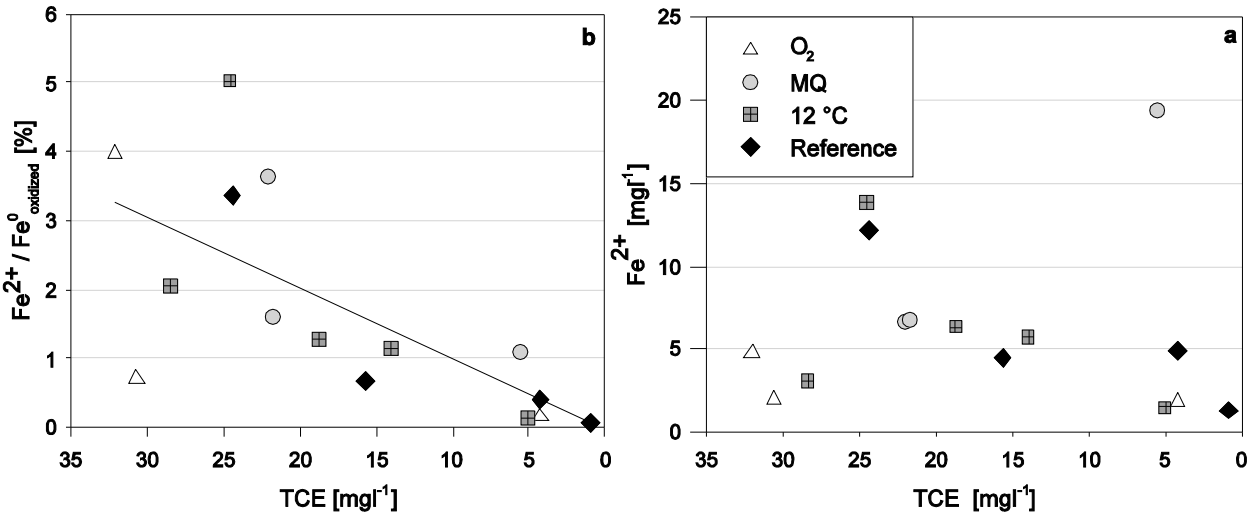

Figure S13: Development of (a) total dissolved Fe-concentration and (b) concentration of dissolved Fe-ions in relationship to oxidized amount of Fe^0 in the course of TCE dehalogenation under different conditions. Reference conditions (GW, 22°C), Millipore water (MQ), reduced temperature (12 °C) and oxic conditions (O_2). TCE concentrations represent measured concentrations that were not corrected for losses induced by overpressure.

Section 8: References in supporting information

Klimkova, S., Cernik, M., Lacinova, L., Filip, J., Jancik, D., Zboril, R., 2011. Zero-valent iron nanoparticles in treatment of acid mine water from in situ uranium leaching. Chemosphere 82, 1178–1184. doi:10.1016/j.chemosphere.2010.11.075

Lottermoser, W., Kaliba, P., Forcher, K., Amthauer, G., 1993. MOESALZ: a computer program for the evaluation of Mössbauer data. University of Salzburg, Austria.

Stevens, J.G., Khasanov, A.M., Miller, J.W., Pollak, H., Li, Z. (Eds.), 1998. Mössbauer Mineral Handbook. Bittmore Press, Asheville, NC USA.

Zhuang, Y., Jin, L., Luthy, R.G., 2012. Kinetics and pathways for the debromination of polybrominated diphenyl ethers by bimetallic and nanoscale zerovalent iron: Effects of particle properties and catalyst. Chemosphere 89, 426–432. doi:10.1016/j.chemosphere.2012.05.078

INTERNATIONAL JOURNAL OF PHYTOREMEDIATION
2016, VOL. 18, NO. 7, 686–692
http://dx.doi.org/10.1080/15226514.2015.1131228

Taylor & Francis
Taylor & Francis Group

Transpiration and metabolisation of TCE by willow plants – a pot experiment

Philipp Schöftner, Andrea Watzinger, Philipp Holzknecht, Bernhard Wimmer, and Thomas G. Reichenauer

AIT Austrian Institute of Technology GmbH, Health & Environment Department, Environmental Resources & Technologies, Konrad-Lorenz-Strasse, Tulln, Austria

ABSTRACT

Willows were grown in glass cylinders filled with compost above water-saturated quartz sand, to trace the fate of TCE in water and plant biomass. The experiment was repeated once with the same plants in two consecutive years. TCE was added in nominal concentrations of 0, 144, 288, and 721 mg l^{-1}. Unplanted cylinders were set-up and spiked with nominal concentrations of 721 mg l^{-1} TCE in the second year. Additionally, ^{13}C-enriched TCE solution ($\delta^{13}C$ = 110.3 ‰) was used. Periodically, TCE content and metabolites were analyzed in water and plant biomass. The presence of TCE-degrading microorganisms was monitored via the measurement of the isotopic ratio of carbon ($^{13}C/^{12}C$) in TCE, and the abundance of ^{13}C-labeled microbial PLFAs (phospholipid fatty acids). More than 98% of TCE was lost via evapotranspiration from the planted pots within one month after adding TCE. Transpiration accounted to 94 to 78% of the total evapotranspiration loss. Almost 1% of TCE was metabolized in the shoots, whereby trichloroacetic acid (TCAA) and dichloroacetic acid (DCAA) were dominant metabolites; less trichloroethanol (TCOH) and TCE accumulated in plant tissues. Microbial degradation was ruled out by $\delta^{13}C$ measurements of water and PLFAs. TCE had no detected influence on plant stress status as determined by chlorophyll-fluorescence and gas exchange.

KEYWORDS

Phytoremediation; trichloroethene; *Salix viminalis*; degradation; PLFAs; ^{13}C

Introduction

Chlorinated hydrocarbons (CHCs), especially trichloroethene, tetrachloroethene, 1,1,1-trichloroethane and dichloromethane, are—together with hydrocarbons—the most frequent pollutants and can therefore be found at numerous industrial sites (Weisgram *et al.* 2012). Using plants for phytoremediation of CHCs is a cost-effective, noninvasive technology that uses sun energy to pump up contaminated groundwater. Phytoremediation of CHCs can be applied at sites that provide enough space for planting of vegetation, exhibit a shallow water table, and have a thin aquifer with low to medium discharge (Matthews, Massmann, and Strand 2003). Willow (*Salix*) and poplar (*Populus*) species have promising remediation properties due to their extensive rooting systems, high water consumption, high toxicity tolerance, rapid growth, and wide regional distribution (Miller, Khan, and Doty 2011). CHCs exhibit physical and chemical properties ideal for uptake by plant roots. These include K_{ow} values (octanol-water partition coefficient) between 1.8 (Briggs, Bromilow, and Evans 1982) and 3.1 (Hsu, Marxmiller, and Yang 1990) as well as low ionization potential, strong polarity and water solubility (Dettenmaier, Doucette, and Bugbee 2009). Once organic xenobiotics such as CHCs are taken up, plants can metabolize and integrate them into their tissue to a certain extent according to the "green liver concept" of Sandermann (1992) or mineralize them to CO_2 and H_2O (Newman *et al.* 1997; Shang and Gordon 2002; Shang *et al.* 2001). Incomplete metabolization of CHCs can cause volatilization with the transpiration stream into the atmosphere (Ma and Burken 2004; Orchard *et al.* 2000; Wang *et al.* 2004; Winters 2008). In the case of TCE uptake, oxidative transformation has already been verified for poplar and willow trees. Trichloroethanol, dichloroacetic acid, and trichloroacetic acid were the main identified products (Gordon *et al.* 1998; James *et al.* 2009; Miller *et al.* 2011; Newman and Reynolds 2004; Newman *et al.* 1997, 1999). Willows and poplars are toxicity-tolerant species that can even grow at high TCE concentrations of around 200 mg l^{-1} (Miller *et al.* 2011). We are unaware of further studies on the toxicity of chlorinated ethenes in willows. Studies on the physiologically similar poplars, however, revealed that 60 mg l^{-1} TCE did not influence cell growth and that 8 months exposure to 50 mg l^{-1} TCE hardly reduced plant growth of one-year-old poplar cuttings (Newman *et al.* 1997). Even at a TCE concentration of 550 mg l^{-1}, (Ma and Burken 2003) did not observe toxic effects in rooted poplar cuttings. In contrast, zero-growth of poplar cuttings was observed at 45 mg l^{-1} PCE, 118 mg l^{-1} TCE, 465 mg l^{-1} 1,2-trans-DCE, 543 mg l^{-1} 1,1-DCE, or 582 mg l^{-1} 1,2-cis-DCE (Dietz and Schnoor 2001). All tested concentrations for poplars were far above expected plume concentrations at field sites. Moreover, bigger trees are probably even more tolerant than the tested cuttings. Thus, according to the present state of knowledge, phytotoxic effects at field sites are unlikely. To enhance CHC degradation in plants, they can be inoculated with endophytes (Weyens *et al.* 2010a; Weyens *et al.* 2009a; Weyens

CONTACT Andrea Watzinger andrea.watzinger@ait.ac.at AIT Austrian Institute of Technology GmbH, Health & Environment Department, Environmental Resources & Technologies, Konrad-Lorenz-Strasse 24, 3430 Tulln, Austria.

Supplemental data for this article can be accessed on the publisher's website.

et al. 2009b). Plants can also be used to support microbial degradation in the rhizosphere (Anderson and Walton 1995; Godsy, Warren, and Paganelli 2003; James *et al.* 2009) by (i) release of plant exudates as nutrients, sugars, amino acids and secondary metabolites such as organic acids (Brigmon *et al.* 2003; Reichenauer and Germida 2008; Walton and Anderson 1990) and (ii) physical changes of soil structure such as gas exchange and soil moisture (McCully 1999). Since roots need oxygen for their growth, microbial degradation in the rhizosphere is assumed to largely follow an aerobic pathway. Microbial degradation leads to a shift in the signature of stable isotopes in the original contaminant towards heavier ^{13}C isotopes. Accordingly, compound specific isotope analysis (CSIA) of the isotope ratio of TCE can be used to discriminate between plant uptake and microbial degradation of CHCs (Hunkeler, Aravena, and Butler 1999; Hunkeler and Aravena 2000; Meckenstock *et al.* 2004). This study was designed to assess the capability of willows to remediate TCE-contaminated sites. For this purpose, willows were grown in artificial aquifers; TCE uptake, TCE transformation in plant tissues, microbial degradation of TCE in the water and plant health status were investigated following a single TCE application. The experiment was repeated within two consecutive years using the same plants. CSIA was used to distinguish between microbial degradation and TCE elimination via plant uptake.

Materials and methods

Experimental design

Rooted cuttings of willow (*Salix viminalis* L.) were planted in a greenhouse in glass pots which were open to the atmosphere. Each of the pots was filled with a 25 cm layer of quartz sand (0.5–2 mm) that was covered by a 20 cm compost layer (Einheitserde ED 73, Germany), whereby 2/3 of the quartz sand layer was water saturated. Pots were wrapped with aluminium foil to avoid algae growth. A similar experimental set-up was successfully used by Newman *et al.* (1997). Two liters of TCE-containing solution was added via a ®Teflon (PTFE) tube into each quartz layer. Before applying the TCE, water was pumped out and residual water was taken up by the plants for half a day of transpiration. Hereafter, 2 l solutions with nominal TCE concentrations of 0, 144, 288, and 721 mg l^{-1} were applied once at each pot. The water level was kept between 18 and 22 cm during the experiment by repeatedly adding TCE-free water via the PTFE tubes described above, which diluted the TCE solutions. The amount of water that was added was measured gravimetrically. The compost layer was kept free of the TCE solution. The experiment was repeated once with the same plants and pots and with 5 replicates for each concentration in two consecutive years, starting on the 23 August 2010 and the 6 July 2011. The duration of the experiment was 45 days in 2010 and 29 days in 2011. In 2011, we added unplanted pots filled with a TCE solution with a nominal concentration of 721 mg l^{-1}. These were covered with moist compost (5 replicates) and with dry compost (5 replicates). Additionally, ^{13}C-labeled TCE ($\delta^{13}C$ = 110.3 ‰) was used for the experiment in 2011.

Water samples were taken via a second perforated PTFE tube that was arranged in the middle of the quartz layer as a horizontal ring. Water samples were stored in PTFE-sealed vials at 4°C until analysis of TCE concentration and isotope analysis of $\delta\ ^{13}C$. Leaves and bark (2 g moist weight) were sampled and stored immediately in liquid N_2 until extraction and measurement of TCE, TCOH, DCAA, and TCAA. Leaves and branches (1.5 cm diameter) were collected 45 days after TCE application in 2010. The branches were dissected into bark and wood. In 2011, samples were taken from shoots of the upper compartments (0.5 cm diameter) at days 4 and 9 and of the lower compartments (0.5–1 cm diameter) at days 19 and 29 after TCE application. Also in 2011, compost samples were taken with a soil auger (Ø 25 mm) from the quartz and the compost layer of each pot and were frozen at −20°C until analysis of composition and the $^{13}C/^{12}C$ isotope ratio of phospholipid fatty acids (PLFAs). Finally, dark-adapted chlorophyll fluorescence was measured using a portable instrument on days 0, 1, 5, 6, 8, 9, 12, 13, 14, and 19 in 2010 and on day 17 in 2011 to evaluate plant stress status.

Analytical methods

Detailed information about the chemicals and materials used is listed in the supplementary data. Water samples (concentration of TCE and $\delta^{13}C$) were measured via Purge and Trap—Gas Chromatography—combustion—Isotope Ratio Mass Spectrometry (P&T-GC-c-IRMS). Here, a HP 5890 Series II GC (Hewlett-Packard, Wilmington, Delaware, USA) equipped with an oxidation oven was connected to a Delta S Isotope Ratio Mass Spectrometer (Finnigan, Bremen, Germany). Samples were injected via a VSP 4000 purge and trap unit (IMT, Innovative Messtechnik GmbH, Germany) using the following settings: 40°C sample temperature, 20 min purge time, 20 ml min^{-1} purge flow, 80°C valve temperature, –50°C trap temperature, 200°C desorption temperature, 7 min desorption time, 50 sec transfer time, 0 ml min^{-1} split flow, 200°C transfer line temperature, 1000 mbar constant helium pressure. Analytes were separated with an Agilent Technologies DB-VRX capillary column (60m, I.D. 0.32 mm, widebore film 1.8 μm) with He (5.0) as carrier gas (1.5 bar) and with the following temperature program: 200°C injection temperature, 40°C initial temperature hold for 10 min, ramp (40°C min^{-1}) to 100°C (hold for 2 min), ramp (10°C min^{-1}) to 200°C (hold for 2 min), ramp (20°C min^{-1}) to 240°C (hold for 2 min). The oxidation oven was operated at 940°C and was oxidized for 20 min with O_2 (0.4 bar) at 620°C prior to every measuring sequence. Within one measuring sequence a 2 s oxygen pulse was added to the oven after every sample at 940°C to prolong the oven's reactive period.

TCE, TCOH, DCAA, and TCAA contents of plant tissues were extracted via solvent extraction according to James *et al.* (2009), Newman *et al.* (1997) and Shang *et al.* (2001) with minor adaptions. Detailed information regarding extraction procedure and its adaptions can be found in SI. Analytes were detected with an Agilent Technologies 6890 gas chromatograph coupled with an Agilent Technologies 5975 inert mass selective detector (MSD) in 2010; in 2011, analytes were detected with an Agilent Technologies (USA) G1223A electron capture

detector (ECD) on a HP 5890 Series II GC (Hewlett-Packard, Wilmington, Delaware, USA). Detailed extraction and analytical procedures are described in the supplementary information.

Composition and $\delta^{13}C$ of PLFAs from compost and quartz sand samples were analyzed according to the methodology of Bligh and Dyer (1959), which was concretized by Frostegård, Tunlid, and Bååth (1991). The composition of fatty acids was detected by GC-FID (flame ionisation detector), and ^{13}C fractionation was detected by GC-c-IRMS. PLFA extraction and measurement was conducted according to Watzinger *et al.* (2014). Dark-adapted chlorophyll fluorescence was measured with a Handy-PEA Fluorimeter (Hansatech Instruments, Norfolk, England). Leaves were dark adapted for 20 minutes prior to measurement. Chlorophyll fluorescence measurements were used to calculate the ratio F_v/F_m as a parameter for "potential photochemical efficiency" of photosystem 2 (PS2). Here, F_m represents the maximal fluorescence level at high light intensity and F_v represents the variable fluorescence, which is derived from the difference between F_m and minimal fluorescence F_0 at darkness (F_m - $F_{0)}$.

Statistical analysis

For the PLFAs, all analytical results were calculated based on oven-dry (105°C) weight of soil. Statistics were performed with SPSS 17.0 for Windows. Impacts were tested by ANOVA and Tamhane post-hoc test because inhomogeneity of variance was confirmed. Significance was accepted at $p < 0.05$. Additionally, the factors substrate (sand - compost), plants (planted - unplanted pots) and TCE concentration (0, 144, 288, and 721 mg l^{-1}) were tested in a multivariate general linear model (full factorial model III, intercept included). Significant differences of PLFAs between TCE concentrations were determined separately for each substrate of the planted pots.

Results and discussion

Uptake of TCE by willows

The average initial TCE concentrations of replicates were 390 ± 192, 11 ± 2, and 6 ± 3 mg l^{-1} in 2010 and 76 ± 50, 21 ± 11, and 12 ± 5 mg l^{-1} in planted pots in 2011 and 28 ± 9 and 26 ± 11 mg l^{-1} in unplanted pots (Fig. 1 a, b). These values are lower than the nominal added 721, 288, and 144 mg l^{-1} TCE. Additionally, slightly increasing TCE concentrations were observed within the first days in 2011. The potential reasons likely were (i) TCE loss during filling of the pots via volatilization, (ii) incomplete dissolution of TCE in the solutions. Two sinks with minor influence may have been (iii) dilution by residual water in the sand, or (iv) adsorption of TCE on organic matter (Brigmon *et al.* 2003) impurities in the sand layer. TCE solutions were filled directly into the inorganic sand layer, but thereafter minor amounts of organic matter moved from the top soil layer into the quartz sand layer. The TCE concentration in water decreased with time (Fig. 1 a, b). More than 95 % of TCE was eliminated during the experiment in the planted pots, whereas TCE concentrations in unplanted pots with wet and dry compost did not decrease. Willows took up TCE from the water phase. The TCE concentrations decreased according to the calculated dilution effect caused by watering with TCE-free water (Fig. S1). The dilution was computed based on the initially measured TCE concentrations. In conclusion, the TCE decrease was controlled by transpiration. Loss of TCE by evaporation was negligible, independent of the water content of the compost layer (wet or dry).

Evapotranspiration (ET) rates of planted pots were constant at 0.42 ± 0.05 l day^{-1} during the whole experimental period in 2010. In 2011, pots with initial concentration of 76 mg l^{-1} TCE showed significantly reduced ET of 0.38 ± 0.05 l day^{-1}, whilst ET of other planted pots was constant at 0.50 ± 0.09 l day^{-1} in the first 9 days. This probably reflects the coincidentally lower leaf area of 76 mg l^{-1} TCE-treated plants. Independent of the TCE concentration, the ET rate dropped after 9 days to 0.22 ± 0.04 l day^{-1}, probably the result of the reduced leaf area due to sampling of plant tissues as well as a continuously decreasing air temperature. Maximum temperature outside the greenhouse dropped from ~31°C to 20°C and minimum temperature from ~17°C to 13°C (ZAMG - Zentralanstalt für Meterologie und Geodynamik, Austria 2012). Leaf area data of single willow plants were unknown, hindering a more precise evaluation of the influence of TCE concentration on ET and a normalization of transpiration rates. Evaporation in unplanted pots in 2011 was 0.071 ± 0.007 l day^{-1} when the overlying compost layer was wet and 0.035 ± 0.005 l day^{-1} when the compost layer was dry. Hence, compared to the ET of planted pots, total evaporation (liters) in unplanted pots accounted for 13% of ET (wet compost) and 6% of ET (dry compost) in total.

Plant metabolism of TCE

Plants, even plants from control pots from the experiment in 2011, contained between one and two nmol g^{-1} TCE without showing temporal changes (Fig. S2 a, b). We assume that TCE that was incorporated in control plants derived from TCE that was transpired by plants with TCE addition because all plants were grown within the same greenhouse chamber. A stomatal uptake of TCE was already shown by Su *et al.* (2010). TCE cross contamination during the extraction procedure was ruled out by blank extractions without plant material. Total TCOH concentrations in leaf and bark samples of plants spiked with 76 mg l^{-1} TCE varied between 1.5 and 0.3 nmol g^{-1} without a distinguishable temporal pattern (Fig. S2 a,b). TCOH concentrations in plants that were spiked with 21 mg l^{-1} TCE decreased from day 9 to day 29 from 0.56 to 0.06 nmol g^{-1} in leaf samples ($p \leq 0.05$) and from 0.25 to 0.02 nmol g^{-1} in bark samples (insufficient data for statistical analysis). TCOH was not detected in leaf samples of control plants and was negligible (<0.08 nmol g^{-1}) in bark samples of control plants. TCOH was mostly glycolized: non glycolized TCOH accounted for 22 ± 15% of TCOH in leaves and for 4 ± 3% in bark. In 2010, plant tissue was sampled 45 days after TCE addition. No TCE was found in these samples, and TCOH was detected in small amounts (<0.5 nmol g^{-1}) solely in leaves and bark of plants that were spiked with high TCE concentrations (Fig. S2 a, b). We assume that residual volatile analytes - TCE and non-glycolized TCOH—were further metabolized as proposed by

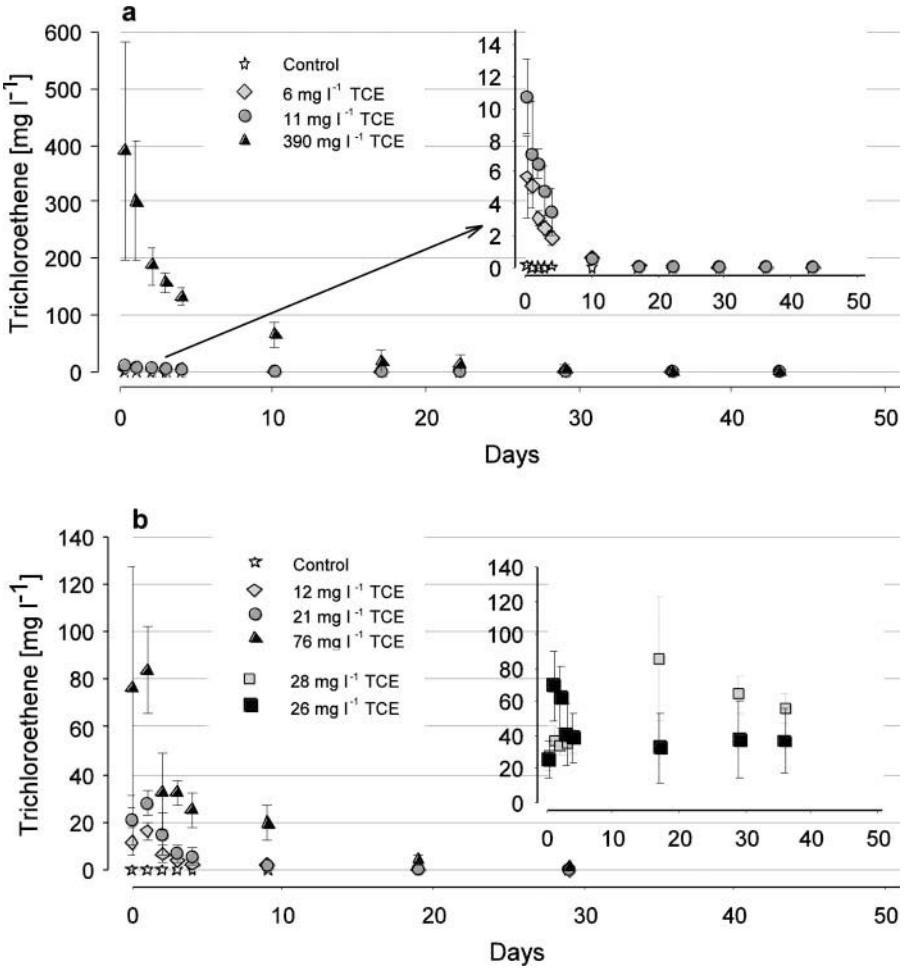

Figure 1. Measured TCE concentrations of the experiments in (a) 2010 and (b) 2011. In (a) 2010 the insert shows control pots without TCE (stars), pots with initially measured TCE concentrations of 6 mg l^{-1} (◊) and pots concentration of 11 mg l^{-1} (◯). In (b) 2011 the insert shows unplanted pots with initial TCE concentrations of 28 mgl l^{-1} (gray = dry compost layer) and 26 mgl l^{-1} (black = wet compost layer). Concentrations stated in the legend refer to initial measurements of TCE concentrations. Symbols show mean ± standard deviation (n = 5).

Shang *et al.* (2001) and vaporized out of plant tissues. This was congruent with TCE water concentrations, which approached near-zero values after 30 days (Fig. 1 a, b). This explains why TCE was hardly detectable after 45 days in 2010 and why TCOH concentrations decreased in 2011.

In contrast, concentrations of the non-volatile metabolites DCAA and TCAA in leaf samples of 2011 increased with time (Fig. S2 a), albeit not significantly. Bark sample DCAA concentrations increased between days 9 and 19 and decreased between days 19 and 29, whereas TCAA bark concentrations decreased (but not significantly) between days 9 and 29. DCAA concentrations in leaf and bark samples were between 0.5 and 3.0 nmol g^{-1} and TCAA concentrations between 0.5 and 8 nmol g^{-1}, whilst control sample concentrations were < 0.3 nmol g^{-1} in 2011 (Fig. S2). Differences between DCAA and TCAA concentrations of controls and TCE-spiked samples were significant for DCAA bark samples and TCAA leaf samples, but not for DCAA leaf samples or TCAA bark samples. In 2010, 45 days after TCE addition, DCAA and TCAA were mainly found in leaves and hardly in bark samples. Detailed concentrations of samples from 2010 are illustrated in (Fig. S2 a, b).

Using solvent extractions, only a small amount of incorporated analytes are extractable (Orchard *et al.* 2000). Regarding TCE extraction, efficiencies between 50 and 90 % can be assumed (Gopalakrishnan, Werth and Negri 2009). The sum of TCE and its metabolites were compared to the initially dosed molar TCE equivalents. The measured amounts in plant biomass represented a very minor part of the TCE eliminated from the aqueous phase, which agrees with previous studies (James *et al.* 2009; Newman *et al.* 1997, 1999; Shang *et al.* 2001). In 2010, summed metabolites of leaves and bark accounted for 0.57 % in the case of 11 mg l^{-1} TCE dosage and for 0.04% at 390 mg l^{-1} TCE dosage. In 2011, extracts accounted for 0.9% at 21 mg l^{-1} and for 0.28% at 76 mg l^{-1}. Total amounts per willow (nmol) were determined by extrapolating of TCE and its metabolite concentrations from the last extractions on day 45 in 2010 and on day 29 in 2011 to total biomass. To calculate total TCE and metabolite amounts, a total leaf mass per willow of 0.1 kg and total bark mass of 1 kg were estimated.

Previous studies showed great differences regarding transformation and transpiration of chlorinated hydrocarbons by plants, whereby differences were even obtained between different genotypes of willow and poplar (Miller *et al.* 2011). Some

authors obtained high transpiration rates (Ma and Burken 2003; Orchard *et al.* 2000; Wang *et al.* 2004; Winters 2008), while others found that trees are capable of metabolizing TCE (Gordon *et al.* 1998; Newman *et al.* 1997; Shang and Gordon 2002; Shang *et al.* 2001) and that near-zero transpiration of CHCs is possible (James *et al.* 2009; Newman *et al.* 1999; Orchard *et al.* 2000). Our data showed higher TCE loss via transpiration compared to plant metabolization. Once in the atmosphere TCE reacts with photochemically produced hydroxyl radicals. Due to this process TCE shows half-life times of a few days (Brunce and Schneider 1994). The major products of atmospheric oxidation were dichloroacetyl chloride, formyl chloride and phosgene (Christiansen and Francisco 2010), the latter being very toxic. To overcome the limitation of excessive TCE transpiration it seems promising to investigate the combination of phytoremediation with plant-associated remediation technologies. Thus, supporting microbial degradation in the rhizosphere can increase CHC decontamination (Anderson and Walton 1995; Lee, Wood and Chen 2006; Walton and Anderson 1990; Yee, Maynard and Wood 1998). Previous studies showed that almost all perchloroethene (PCE) or carbon tetrachloride could be degraded in the rhizosphere of poplars (Orchard *et al.* 2000; Wang *et al.* 2004), especially if supporting soil amendments as fertilizers or vegetable oil were applied (Brigmon *et al.* 2003). Furthermore, inoculating trees with endophytic microorganisms may be necessary to ensure sufficient degradation of chlorinated hydrocarbons (Barac *et al.* 2004; Doty 2008; Kang, Khan, and Doty 2012; Khan and Doty 2011; Weyens *et al.* 2010a,b; Weyens *et al.* 2009a,b,c).

Microbial degradation of TCE in the rhizosphere

In 2010, the δ^{13}C-values of TCE in water were −29.9 ± 0.9 ‰ and in 2011 113.7 ± 0.7 ‰. No temporal trend was evident. In addition, no degradation metabolites, such as dichloroethene, were found in the water. Consequently, microbial degradation is negligible as an elimination pathway in the water of our experimental pots. This conclusion was strengthened by constant δ^{13}C values of soil microbial PLFAs (phospholipid fatty acids). ^{13}C/^{12}C ratios of single PLFAs were between –25 and –30 ‰, i.e., close to the natural δ^{13}C values of plant-derived organic carbon. No ^{13}C-labeled TCE (δ^{13}C = 110.3 ‰) was incorporated into the microbial biomembranes.

The PLFA composition was mainly influenced by the set-up time and/or planting of pots (unplanted pots were set-up one year later) and by the different layers (sand and compost, wet and dry compost); TCE concentration had only minor effects (Fig. 2). The amounts of PLFAs in the sand and compost layer were significantly higher in planted (older) versus unplanted (newer) pots (Fig. 2). No significant differences in PLFA concentration were recorded between unplanted pots with wet or dry compost, and PLFA values were significantly higher in the compost than in the sand layer, independent of other factors (Fig. 2). With increasing TCE concentration, PLFA values in the compost layer decreased, but increased in the sand layer (Fig. 2, Fig. 3). Significant effect of various TCE concentrations on PLFA amounts was not confirmed by Tamhane post doc tests.

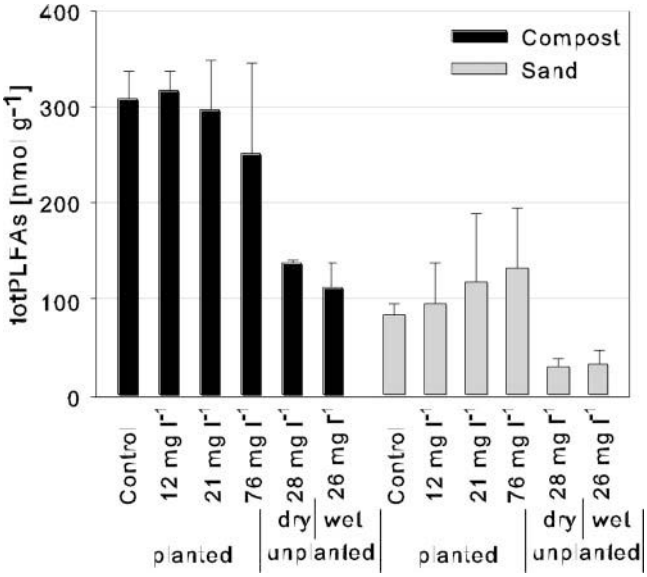

Figure 2. Amount of total microbial biomass (total PLFAs) in compost (black) and sand (gray) in 2011 in replicates with 0, 12, 21, and 76 mg l^{-1} TCE. "Dry" represents compost and sand layers of unplanted pots with dry compost layer. "Wet" represents compost and sand layers of unplanted pots with wet compost layer. Error bars represent standard deviation.

Summarizing, (i) TCE was apparently not degraded by microbes and (ii) the slight influence of TCE on PLFA amounts probably reflected secondary effects in our pot experiment.

Phytotoxicity of TCE

Chlorophyll fluorescence was used as a method for measuring plant stress at the leaf level. Values of F_v/F_m (i.e. actual photochemical potential of PS2) were 0.82 ± 0.03 in 2010 and 0.84 ± 0.02 in 2011, indicating non-stressed leaves at all TCE concentrations. F_v/F_m values did not differ significantly under different TCE concentrations, neither in 2010 nor in 2011 on any measuring day. Hence, TCE had no influence on photosynthesis or on plant stress status, which is consistent with the observation that TCE did not influence transpiration substantially. Six days after TCE application in 2010, however, fluorescence values decreased significantly, but values still indicated non-stressed leaves (Fig. 4).

Conclusion

Willows took up TCE without excluding TCE during the transpiration process, whereby even high TCE concentrations of about 390 mg l^{-1} did not cause detectable toxic effects in plants. In our experiments, TCE was only minimally metabolized by willows. The degradation efficiency of TCE in the plants may be higher at the field scale due to bigger tree size and lower TCE concentrations. Nevertheless, our results suggest that, metabolization by willows may be insufficient what can cause transition of high amounts of CHC from water to the atmosphere via the transpiration pathway. To prevent such transition and to ensure total decontamination within the phytoremediation process, enhancing microbial degradation in the rhizosphere and by CHC-degrading endophytes might be a future promising strategy.

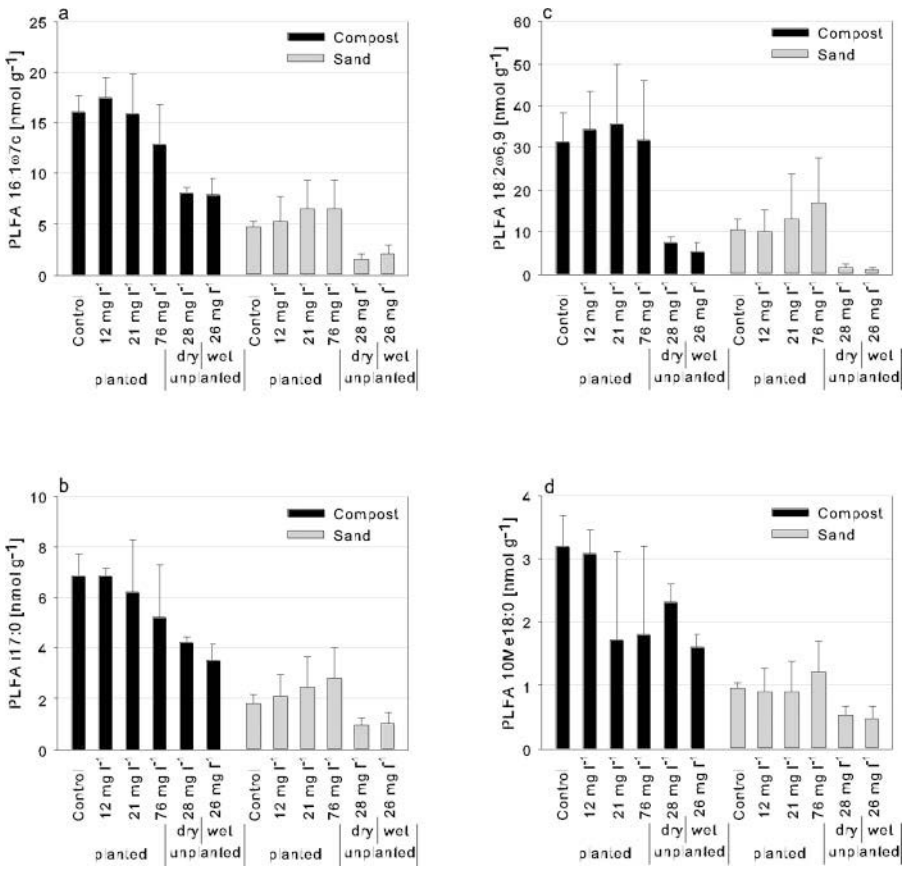

Figure 3. Amounts of microbial PLFAs (a)16:1ω7c (gram negative bacteria), (b) i17:0 (gram positive bacteria), (c) 18:2ω6,9 (saprophytic fungi biomarker) and (d) 10Me18:0 (actinomycetes) biomass in compost (black) and sand (gray). "Dry" represents compost and sand layers of unplanted pots with dry compost layer. "Wet" represents compost and sand layers of unplanted pots with wet compost layer.

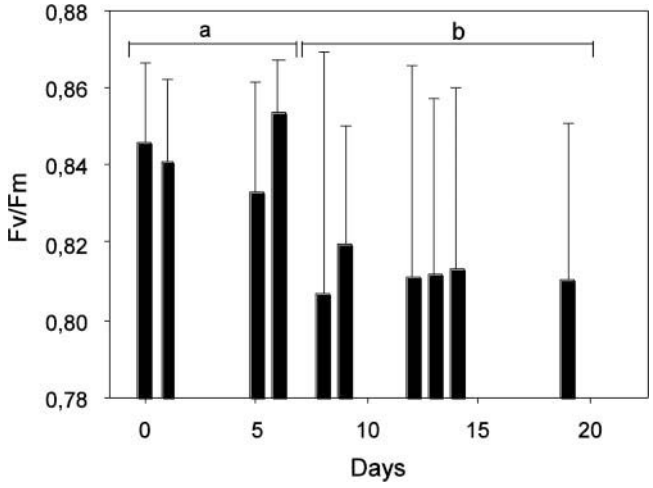

Figure 4 Chlorophyll fluorescence values in 2010. Bars show means ± standard deviations of each measuring day (n = between 30–67). Two groups were identified (a, b) showing slightly decreased Fv/Fm values after day 8 (Tamhane post-hoc test, $n < 0.05$).

Acknowledgment

The authors thank Sonja Feichtmaier, Joachim Heindler, Christian Mayer, Patrick Kobe, Christopher Nastl, Martha Klampfer, and Anton Grahsl for technical support.

Funding

This research was funded by the Federal Ministry of Agriculture, Forestry, Environment and Water Management of Austria. Funding Management by KPC Kommunalkredit Public Consulting (project number A820014).

Conflict of interest

The authors declare that they have no conflict of interest.

References

Anderson TA, Walton BT. 1995. Comparative fate of [^{14}C] trichloroethylene in the root zone of plants from a former solvent disposal site. Environ Toxicol Chem 14:2041–2047.

Barac T, Taghavi S, Borremans B, Provoost A, Oeyen L, Colpaert JV, Vangronsveld J, Van der Lelie D. 2004. Engineered endophytic bacteria improve phytoremediation of water-soluble, volatile, organic pollutants. Nat Biotechnol 22:583–588.

Bligh EG, Dyer WJ. 1959. A rapid method of total lipid extraction and purification. Can J Biochem Physiol 37:911–917.

Briggs GG, Bromilow RH, Evans AA. 1982. Relationships between lipophilicity and root uptake and translocation of non-ionised chemicals by barley. Pestic Sci 13:495–504.

Brigmon LR, Saunders FM, Altman D, Wilde E, Berry CJ, Franck M, McKinsey P, Burdick S, Loeffler F, Harris S. 2003. United States Department of Energy. FY02 Final Report on Phytoremediation of Chlorinated Ethenes in Southern Sector Seepline Sediments of the Savannah River Site.

Brunce NJ, Schneider UA. 1994. Chemical lifetime of chlorinated aliphatic priority pollutants in the Canadian troposphere. J Photochem Photobiology A 81:93–101.
Christiansen CJ, Francisco JS. 2010. Atmospheric oxidation of trochloroethylene: An ab initio study. J Phys Chem 114:9163–9176.
Dettenmaier EM, Doucette WJ, Bugbee B. 2009. Chemical hydrophobicity and uptake by plant roots. Environ Sci Technol 43:324–329.
Dietz AC, Schnoor JL. 2001. Phytotoxicity of chlorinated aliphatics to hybrid poplar (Populus deltoides x nigra DN34). Environ Toxicol Chem 20:389–393.
Doty SL. 2008. Enhancing phytoremediation through the use of transgenics and endophytes. New Phytol 179:318–333.
Frostegård Å, Tunlid A, Bååth E. 1991. Microbial biomass measured as total lipid phosphate in soils of different organic content. J Microbiol Methods 14:151–163.
Godsy EM, Warren E, Paganelli VV. 2003. The role of microbial reductive dechlorination of TCE at a phytoremediation site. Int J Phytorem 5:73–87.
Gopalakrishnan G, Werth CJ, Negri MC. 2009. Mass recovery methods for trichloroethylene in plant tissue. Environ Toxicol Chem 28:1185–1190.
Gordon M, Choe N, Duffy J, Ekuan G, Heilman P, Muiznieks IA, Ruszaj M, Shurtleff BB, Strand SE, Wilmoth J, Newman LA. 1998. Phytoremediation of trichloroethylene with hybrid poplars. Environ Health Perspect Suppl 106:1001–1004.
Hsu FC, Marxmiller RL, Yang AY. 1990. Study of root uptake and xylem translocation of cinmethylin and related compounds in detopped soybean roots using a pressure chamber technique. Plant Physiol 93:1573–1578.
Hunkeler D, Aravena R. 2000. Determination of compound-specific carbon isotope ratios of chlorinated methanes, ethanes, and ethenes in aqueous samples. Environ Sci Technol 34:2839–2844.
Hunkeler D, Aravena R, Butler BJ. 1999. Monitoring microbial dechlorination of tetrachloroethene (PCE) in groundwater using compound-specific stable carbon isotope ratios: microcosm and field studies. Environ Sci Technol 33:2733–2738.
James CA, Xin G, Doty SL, Muiznieks I, Newman L, Strand SE. 2009. A mass balance study of the phytoremediation of perchloroethylene-contaminated groundwater. Environ Pollut (Oxford UK) 157:2564–2569.
Kang JW, Khan Z, Doty SL. 2012. Biodegradation of trichloroethylene by an endophyte of hybrid poplar. Appl Environ Microbiol 78:3504–3507.
Khan Z, Doty S. 2011. Endophyte-assisted phytoremediation. Curr Top Plant Biol 12:97–105.
Lee W, Wood TK, Chen W. 2006. Engineering TCE-degrading rhizobacteria for heavy metal accumulation and enhanced TCE degradation. Biotechnol Bioeng 95:399–403.
Ma X, Burken J. 2004. Modeling of TCE Diffusion to the atmosphere and distribution in plant stems. Environ Sci Technol 38:4580–4586.
Ma X, Burken JG. 2003. TCE diffusion to the atmosphere in phytoremediation applications. Environ Sci Technol 37:2534–2539.
Matthews DW, Massmann J, Strand SE. 2003. Influence of aquifer properties on phytoremediation effectiveness. Groundwater 41:41–47.
McCully ME. 1999. Roots in soil: Unearthing the complexities of roots and their rhizospheres. Annu Rev Plant Physiol Plant Mol Biol 50:695–718.
Meckenstock RU, Morasch B, Griebler C, Richnow HH. 2004. Stable isotope fractionation analysis as a tool to monitor biodegradation in contaminated acquifers. J Contam Hydrol 75:215–255.
Miller RS, Khan Z, Doty SL. 2011. Comparison of trichloroethylene toxicity, removal and degradation by varieties of Populus and Salix for improved phytoremediation applications. J Biorem Biodegrad S7:1–8.
Newman LA, Reynolds CM. 2004. Phytodegradation of organic compounds. Curr Opin Biotechnol 15:225–230.
Newman LA, Strand SE, Choe N, Duffy J, Ekuan G, Ruszaj M, Shurtleff BB, Wilmoth J, Heilman P, Gordon MP. 1997. Uptake and biotransformation of trichloroethylene by hybrid poplars. Environ Sci Technol 31:1062–1067.
Newman LA, Wang X, Muiznieks IA, Ekuan G, Ruszaj M, Cortellucci R, Domroes D, Karscig G, Newman T, Crampton RS, Hashmonay RA, Yost MG, Heilman PE, Duffy J, Gordon MP, Strand SE. 1999. Remediation of trichloroethylene in an artificial aquifer with trees: A controlled field study. Environ Sci Technol 33:2257–2265.
Orchard BJ, Doucette WJ, Chard JK, Bugbee B. 2000. Uptake of trichloroethylene by hybrid poplar trees grown hydroponically in flow-through plant growth chambers. Environ Toxicol Chem 19:895–903.
Reichenauer TG, Germida JJ. 2008. Phytoremediation of organic contaminants in soil and groundwater. ChemSusChem 1:708–717.
Sandermann H. 1992. Plant metabolism of xenobiotics. Trends Biochem Sci 17:82–84.
Shang TQ, Gordon MP. 2002. Transformation of [14C] trichloroethylene by poplar suspension cells. Chemosphere 47:957–962.
Shang TQ, Doty SL, Wilson AM, Howald WN, Gordon MP. 2001. Trichloroethylene oxidative metabolism in plants: the trichloroethanol pathway. Phytochemistry (Elsevier) 58:1055–1065.
Shang TQ, Gordon MP. 2002. Transformation of [14C] trichloroethylene by poplar suspension cells. Chemosphere 47:957–962.
Su YH, Liu T, Liang YC. 2010. Transport via xylem of trichloroethylene in wheat, corn, and tomato seedlings. J Hazard Mater 182:472–476.
Walton BT, Anderson TA. 1990. Microbial degradation of trichloroethylene in the rhizosphere: potential application to biological remediation of waste sites. Appl Environ Microbiol 56:1012–1016.
Wang X, Dossett MP, Gordon MP, Strand SE. 2004. Fate of carbon tetrachloride during phytoremediation with poplar under controlled field conditions. Environ Sci Technol 38:5744–5749.
Watzinger A, Feichtmair S, Kitzler B, Zehetner F, Kloss S, Wimmer B, Zechmeister-Boltenstern S, Soja G. 2014. Soil microbial communities responded to biochar application in temperate soils and slowly metabolized ^{13} C-labelled biochar as revealed by ^{13} C PLFA analyses: results from a short-term incubation and pot experiment: Response of soil microbial communities to biochar. Eur J Soil Sci 65:40–51.
Weisgram M, Brandner P, Foditsch S, Dörrie T, Müller D. 2012. Umweltbundesamt and Österreichischer Verein für Altlastenmanagement, Vienna. Arbeitshilfe - CKW kontaminierte Standorte, Erkundung, Beurteilung und Sanierung.
Weyens N, Taghavi S, Barac T, Lelie D, Boulet J, Artois T, Carleer R, Vangronsveld J. 2009a. Bacteria associated with oak and ash on a TCE-contaminated site: characterization of isolates with potential to avoid evapotranspiration of TCE. Environ Sci Pollut Res 16: 830–843.
Weyens N, Van der Lelie D, Artois T, Smeets K, Taghavi S, Newman L, Carleer R, Vangronsveld J. 2009b. Bioaugmentation with engineered endophytic bacteria improves contaminant fate in phytoremediation. Environ Sci Technol 43:9413–9418.
Weyens N, Van der Lelie D, Taghavi S, Vangronsveld J. 2009c. Phytoremediation: plant–endophyte partnerships take the challenge. Curr Opin Biotechnol 20:248–254.
Weyens N, Truyens S, Dupae J, Newman L, Taghavi S, Van der Lelie D, Carleer R, Vangronsveld J. 2010a. Potential of the TCE-degrading endophyte Pseudomonas putida W619-TCE to improve plant growth and reduce TCE phytotoxicity and evapotranspiration in poplar cuttings. Environ Pollut (Oxford UK) 158:2915–2919.
Weyens N, Croes S, Dupae J, Newman L, Van der Lelie D, Carleer R, Vangronsveld J. 2010b. Endophytic bacteria improve phytoremediation of Ni and TCE co-contamination. Environ Pollut (Oxford UK) 158:2422–2427.
Winters RM. 2008. Volatilization of trichloroethylene from shallow subsurface environments: trees and soil. [master's thesis]. Logan (UT): Utah State University.
Yee DC, Maynard JA, Wood TK. 1998. Rhizoremediation of trichloroethylene by a recombinant, root-colonizing pseudomonas fluorescens strain expressing toluene ortho-monooxygenase constitutively. Appl Environ Microbiol 64:112–118.
Zentralanstalt für Meterologie und Geodynamik, Austria (ZAMG). 2012. Measuring station Langenlebarn.

permeable layers. By that the DNAPL pools vanish. Once the DNAPL pools do not exist anymore the back diffusion of TCE from the less permeable layers to the more permeable layers dominates the plume formation. At this stage the mass discharge of TCE via the plume is already greatly reduced. Still the concentrations in the plume and the total amount of undissolved TCE can be quite high.

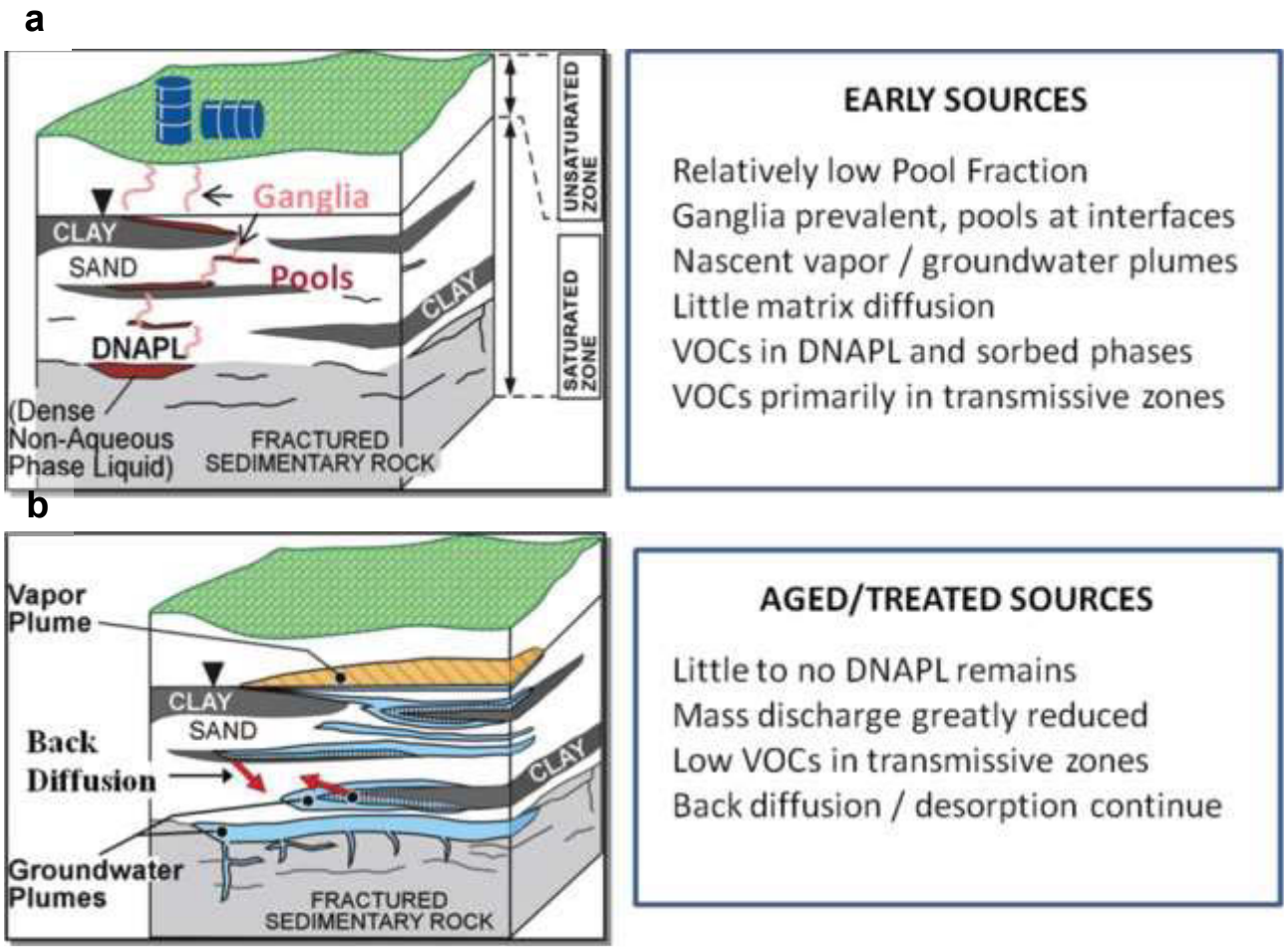

Figure 1: Evolution of a DNAPL source zone and key features of different stages (Stroo et al., 2012)

Remediation of all expected severely contaminated sites in Austria will cause estimated total costs of about 5 to 12 billion Euros (BMLFUW, 2007) if state of the art technologies will be applied for remediation of these sites. Decontamination of contaminated sites by such state of the art methods as “dig & dump” and “pump & treat” is very cost extensive. “Dig & dump” technologies are expensive since the infrastructure for digging, transport and the controlled disposal of contaminated soil is cost intensive. “Pump & treat” technologies pump contaminated water or air from the underground to the surface where the contaminated medium is treated. By that it is not possible to treat the contaminant source but solely the plume downstream of the source. The

1.2.2. Application of willow plants for remediation of TCE

Phytoremediation means using plant physiological mechanisms for the remediation of contaminated sites. By that it is possible to remediate inorganic and organic contaminations. Initially - beginning with about 1990 - phytoremediation was used mainly to remediate sites that were contaminated by heavy metals. Heavy metals can be taken up by plants and are stored in plant tissues. After harvesting of the plants it is possible to extract these heavy metals from plant tissues. Later the focus moved to organic contaminants, especially pesticides. Organic contaminants as TCE are not just stored in plant tissues but can be metabolized into other, less toxic substances. This metabolization can be compared with the metabolization of organic substances in the liver of mammals. Accordingly the "green liver concept" was established by Sandermann (1992).

In case of DNAPL contaminations, plants are planted around the source zone and downstream of the source zone (Figure 3). Plants take up the groundwater and redirect the groundwater stream towards the surface along the transpiration pathway (roots-stem-leaves-atmosphere). By that the plants act as a hydraulic barrier and prevent spreading of the dissolved DNAPL downstream. Additionally the plants can metabolize and detoxify the contaminant in their plant tissue according to the green liver concept. A site contaminated with DNAPL has to exhibit some requirements to be suitable for remediation by phytoremediation:

- The contaminated site has to be suitable for planting of trees at a scale that is big enough that the plants can act as a hydraulic barrier (surface sealing alone is no exclusion criterion).
- Rather low depth to water table so the plants can root into the aquifer
- Shallow aquifer and a low groundwater flow velocity

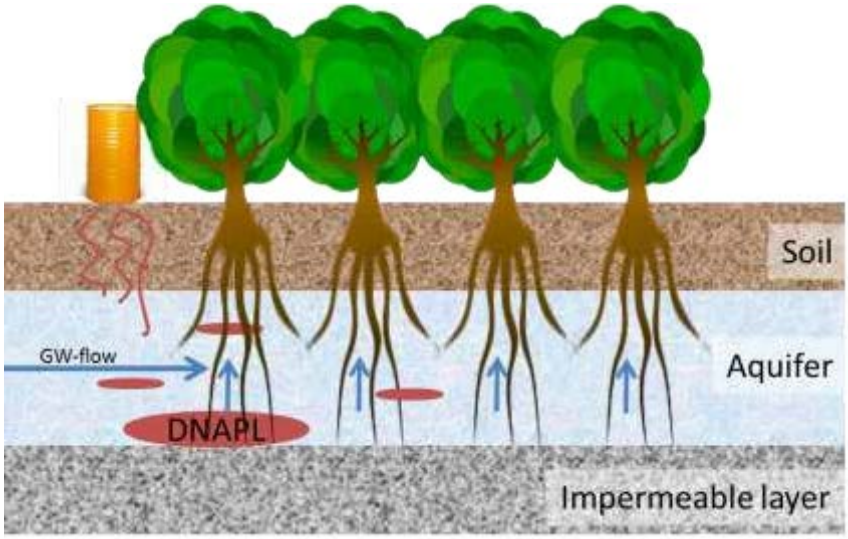

Figure 3: Schematic representation of a remediation set-up to remediate a site contaminated by DNAPL

1.2.3. Isotopic fractionation of TCE during remediation

Isotopic fractionation is an analytical tool that was used within this study. It can be used to prove if a decrease of contaminant concentrations in water is caused by degradation of the contaminant or by dilution, by adsorption or by absorption of the contaminant. This method is based on the difference of the binding energy of different stable isotopes. Isotopes are variants of a chemical element as Carbon (C) which exhibit different numbers of neutrons in the nucleus of an atom but the same number of electrons and protons. The more neutrons an atom exhibit the higher the molecular mass of the isotope. Stable isotopes are is

topes which do not decay radioactively but are stable over time. In the case of carbon two stable isotopes with higher abundance exist; one with 12 neutrons (^{12}C) and one with 13 (^{13}C) neutrons. The heavier isotope (e.g. ^{13}C) is bound stronger within the initial product (e.g. TCE) than the lighter isotope (e.g. ^{12}C). So it is harder for microbes and chemical reactants to degrade organic substances which contain the heavier isotope. Therefore the molecules containing heavier isotopes accumulate during a degradation process while the molecules containing lighter isotopes are degraded preferentially. Figure 5 illustrates exemplary the accumulation of ^{13}C containing TCE molecules during degradation of TCE in a closed system. If the concentration in water decreases without accumulation of the heavier isotope the contaminant was not degraded but diluted, adsorbed or absorbed. Volatilization of TCE causes only minor shifts in isotopic composition of the residual contaminant compared to degradation processes. The intensity of this fractionation with degradation depends on specific degradation processes and vary significantly for different microbial communities and different nZVI particle types. The extent at which stable isotopes fractionate during degradation is described as C-enrichment factor or fractionation factor. This factor has to be defined for every microbial community and particle type in lab experiments. Carbon fractionation factors have already been defined for numerous (n)ZVI particles (Dayan et al., 1999; Elsner et al., 2008; Lojkasek-Lima et al., 2012; Slater et al., 2002) and microbial communities (Harding et al., 2013; Marco-Urrea et al., 2011; Numata et al., 2002).

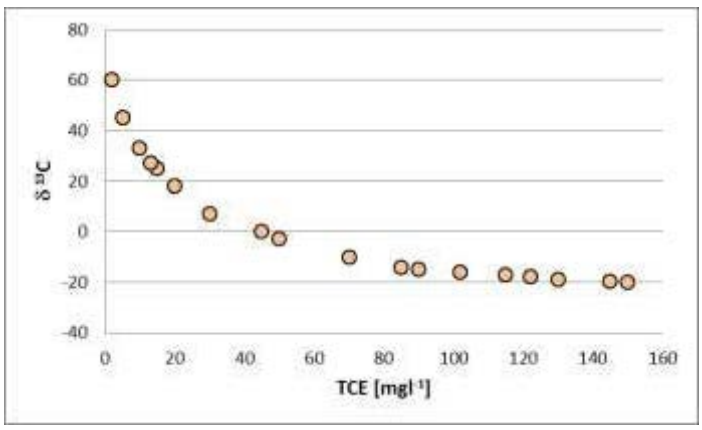

Figure 5: Schematic representation of accumulation of 13C during degradation of TCE in a closed system

INTERNATIONAL JOURNAL OF PHYTOREMEDIATION
2016, VOL. 18, NO. 7, 686–692
http://dx.doi.org/10.1080/15226514.2015.1131228

Taylor & Francis
Taylor & Francis Group

Transpiration and metabolisation of TCE by willow plants – a pot experiment

Philipp Schöftner, Andrea Watzinger, Philipp Holzknecht, Bernhard Wimmer, and Thomas G. Reichenauer

AIT Austrian Institute of Technology GmbH, Health & Environment Department, Environmental Resources & Technologies, Konrad-Lorenz-Strasse, Tulln, Austria

ABSTRACT

Willows were grown in glass cylinders filled with compost above water-saturated quartz sand, to trace the fate of TCE in water and plant biomass. The experiment was repeated once with the same plants in two consecutive years. TCE was added in nominal concentrations of 0, 144, 288, and 721 mg l^{-1}. Unplanted cylinders were set-up and spiked with nominal concentrations of 721 mg l^{-1} TCE in the second year. Additionally, ^{13}C-enriched TCE solution ($d^{13}C$ = 110.3 %) was used. Periodically, TCE content and metabolites were analyzed in water and plant biomass. The presence of TCE-degrading microorganisms was monitored via the measurement of the isotopic ratio of carbon ($^{13}C/^{12}C$) in TCE, and the abundance of ^{13}C-labeled microbial PLFAs (phospholipid fatty acids). More than 98% of TCE was lost via evapotranspiration from the planted pots within one month after adding TCE. Transpiration accounted to 94 to 78% of the total evapotranspiration loss. Almost 1% of TCE was metabolized in the shoots, whereby trichloroacetic acid (TCAA) and dichloroacetic acid (DCAA) were dominant metabolites; less trichloroethanol (TCOH) and TCE accumulated in plant tissues. Microbial degradation was ruled out by $d^{13}C$ measurements of water and PLFAs. TCE had no detected influence on plant stress status as determined by chlorophyll-fluorescence and gas exchange.

KEYWORDS
Phytoremediation; trichloroethene; Salix viminalis; degradation; PLFAs; ^{13}C

Introduction

Chlorinated hydrocarbons (CHCs), especially trichloroethene, tetrachloroethene, 1,1,1-trichloroethane and dichloromethane, are—together with hydrocarbons—the most frequent pollutants and can therefore be found at numerous industrial sites (Weisgram et al. 2012). Using plants for phytoremediation of CHCs is a cost-effective, noninvasive technology that uses sun energy to pump up contaminated groundwater. Phytoremediation of CHCs can be applied at sites that provide enough space for planting of vegetation, exhibit a shallow water table, and have a thin aquifer with low to medium discharge (Matthews, Massmann, and Strand 2003). Willow (Salix) and poplar (Populus) species have promising remediation properties due to their extensive rooting systems, high water consumption, high toxicity tolerance, rapid growth, and wide regional distribution (Miller, Khan, and Doty 2011). CHCs exhibit physical and chemical properties ideal for uptake by plant roots. These include K_{ow} values (octanol-water partition coefficient) between 1.8 (Briggs, Bromilow, and Evans 1982) and 3.1 (Hsu, Marxmiller, and Yang 1990) as well as low ionization potential, strong polarity and water solubility (Dettenmaier, Doucette, and Bugbee 2009). Once organic xenobiotics such as CHCs are taken up, plants can metabolize and integrate them into their tissue to a certain extent according to the "green liver concept" of Sandermann (1992) or mineralize them to CO_2 and H_2O (Newman et al. 1997; Shang and Gordon 2002; Shang et al. 2001). Incomplete metabolization of CHCs can cause volatilization with the transpiration stream into the atmosphere (Ma and Burken 2004; Orchard et al. 2000; Wang et al. 2004; Winters 2008). In the case of TCE uptake, oxidative transformation has already been verified for poplar and willow trees. Trichloroethanol, dichloroacetic acid, and trichloroacetic acid were the main identified products (Gordon et al. 1998; James et al. 2009; Miller et al. 2011; Newman and Reynolds 2004; Newman et al. 1997, 1999). Willows and poplars are toxicity-tolerant species that can even grow at high TCE concentrations of around 200 mg l^{-1} (Miller et al. 2011). We are unaware of further studies on the toxicity of chlorinated ethenes in willows. Studies on the physiologically similar poplars, however, revealed that 60 mg l^{-1} TCE did not influence cell growth and that 8 months exposure to 50 mg l^{-1} TCE hardly reduced plant growth of one-year-old poplar cuttings (Newman et al. 1997). Even at a TCE concentration of 550 mg l^{-1}, (Ma and Burken 2003) did not observe toxic effects in rooted poplar cuttings. In contrast, zero-growth of poplar cuttings was observed at 45 mg l^{-1} PCE, 118 mg l^{-1} TCE, 465 mg l^{-1} 1,2-trans-DCE, 543 mg l^{-1} 1,1-DCE, or 582 mg l^{-1} 1,2-cis-DCE (Dietz and Schnoor 2001). All tested concentrations for poplars were far above expected plume concentrations at field sites. Moreover, bigger trees are probably even more tolerant than the tested cuttings. Thus, according to the present state of knowledge, phytotoxic effects at field sites are unlikely. To enhance CHC degradation in plants, they can be inoculated with endophytes (Weyens et al. 2010a; Weyens et al. 2009a; Weyens

CONTACT Andrea Watzinger andrea.watzinger@ait.ac.at AIT Austrian Institute of Technology GmbH, Health & Environment Department, Environmental Resources & Technologies, Konrad-Lorenz-Strasse 24, 3430 Tulln, Austria.

Supplemental data for this article can be accessed on the publisher's website.

et al. 2009b). Plants can also be used to support microbial degradation in the rhizosphere (Anderson and Walton 1995; Godsy, Warren, and Paganelli 2003; James et al. 2009) by (i) release of plant exudates as nutrients, sugars, amino acids and secondary metabolites such as organic acids (Brigmon et al. 2003; Reichenauer and Germida 2008; Walton and Anderson 1990) and (ii) physical changes of soil structure such as gas exchange and soil moisture (McCully 1999). Since roots need oxygen for their growth, microbial degradation in the rhizosphere is assumed to largely follow an aerobic pathway. Microbial degradation leads to a shift in the signature of stable isotopes in the original contaminant towards heavier ^{13}C isotopes. Accordingly, compound specific isotope analysis (CSIA) of the isotope ratio of TCE can be used to discriminate between plant uptake and microbial degradation of CHCs (Hunkeler, Aravena, and Butler 1999; Hunkeler and Aravena 2000; Meckenstock et al. 2004). This study was designed to assess the capability of willows to remediate TCE-contaminated sites. For this purpose, willows were grown in artificial aquifers; TCE uptake, TCE transformation in plant tissues, microbial degradation of TCE in the water and plant health status were investigated following a single TCE application. The experiment was repeated within two consecutive years using the same plants. CSIA was used to distinguish between microbial degradation and TCE elimination via plant uptake.

Materials and methods

Experimental design

Rooted cuttings of willow (Salix viminalis L.) were planted in a greenhouse in glass pots which were open to the atmosphere. Each of the pots was filled with a 25 cm layer of quartz sand (0.5–2 mm) that was covered by a 20 cm compost layer (Einheitserde ED 73, Germany), whereby 2/3 of the quartz sand layer was water saturated. Pots were wrapped with aluminium foil to avoid algae growth. A similar experimental set-up was successfully used by Newman et al. (1997). Two liters of TCE-containing solution was added via a ®Teflon (PTFE) tube into each quartz layer. Before applying the TCE, water was pumped out and residual water was taken up by the plants for half a day of transpiration. Hereafter, 2 l solutions with nominal TCE concentrations of 0, 144, 288, and 721 mg l^{-1} were applied once at each pot. The water level was kept between 18 and 22 cm during the experiment by repeatedly adding TCE-free water via the PTFE tubes described above, which diluted the TCE solutions. The amount of water that was added was measured gravimetrically. The compost layer was kept free of the TCE solution. The experiment was repeated once with the same plants and pots and with 5 replicates for each concentration in two consecutive years, starting on the 23 August 2010 and the 6 July 2011. The duration of the experiment was 45 days in 2010 and 29 days in 2011. In 2011, we added unplanted pots filled with a TCE solution with a nominal concentration of 721 mg l^{-1}. These were covered with moist compost (5 replicates) and with dry compost (5 replicates). Additionally, ^{13}C-labeled TCE ($\delta^{13}C = 110.3$ ‰) was used for the experiment in 2011.

Water samples were taken via a second perforated PTFE tube that was arranged in the middle of the quartz layer as a horizontal ring. Water samples were stored in PTFE-sealed vials at 4°C until analysis of TCE concentration and isotope analysis of $\delta^{13}C$. Leaves and bark (2 g moist weight) were sampled and stored immediately in liquid N_2 until extraction and measurement of TCE, TCOH, DCAA, and TCAA. Leaves and branches (1.5 cm diameter) were collected 45 days after TCE application in 2010. The branches were dissected into bark and wood. In 2011, samples were taken from shoots of the upper compartments (0.5 cm diameter) at days 4 and 9 and of the lower compartments (0.5–1 cm diameter) at days 19 and 29 after TCE application. Also in 2011, compost samples were taken with a soil auger (Ø 25 mm) from the quartz and the compost layer of each pot and were frozen at −20°C until analysis of composition and the $^{13}C/^{12}C$ isotope ratio of phospholipid fatty acids (PLFAs). Finally, dark-adapted chlorophyll fluorescence was measured using a portable instrument on days 0, 1, 5, 6, 8, 9, 12, 13, 14, and 19 in 2010 and on day 17 in 2011 to evaluate plant stress status.

Analytical methods

Detailed information about the chemicals and materials used is listed in the supplementary data. Water samples (concentration of TCE and $\delta^{13}C$) were measured via Purge and Trap—Gas Chromatography—combustion—Isotope Ratio Mass Spectrometry (P&T-GC-c-IRMS). Here, a HP 5890 Series II GC (Hewlett-Packard, Wilmington, Delaware, USA) equipped with an oxidation oven was connected to a Delta S Isotope Ratio Mass Spectrometer (Finnigan, Bremen, Germany). Samples were injected via a VSP 4000 purge and trap unit (IMT, Innovative Messtechnik GmbH, Germany) using the following settings: 40°C sample temperature, 20 min purge time, 20 ml min^{-1} purge flow, 80°C valve temperature, –50°C trap temperature, 200°C desorption temperature, 7 min desorption time, 50 sec transfer time, 0 ml min^{-1} split flow, 200°C transfer line temperature, 1000 mbar constant helium pressure. Analytes were separated with an Agilent Technologies DB-VRX capillary column (60m, I.D. 0.32 mm, widebore film 1.8 µm) with He (5.0) as carrier gas (1.5 bar) and with the following temperature program: 200°C injection temperature, 40°C initial temperature hold for 10 min, ramp (40°C min^{-1}) to 100°C (hold for 2 min), ramp (10°C min^{-1}) to 200°C (hold for 2 min), ramp (20°C min^{-1}) to 240°C (hold for 2 min). The oxidation oven was operated at 940°C and was oxidized for 20 min with O_2 (0.4 bar) at 620°C prior to every measuring sequence. Within one measuring sequence a 2 s oxygen pulse was added to the oven after every sample at 940°C to prolong the oven's reactive period.

TCE, TCOH, DCAA, and TCAA contents of plant tissues were extracted via solvent extraction according to James et al. (2009), Newman et al. (1997) and Shang et al. (2001) with minor adaptions. Detailed information regarding extraction procedure and its adaptions can be found in SI. Analytes were detected with an Agilent Technologies 6890 gas chromatograph coupled with an Agilent Technologies 5975 inert mass selective detector (MSD) in 2010; in 2011, analytes were detected with an Agilent Technologies (USA) G1223A electron capture

detector (ECD) on a HP 5890 Series II GC (Hewlett-Packard, Wilmington, Delaware, USA). Detailed extraction and analytical procedures are described in the supplementary information.

Composition and $\delta^{13}C$ of PLFAs from compost and quartz sand samples were analyzed according to the methodology of Bligh and Dyer (1959), which was concretized by Frostegård, Tunlid, and Bååth (1991). The composition of fatty acids was detected by GC-FID (flame ionisation detector), and ^{13}C fractionation was detected by GC-c-IRMS. PLFA extraction and measurement was conducted according to Watzinger et al. (2014). Dark-adapted chlorophyll fluorescence was measured with a Handy-PEA Fluorimeter (Hansatech Instruments, Norfolk, England). Leaves were dark adapted for 20 minutes prior to measurement. Chlorophyll fluorescence measurements were used to calculate the ratio F_v/F_m as a parameter for "potential photochemical efficiency" of photosystem 2 (PS2). Here, F_m represents the maximal fluorescence level at high light intensity and F_v represents the variable fluorescence, which is derived from the difference between F_m and minimal fluorescence F_0 at darkness (F_m - $F_{0)}$.

Statistical analysis

For the PLFAs, all analytical results were calculated based on oven-dry (105°C) weight of soil. Statistics were performed with SPSS 17.0 for Windows. Impacts were tested by ANOVA and Tamhane post-hoc test because inhomogeneity of variance was confirmed. Significance was accepted at $p < 0.05$. Additionally, the factors substrate (sand - compost), plants (planted - unplanted pots) and TCE concentration (0, 144, 288, and 721 mg l^{-1}) were tested in a multivariate general linear model (full factorial model III, intercept included). Significant differences of PLFAs between TCE concentrations were determined separately for each substrate of the planted pots.

Results and discussion

Uptake of TCE by willows

The average initial TCE concentrations of replicates were 390 ± 192, 11 ± 2, and 6 ± 3 mg l^{-1} in 2010 and 76 ± 50, 21 ± 11, and 12 ± 5 mg l^{-1} in planted pots in 2011 and 28 ± 9 and 26 ± 11 mg l^{-1} in unplanted pots (Fig. 1 a, b). These values are lower than the nominal added 721, 288, and 144 mg l^{-1} TCE. Additionally, slightly increasing TCE concentrations were observed within the first days in 2011. The potential reasons likely were (i) TCE loss during filling of the pots via volatilization, (ii) incomplete dissolution of TCE in the solutions. Two sinks with minor influence may have been (iii) dilution by residual water in the sand, or (iv) adsorption of TCE on organic matter (Brigmon et al. 2003) impurities in the sand layer. TCE solutions were filled directly into the inorganic sand layer, but thereafter minor amounts of organic matter moved from the top soil layer into the quartz sand layer. The TCE concentration in water decreased with time (Fig. 1 a, b). More than 95 % of TCE was eliminated during the experiment in the planted pots, whereas TCE concentrations in unplanted pots with wet and dry compost did not decrease. Willows took up TCE from the water phase. The TCE concentrations decreased according to the calculated dilution effect caused by watering with TCE-free water (Fig. S1). The dilution was computed based on the initially measured TCE concentrations. In conclusion, the TCE decrease was controlled by transpiration. Loss of TCE by evaporation was negligible, independent of the water content of the compost layer (wet or dry).

Evapotranspiration (ET) rates of planted pots were constant at 0.42 ± 0.05 l day^{-1} during the whole experimental period in 2010. In 2011, pots with initial concentration of 76 mg l^{-1} TCE showed significantly reduced ET of 0.38 ± 0.05 l day^{-1}, whilst ET of other planted pots was constant at 0.50 ± 0.09 l day^{-1} in the first 9 days. This probably reflects the coincidentally lower leaf area of 76 mg l^{-1} TCE-treated plants. Independent of the TCE concentration, the ET rate dropped after 9 days to 0.22 ± 0.04 l day^{-1}, probably the result of the reduced leaf area due to sampling of plant tissues as well as a continuously decreasing air temperature. Maximum temperature outside the greenhouse dropped from ~31°C to 20°C and minimum temperature from ~17°C to 13°C (ZAMG - Zentralanstalt für Meterologie und Geodynamik, Austria 2012). Leaf area data of single willow plants were unknown, hindering a more precise evaluation of the influence of TCE concentration on ET and a normalization of transpiration rates. Evaporation in unplanted pots in 2011 was 0.071 ± 0.007 l day^{-1} when the overlying compost layer was wet and 0.035 ± 0.005 l day^{-1} when the compost layer was dry. Hence, compared to the ET of planted pots, total evaporation (liters) in unplanted pots accounted for 13% of ET (wet compost) and 6% of ET (dry compost) in total.

Plant metabolism of TCE

Plants, even plants from control pots from the experiment in 2011, contained between one and two nmol g^{-1} TCE without showing temporal changes (Fig. S2 a, b). We assume that TCE that was incorporated in control plants derived from TCE that was transpired by plants with TCE addition because all plants were grown within the same greenhouse chamber. A stomatal uptake of TCE was already shown by Su et al. (2010). TCE cross contamination during the extraction procedure was ruled out by blank extractions without plant material. Total TCOH concentrations in leaf and bark samples of plants spiked with 76 mg l^{-1} TCE varied between 1.5 and 0.3 nmol g^{-1} without a distinguishable temporal pattern (Fig. S2 a,b). TCOH concentrations in plants that were spiked with 21 mg l^{-1} TCE decreased from day 9 to day 29 from 0.56 to 0.06 nmol g^{-1} in leaf samples ($p \leq 0.05$) and from 0.25 to 0.02 nmol g^{-1} in bark samples (insufficient data for statistical analysis). TCOH was not detected in leaf samples of control plants and was negligible (<0.08 nmol g^{-1}) in bark samples of control plants. TCOH was mostly glycolized: non glycolized TCOH accounted for 22 ± 15% of TCOH in leaves and for 4 ± 3% in bark. In 2010, plant tissue was sampled 45 days after TCE addition. No TCE was found in these samples, and TCOH was detected in small amounts (<0.5 nmol g^{-1}) solely in leaves and bark of plants that were spiked with high TCE concentrations (Fig. S2 a, b). We assume that residual volatile analytes - TCE and non-glycolized TCOH—were further metabolized as proposed by

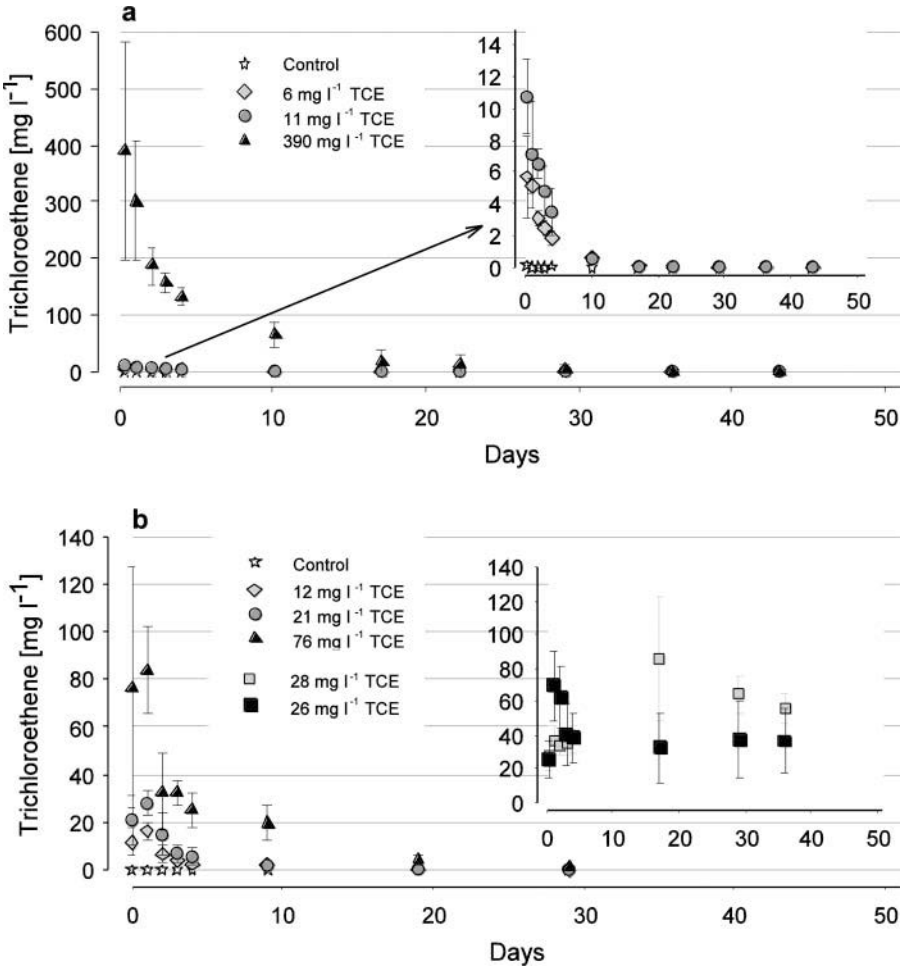

Figure 1. Measured TCE concentrations of the experiments in (a) 2010 and (b) 2011. In (a) 2010 the insert shows control pots without TCE (stars), pots with initially measured TCE concentrations of 6 mg l^{-1} (◊) and pots concentration of 11 mg l^{-1} (◯). In (b) 2011 the insert shows unplanted pots with initial TCE concentrations of 28 mgl l^{-1} (gray = dry compost layer) and 26 mgl l^{-1} (black = wet compost layer). Concentrations stated in the legend refer to initial measurements of TCE concentrations. Symbols show mean ± standard deviation (n = 5).

Shang et al. (2001) and vaporized out of plant tissues. This was congruent with TCE water concentrations, which approached near-zero values after 30 days (Fig. 1 a, b). This explains why TCE was hardly detectable after 45 days in 2010 and why TCOH concentrations decreased in 2011.

In contrast, concentrations of the non-volatile metabolites DCAA and TCAA in leaf samples of 2011 increased with time (Fig. S2 a), albeit not significantly. Bark sample DCAA concentrations increased between days 9 and 19 and decreased between days 19 and 29, whereas TCAA bark concentrations decreased (but not significantly) between days 9 and 29. DCAA concentrations in leaf and bark samples were between 0.5 and 3.0 nmol g^{-1} and TCAA concentrations between 0.5 and 8 nmol g^{-1}, whilst control sample concentrations were < 0.3 nmol g^{-1} in 2011 (Fig. S2). Differences between DCAA and TCAA concentrations of controls and TCE-spiked samples were significant for DCAA bark samples and TCAA leaf samples, but not for DCAA leaf samples or TCAA bark samples. In 2010, 45 days after TCE addition, DCAA and TCAA were mainly found in leaves and hardly in bark samples. Detailed concentrations of samples from 2010 are illustrated in (Fig. S2 a, b).

Using solvent extractions, only a small amount of incorporated analytes are extractable (Orchard et al. 2000). Regarding TCE extraction, efficiencies between 50 and 90 % can be assumed (Gopalakrishnan, Werth and Negri 2009). The sum of TCE and its metabolites were compared to the initially dosed molar TCE equivalents. The measured amounts in plant biomass represented a very minor part of the TCE eliminated from the aqueous phase, which agrees with previous studies (James et al. 2009; Newman et al. 1997, 1999; Shang et al. 2001). In 2010, summed metabolites of leaves and bark accounted for 0.57 % in the case of 11 mg l^{-1} TCE dosage and for 0.04% at 390 mg l^{-1} TCE dosage. In 2011, extracts accounted for 0.9% at 21 mg l^{-1} and for 0.28% at 76 mg l^{-1}. Total amounts per willow (nmol) were determined by extrapolating of TCE and its metabolite concentrations from the last extractions on day 45 in 2010 and on day 29 in 2011 to total biomass. To calculate total TCE and metabolite amounts, a total leaf mass per willow of 0.1 kg and total bark mass of 1 kg were estimated.

Previous studies showed great differences regarding transformation and transpiration of chlorinated hydrocarbons by plants, whereby differences were even obtained between different genotypes of willow and poplar (Miller et al. 2011). Some

authors obtained high transpiration rates (Ma and Burken 2003; Orchard et al. 2000; Wang et al. 2004; Winters 2008), while others found that trees are capable of metabolizing TCE (Gordon et al. 1998; Newman et al. 1997; Shang and Gordon 2002; Shang et al. 2001) and that near-zero transpiration of CHCs is possible (James et al. 2009; Newman et al. 1999; Orchard et al. 2000). Our data showed higher TCE loss via transpiration compared to plant metabolization. Once in the atmosphere TCE reacts with photochemically produced hydroxyl radicals. Due to this process TCE shows half-life times of a few days (Brunce and Schneider 1994). The major products of atmospheric oxidation were dichloroacetyl chloride, formyl chloride and phosgene (Christiansen and Francisco 2010), the latter being very toxic. To overcome the limitation of excessive TCE transpiration it seems promising to investigate the combination of phytoremediation with plant-associated remediation technologies. Thus, supporting microbial degradation in the rhizosphere can increase CHC decontamination (Anderson and Walton 1995; Lee, Wood and Chen 2006; Walton and Anderson 1990; Yee, Maynard and Wood 1998). Previous studies showed that almost all perchloroethene (PCE) or carbon tetrachloride could be degraded in the rhizosphere of poplars (Orchard et al. 2000; Wang et al. 2004), especially if supporting soil amendments as fertilizers or vegetable oil were applied (Brigmon et al. 2003). Furthermore, inoculating trees with endophytic microorganisms may be necessary to ensure sufficient degradation of chlorinated hydrocarbons (Barac et al. 2004; Doty 2008; Kang, Khan, and Doty 2012; Khan and Doty 2011; Weyens et al. 2010a,b; Weyens et al. 2009a,b,c).

Microbial degradation of TCE in the rhizosphere

In 2010, the $\delta^{13}C$-values of TCE in water were −29.9 ± 0.9 ‰ and in 2011 113.7 ± 0.7 ‰. No temporal trend was evident. In addition, no degradation metabolites, such as dichloroethene, were found in the water. Consequently, microbial degradation is negligible as an elimination pathway in the water of our experimental pots. This conclusion was strengthened by constant $\delta^{13}C$ values of soil microbial PLFAs (phospholipid fatty acids). $^{13}C/^{12}C$ ratios of single PLFAs were between –25 and –30 ‰, i.e., close to the natural $\delta^{13}C$ values of plant-derived organic carbon. No ^{13}C-labeled TCE ($\delta^{13}C$ = 110.3 ‰) was incorporated into the microbial biomembranes.

The PLFA composition was mainly influenced by the set-up time and/or planting of pots (unplanted pots were set-up one year later) and by the different layers (sand and compost, wet and dry compost); TCE concentration had only minor effects (Fig. 2). The amounts of PLFAs in the sand and compost layer were significantly higher in planted (older) versus unplanted (newer) pots (Fig. 2). No significant differences in PLFA concentration were recorded between unplanted pots with wet or dry compost, and PLFA values were significantly higher in the compost than in the sand layer, independent of other factors (Fig. 2). With increasing TCE concentration, PLFA values in the compost layer decreased, but increased in the sand layer (Fig. 2, Fig. 3). Significant effect of various TCE concentrations on PLFA amounts was not confirmed by Tamhane post doc tests.

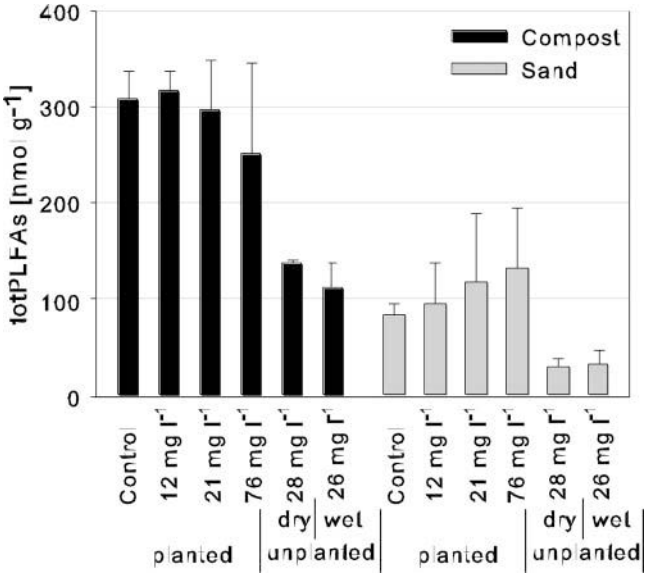

Figure 2. Amount of total microbial biomass (total PLFAs) in compost (black) and sand (gray) in 2011 in replicates with 0, 12, 21, and 76 mg l^{-1} TCE. "Dry" represents compost and sand layers of unplanted pots with dry compost layer. "Wet" represents compost and sand layers of unplanted pots with wet compost layer. Error bars represent standard deviation.

Summarizing, (i) TCE was apparently not degraded by microbes and (ii) the slight influence of TCE on PLFA amounts probably reflected secondary effects in our pot experiment.

Phytotoxicity of TCE

Chlorophyll fluorescence was used as a method for measuring plant stress at the leaf level. Values of F_v/F_m (i.e. actual photochemical potential of PS2) were 0.82 ± 0.03 in 2010 and 0.84 ± 0.02 in 2011, indicating non-stressed leaves at all TCE concentrations. F_v/F_m values did not differ significantly under different TCE concentrations, neither in 2010 nor in 2011 on any measuring day. Hence, TCE had no influence on photosynthesis or on plant stress status, which is consistent with the observation that TCE did not influence transpiration substantially. Six days after TCE application in 2010, however, fluorescence values decreased significantly, but values still indicated non-stressed leaves (Fig. 4).

Conclusion

Willows took up TCE without excluding TCE during the transpiration process, whereby even high TCE concentrations of about 390 mg l^{-1} did not cause detectable toxic effects in plants. In our experiments, TCE was only minimally metabolized by willows. The degradation efficiency of TCE in the plants may be higher at the field scale due to bigger tree size and lower TCE concentrations. Nevertheless, our results suggest that, metabolization by willows may be insufficient what can cause transition of high amounts of CHC from water to the atmosphere via the transpiration pathway. To prevent such transition and to ensure total decontamination within the phytoremediation process, enhancing microbial degradation in the rhizosphere and by CHC-degrading endophytes might be a future promising strategy.

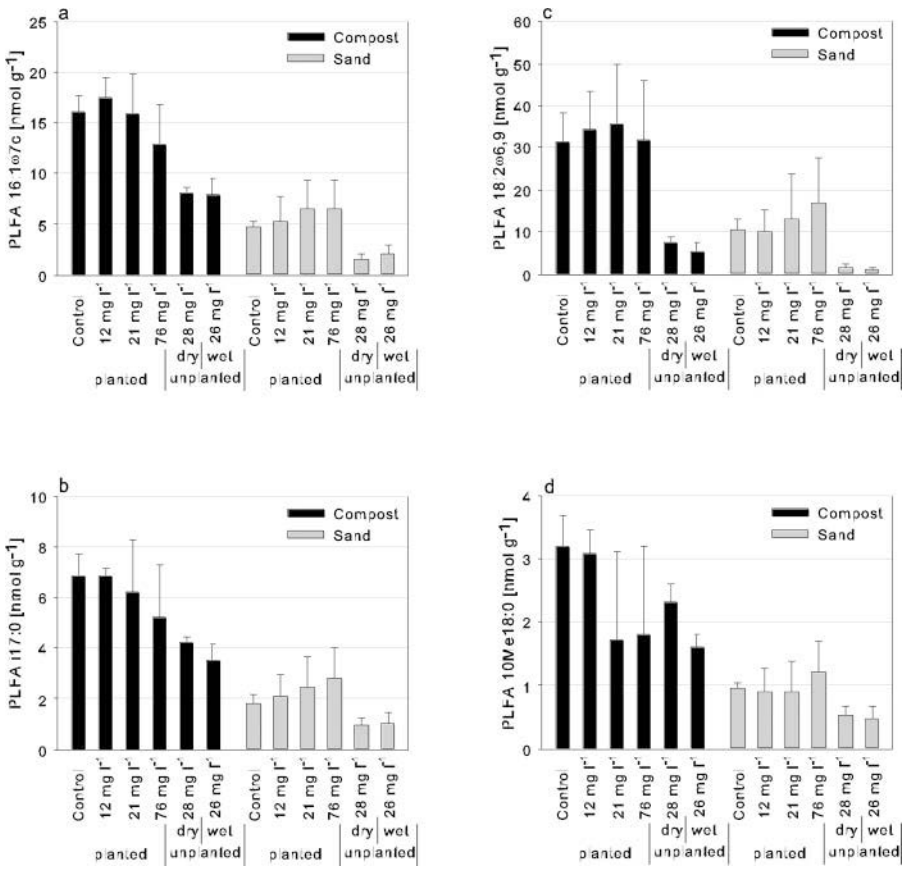

Figure 3. Amounts of microbial PLFAs (a)16:1ω7c (gram negative bacteria), (b) i17:0 (gram positive bacteria), (c) 18:2ω6,9 (saprophytic fungi biomarker) and (d) 10Me18:0 (actinomycetes) biomass in compost (black) and sand (gray). "Dry" represents compost and sand layers of unplanted pots with dry compost layer. "Wet" represents compost and sand layers of unplanted pots with wet compost layer.

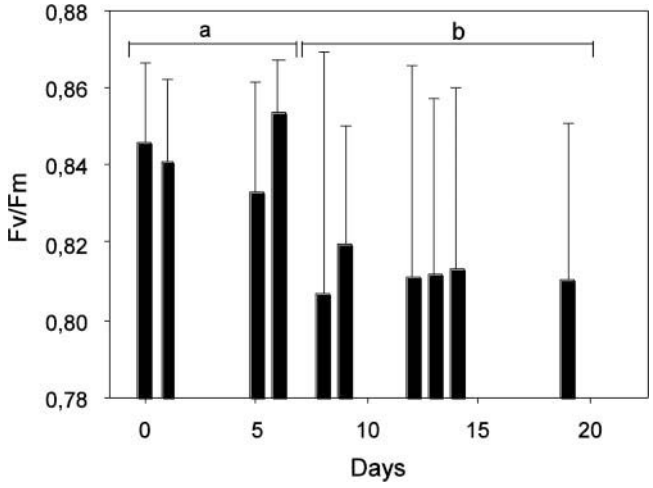

Figure 4 Chlorophyll fluorescence values in 2010. Bars show means ± standard deviations of each measuring day (n = between 30–67). Two groups were identified (a, b) showing slightly decreased Fv/Fm values after day 8 (Tamhane post-hoc test, $n < 0.05$).

Acknowledgment

The authors thank Sonja Feichtmaier, Joachim Heindler, Christian Mayer, Patrick Kobe, Christopher Nastl, Martha Klampfer, and Anton Grahsl for technical support.

Funding

This research was funded by the Federal Ministry of Agriculture, Forestry, Environment and Water Management of Austria. Funding Management by KPC Kommunalkredit Public Consulting (project number A820014).

Conflict of interest

The authors declare that they have no conflict of interest.

References

Anderson TA, Walton BT. 1995. Comparative fate of [^{14}C] trichloroethylene in the root zone of plants from a former solvent disposal site. Environ Toxicol Chem 14:2041–2047.

Barac T, Taghavi S, Borremans B, Provoost A, Oeyen L, Colpaert JV, Vangronsveld J, Van der Lelie D. 2004. Engineered endophytic bacteria improve phytoremediation of water-soluble, volatile, organic pollutants. Nat Biotechnol 22:583–588.

Bligh EG, Dyer WJ. 1959. A rapid method of total lipid extraction and purification. Can J Biochem Physiol 37:911–917.

Briggs GG, Bromilow RH, Evans AA. 1982. Relationships between lipophilicity and root uptake and translocation of non-ionised chemicals by barley. Pestic Sci 13:495–504.

Brigmon LR, Saunders FM, Altman D, Wilde E, Berry CJ, Franck M, McKinsey P, Burdick S, Loeffler F, Harris S. 2003. United States Department of Energy. FY02 Final Report on Phytoremediation of Chlorinated Ethenes in Southern Sector Seepline Sediments of the Savannah River Site.

Brunce NJ, Schneider UA. 1994. Chemical lifetime of chlorinated aliphatic priority pollutants in the Canadian troposphere. J Photochem Photobiology A 81:93–101.

Christiansen CJ, Francisco JS. 2010. Atmospheric oxidation of trochloroethylene: An ab initio study. J Phys Chem 114:9163–9176.

Dettenmaier EM, Doucette WJ, Bugbee B. 2009. Chemical hydrophobicity and uptake by plant roots. Environ Sci Technol 43:324–329.

Dietz AC, Schnoor JL. 2001. Phytotoxicity of chlorinated aliphatics to hybrid poplar (Populus deltoides x nigra DN34). Environ Toxicol Chem 20:389–393.

Doty SL. 2008. Enhancing phytoremediation through the use of transgenics and endophytes. New Phytol 179:318–333.

Frostegård Å, Tunlid A, Bååth E. 1991. Microbial biomass measured as total lipid phosphate in soils of different organic content. J Microbiol Methods 14:151–163.

Godsy EM, Warren E, Paganelli VV. 2003. The role of microbial reductive dechlorination of TCE at a phytoremediation site. Int J Phytorem 5:73–87.

Gopalakrishnan G, Werth CJ, Negri MC. 2009. Mass recovery methods for trichloroethylene in plant tissue. Environ Toxicol Chem 28:1185–1190.

Gordon M, Choe N, Duffy J, Ekuan G, Heilman P, Muiznieks IA, Ruszaj M, Shurtleff BB, Strand SE, Wilmoth J, Newman LA. 1998. Phytoremediation of trichloroethylene with hybrid poplars. Environ Health Perspect Suppl 106:1001–1004.

Hsu FC, Marxmiller RL, Yang AY. 1990. Study of root uptake and xylem translocation of cinmethylin and related compounds in detopped soybean roots using a pressure chamber technique. Plant Physiol 93:1573–1578.

Hunkeler D, Aravena R. 2000. Determination of compound-specific carbon isotope ratios of chlorinated methanes, ethanes, and ethenes in aqueous samples. Environ Sci Technol 34:2839–2844.

Hunkeler D, Aravena R, Butler BJ. 1999. Monitoring microbial dechlorination of tetrachloroethene (PCE) in groundwater using compound-specific stable carbon isotope ratios: microcosm and field studies. Environ Sci Technol 33:2733–2738.

James CA, Xin G, Doty SL, Muiznieks I, Newman L, Strand SE. 2009. A mass balance study of the phytoremediation of perchloroethylene-contaminated groundwater. Environ Pollut (Oxford UK) 157:2564–2569.

Kang JW, Khan Z, Doty SL. 2012. Biodegradation of trichloroethylene by an endophyte of hybrid poplar. Appl Environ Microbiol 78:3504–3507.

Khan Z, Doty S. 2011. Endophyte-assisted phytoremediation. Curr Top Plant Biol 12:97–105.

Lee W, Wood TK, Chen W. 2006. Engineering TCE-degrading rhizobacteria for heavy metal accumulation and enhanced TCE degradation. Biotechnol Bioeng 95:399–403.

Ma X, Burken J. 2004. Modeling of TCE Diffusion to the atmosphere and distribution in plant stems. Environ Sci Technol 38:4580–4586.

Ma X, Burken JG. 2003. TCE diffusion to the atmosphere in phytoremediation applications. Environ Sci Technol 37:2534–2539.

Matthews DW, Massmann J, Strand SE. 2003. Influence of aquifer properties on phytoremediation effectiveness. Groundwater 41:41–47.

McCully ME. 1999. Roots in soil: Unearthing the complexities of roots and their rhizospheres. Annu Rev Plant Physiol Plant Mol Biol 50:695–718.

Meckenstock RU, Morasch B, Griebler C, Richnow HH. 2004. Stable isotope fractionation analysis as a tool to monitor biodegradation in contaminated acquifers. J Contam Hydrol 75:215–255.

Miller RS, Khan Z, Doty SL. 2011. Comparison of trichloroethylene toxicity, removal and degradation by varieties of Populus and Salix for improved phytoremediation applications. J Biorem Biodegrad S7:1–8.

Newman LA, Reynolds CM. 2004. Phytodegradation of organic compounds. Curr Opin Biotechnol 15:225–230.

Newman LA, Strand SE, Choe N, Duffy J, Ekuan G, Ruszaj M, Shurtleff BB, Wilmoth J, Heilman P, Gordon MP. 1997. Uptake and biotransformation of trichloroethylene by hybrid poplars. Environ Sci Technol 31:1062–1067.

Newman LA, Wang X, Muiznieks IA, Ekuan G, Ruszaj M, Cortellucci R, Domroes D, Karscig G, Newman T, Crampton RS, Hashmonay RA, Yost MG, Heilman PE, Duffy J, Gordon MP, Strand SE. 1999. Remediation of trichloroethylene in an artificial aquifer with trees: A controlled field study. Environ Sci Technol 33:2257–2265.

Orchard BJ, Doucette WJ, Chard JK, Bugbee B. 2000. Uptake of trichloroethylene by hybrid poplar trees grown hydroponically in flow-through plant growth chambers. Environ Toxicol Chem 19:895–903.

Reichenauer TG, Germida JJ. 2008. Phytoremediation of organic contaminants in soil and groundwater. ChemSusChem 1:708–717.

Sandermann H. 1992. Plant metabolism of xenobiotics. Trends Biochem Sci 17:82–84.

Shang TQ, Gordon MP. 2002. Transformation of [14C] trichloroethylene by poplar suspension cells. Chemosphere 47:957–962.

Shang TQ, Doty SL, Wilson AM, Howald WN, Gordon MP. 2001. Trichloroethylene oxidative metabolism in plants: the trichloroethanol pathway. Phytochemistry (Elsevier) 58:1055–1065.

Shang TQ, Gordon MP. 2002. Transformation of [14C] trichloroethylene by poplar suspension cells. Chemosphere 47:957–962.

Su YH, Liu T, Liang YC. 2010. Transport via xylem of trichloroethylene in wheat, corn, and tomato seedlings. J Hazard Mater 182:472–476.

Walton BT, Anderson TA. 1990. Microbial degradation of trichloroethylene in the rhizosphere: potential application to biological remediation of waste sites. Appl Environ Microbiol 56:1012–1016.

Wang X, Dossett MP, Gordon MP, Strand SE. 2004. Fate of carbon tetrachloride during phytoremediation with poplar under controlled field conditions. Environ Sci Technol 38:5744–5749.

Watzinger A, Feichtmair S, Kitzler B, Zehetner F, Kloss S, Wimmer B, Zechmeister-Boltenstern S, Soja G. 2014. Soil microbial communities responded to biochar application in temperate soils and slowly metabolized ^{13} C-labelled biochar as revealed by ^{13} C PLFA analyses: results from a short-term incubation and pot experiment: Response of soil microbial communities to biochar. Eur J Soil Sci 65:40–51.

Weisgram M, Brandner P, Foditsch S, Dörrie T, Müller D. 2012. Umweltbundesamt and Österreichischer Verein für Altlastenmanagement, Vienna. Arbeitshilfe - CKW kontaminierte Standorte, Erkundung, Beurteilung und Sanierung.

Weyens N, Taghavi S, Barac T, Lelie D, Boulet J, Artois T, Carleer R, Vangronsveld J. 2009a. Bacteria associated with oak and ash on a TCE-contaminated site: characterization of isolates with potential to avoid evapotranspiration of TCE. Environ Sci Pollut Res 16: 830–843.

Weyens N, Van der Lelie D, Artois T, Smeets K, Taghavi S, Newman L, Carleer R, Vangronsveld J. 2009b. Bioaugmentation with engineered endophytic bacteria improves contaminant fate in phytoremediation. Environ Sci Technol 43:9413–9418.

Weyens N, Van der Lelie D, Taghavi S, Vangronsveld J. 2009c. Phytoremediation: plant–endophyte partnerships take the challenge. Curr Opin Biotechnol 20:248–254.

Weyens N, Truyens S, Dupae J, Newman L, Taghavi S, Van der Lelie D, Carleer R, Vangronsveld J. 2010a. Potential of the TCE-degrading endophyte Pseudomonas putida W619-TCE to improve plant growth and reduce TCE phytotoxicity and evapotranspiration in poplar cuttings. Environ Pollut (Oxford UK) 158:2915–2919.

Weyens N, Croes S, Dupae J, Newman L, Van der Lelie D, Carleer R, Vangronsveld J. 2010b. Endophytic bacteria improve phytoremediation of Ni and TCE co-contamination. Environ Pollut (Oxford UK) 158:2422–2427.

Winters RM. 2008. Volatilization of trichloroethylene from shallow subsurface environments: trees and soil. [master's thesis]. Logan (UT): Utah State University.

Yee DC, Maynard JA, Wood TK. 1998. Rhizoremediation of trichloroethylene by a recombinant, root-colonizing pseudomonas fluorescens strain expressing toluene ortho-monooxygenase constitutively. Appl Environ Microbiol 64:112–118.

Zentralanstalt für Meterologie und Geodynamik, Austria (ZAMG). 2012. Measuring station Langenlebarn.